OPTIMAL OPERATION AND CONTROL OF RENEWABLE ENERGY POWERED REVERSE OSMOSIS DESALINATION SYSTEM

by

EWAOCHE JOHN OKAMPO

A thesis submitted to the faculty of Engineering and Built Environment in fulfillment of the requirements for the degree of

PHILOSOPHIAE DOCTOR (PhD)

in

ELECTRICAL AND ELECTRONIC ENGINEERING SCIENCE

at the

UNIVERSITY OF JOHANNESBURG

Supervisor: PROF. NNAMDI NWULU

APRIL 2020

ABSTRACT

Desalination is a viable solution to meet water scarcity but is regarded as cost-intensive. The reverse osmosis (RO) technique of desalination is commonly used for its cost-effectiveness as compared to other methods but still considered energy-intensive. Conventional fossil energy sources emit carbon gas, which has environmental and cost implications, while renewable energy sources are limited by intermittency. This study formulates mathematical optimization models used to determine the optimal energy mix to power a reverse osmosis desalination unit. The models are formulated to ensure balance between power supply and demand, water demand and water produced, cost functions, and a time-of-use demand response (TOU DR) program. The cost functions include carbon emission cost, DR cost and components cost. The objective of The optimization models is to minimize the annualized cost of system (ACS), levelized cost of energy (LCOE), unit cost of water (COW) and carbon emissions, while maximizing the quantity of freshwater production subject to different economic and system reliability constraints.

The first model has an energy mix of grid power, a diesel generator and a photovoltaic (PV) module to supply an RO desalination unit with the objective of maximizing freshwater production at minimal cost. Also considered is the impact of DR and its cost on the quantity of water produced at different hours of the day, and the unit cost of freshwater. Three cases of optimal sizing approaches were compared. Case 1 is a system with only grid power and a diesel generator as energy sources; Case 2 has PV power incorporated in the energy supply mix, while Case 3 has the three energy sources and a TOU DR program on the demand side. The result shows that Case 3 turns out the highest freshwater production (1 520 m^3/day) at low cost of (1.33 \$/m^3) when compared to Case 1 with daily freshwater production of 1 250 m^3/day at a unit cost of 1.54 \$/m^3 and Case 2 with daily freshwater production of 1 501 m^3/day at a unit cost of 1.28 \$/m^3.

The second model is implemented on three similar case scenarios as the first, with the introduction of carbon emission cost. The techno-economic analysis of the three cases was performed considering the economic impact of carbon emission and the results were compared. The results show that Case 3 offers a very significant improvement on the reduction of carbon emission with a value of 751 766 $kgCO_{2\text{-}e}$ and 648 315 $kgCO_{2\text{-}e}$ with the introduction of a DR program and also has the lowest ACS ($1 158 801 with TOU DR). The result of sensitivity analysis shows the impact of increasing the carbon tax rate on the LCOE and COW; again, Case 3 proves to be less affected, as its proportional cost variation is significantly less than that of Case 1 and Case 2.

The third model explores the integration of RO, electro-dialysis (ED) and crystallization methods with the objective of minimizing the LCOE and brine production while maximizing freshwater and salt production. The proposed design is such that the feed water (saline water) is passed through the RO unit for desalination; the brine produced from the RO unit is further desalinated by the ED method, leaving a very high concentrate to be crystallized into soluble salts, thereby achieving zero brine production. Furthermore, for energy-efficient management, optimal sizing of energy sources, which include grid power, wind power and solar power, was carried out considering mitigation of carbon emission and its cost and the intermittent limitation of the renewable energy sources. This integrated design ensures that the internal and external costs of desalination are evaluated and minimized.

Finally, a comparison of results from the three models and sensitivity analyses were performed. Model 3 proved to be a more promising approach to solving the freshwater scarcity problem at a low cost and in an environmentally friendly way.

DEDICATION

This thesis is dedicated to all those who are in scarcity of freshwater around the world,

and to all those making efforts to solve the problem of inadequate potable water for humanity.

To the memory of my late mother, Mrs. Juliana Okampo,

and

to my son, Augustine Okampo.

ACKNOWLEDGEMENT

My profound gratitude is due to God Almighty for His gift of strength and grace. And to the following people I express my heartfelt gratitude for their contributions and support to ensure the success of this study.

- Prof. Nnamdi Nwulu, my supervisor, and Prof Clinton Aigbavboa, thank you for being so approachable, for your insightful comments, your encouragement and your firmness.
- All members of the Centre for Food, Energy, Water and Environment at the Faculty of Engineering and Built Environment for their contributions during seminars and private consultations. Aziza O. Gbadegesin, Gbadamosi Olalekan, Damisa Uyi, Olorunfemi Tope and all others, your contributions are highly appreciated.
- The family of Engr. Emmanuel Adikwu Ukpoju and my friends, Ehorsa Hensley Ogbebor, Douglas Aghimien, Femi Peace Ajayi, Ifije Ohiomah and Mamokete Bokhale, thank you for your hospitality, financial support and encouragement.
- The entire staff of the Department of Electrical and Electronic Engineering, Faculty of Engineering and Built Environment and the School of Postgraduate Studies for the conducive environment, support through consistent seminars and individual contributions.
- My family, for their prayers, support and encouragement; I am grateful.

PUBLICATIONS

1. E.J. Okampo and N. Nwulu. (2020) "Optimal Energy Mix for a Reverse Osmosis Desalination Unit Considering Demand Response" *Journal of Engineering Design and Technology*. Emerald Publishing Limited 1726-0531DOI 10.1108/JEDT-01-2020-0025

2. E.J. Okampo and N. Nwulu. "Optimal Design and Techno-Economic Evaluation of a Renewable Energy Powered Combined Reverse Osmosis Desalination and Brine Treatment Unit". *Desalination and Water Treatment. www.deswater.com 202(2020)27-37, October. doi: 10.5004/dwt.2020.26145.*

3. E.J. Okampo and N. Nwulu. "Optimization of Renewable Energy Powered Reverse Osmosis Desalination Systems: A State-of-The-Art Review" *Renewable and Sustainable Energy Reviews. 2021; 140:110712. https://doi.org/10.1016/j.rser.2021.110712.*

4. E.J. Okampo and N. Nwulu. "Techno-economic evaluation of Reverse Osmosis Desalination System Considering Emission Cost and Demand Response" *Sustainable Energy Technologies and Assessment. Volume 46, August 2021, 101252.*

https://doi.org/10.1016/j.seta.2021.101252.

Table of Contents

CHAPTER 1 1
INTRODUCTION 1
1.1 Background 1
1.2 Problem Statement 3
1.3 Aim and Objectives of Study 4
1.4 Significance of Study 4
1.5 Research Methodology 5
1.6 Delimitation of Study 5
1.7 Organization of Work 6
CHAPTER 2 7
REVIEW OF LITERATURE 7
2.1 Desalination: Overview, Methods and Configurations 7
2.1.1 Humidification Dehumidification Method of Desalination 7
2.1.2 Multi-stage Flash Desalination Method 9
2.1.3 Vapor Compressor Distillation Method of Desalination 10
2.1.4 Multi-effect Distillation 11
2.1.5 Electro-dialysis and Electro-dialysis Reversal Desalination Methods 13
2.1.6 Capacitive Deionization Method 14
2.1.7 Membrane Distillation 16
2.1.8 Reverse Osmosis Method of Desalination 17
2.1.9 Other Desalination Methods 19
2.2 Renewable Energy Sources for Desalination 25
2.2.1 Geothermal Energy 25
2.2.2 Ocean Energy 27
2.2.3 Wind Energy 30
2.2.4 Solar Energy 31
2.2.5 Hybrid RES for Desalination 34
2.3 Optimization of RES-RO Desalination System 35
2.3.1 System Sizing Optimization 40
2.3.2 Operational Optimization 42
2.3.3 Thermodynamic Optimization 45

2.4 Research Output and Trend 47
2.4.1 Cluster 1 (Red): Economic Feasibility of RES Integration with Desalination 49
2.4.2 Cluster 2 (Green): Simulation of RES-powered RO Seawater Desalination Plant 49
2.4.3 Cluster 3 (Blue): Economic Analysis of PV-RO Technologies 49
2.4.4 Cluster 4 (Yellow): Design and Exergy Analysis of Solar-powered Desalination Unit 49
2.4.5 Cluster 5 (Purple): Optimization of PV-RO Desalination Plant 50
2.5 Findings and Conclusions from the Review of Literature 51
CHAPTER 3 54
OPTIMAL ENERGY MIX FOR A REVERSE OSMOSIS DESALINATION UNIT CONSIDERING DEMAND RESPONSE 54
3.1 Introduction 54
3.2 Energy Supply and Demand Modeling 55
3.2.1 Grid Power Model 55
3.2.2 Diesel Generator Power Supply Model 56
3.2.3 PV Power Supply Model 56
3.2.4 RO Desalination Plant Power Demand Model 56
3.2.5 Demand Response Load Model 57
3.3 Component cost model 57
3.3.1 Grid Power Cost 57
3.3.2 Diesel Generator Cost 58
3.3.3 PV cost 58
3.3.4 RO Desalination Cost Model 59
3.3.5 Demand Response Cost 59
3.3.6 Total System Cost 59
3.4 Optimization Model 60
3.5 Case Study 62
3.6 Results and Discussion 64
3.6.1 Results 64
3.6.2 Discussion 68
3.7 SUMMARY 69
CHAPTER 4 71

TECHNO-ECONOMIC EVALUATION OF REVERSE OSMOSIS DESALINATION SYSTEM CONSIDERING EMISSION COST AND DEMAND RESPONSE 71
4.1 Introduction 71
4.2 Energy Supply and Demand Models 72
4.2.1 Grid Power Model 72
4.2.2 Diesel Generator Power Supply Model 72
4.2.3 PV Power Supply Model 72
4.2.4 RO Desalination Plant Power Demand Model 73
4.2.5 Demand Response Load Model 73
4.3 Component Cost Model 73
4.3.1 Grid Power Cost 74
4.3.2 Diesel Generator Cost 74
4.3.3 PV Cost 74
4.3.4 RO Desalination Cost Model 75
4.3.5 Demand Response Cost 75
4.4 Carbon Emission Cost and Global Warming Impact of Energy Source 75
4.5 Optimization Model 76
4.6 Case Study 78
4.7 Results and Discussion 78
4.7.1 Results 79
4.7.2 Discussion of Results 83
4.8 SUMMARY 85
CHAPTER 5 87
OPTIMAL DESIGN AND TECHNO-ECONOMIC EVALUATION OF A RENEWABLE ENERGY POWERED COMBINED REVERSE OSMOSIS DESALINATION AND BRINE TREATMENT UNIT 87
5.1 Introduction 87
5.2 System Models 89
5.2.1 System Architecture 89
5.2.2 Grid Power and Cost Model 90
5.2.3 Renewable Energy Sources and Cost Model 91
5.2.4 RO Desalination Plant Power Demand and Cost Model 92
5.2.5 Brine Treatment Power Demand Model 93

5.2.6 TOU Demand Response Load and Cost Model 94
5.2.7 Carbon Emission Cost and Global Warming Impact of Energy Source 94
5.2.8 Optimization Problem Formulation 95
5.3 Case Study 98
5.4 Results and Discussion 98
5.4.1 Results 98
5.4.2 Discussion 101
5.5 SUMMARY 102
CHAPTER 6 104
COMPARISON OF RESULTS AND SENSITIVITY ANALYSIS 104
6.1 Introduction 104
6.2 Comparative Analysis 105
6.3 Sensitivity Analysis from Model 2 106
6.4 Sensitivity Analysis from Model 3 108
6.5 SUMMARY 110
CHAPTER 7 111
CONCLUSION 111
7.1 Conclusion 111
7.2 Contributions to Knowledge 111
7.3 Future Work 112
REFERENCES 114
APPENDIX A: SAMPLE OF MODEL'S PROGRAM IN AIMMS 144

LIST OF FIGURES

2.1. Classification of major desalination methods……... 7

2.2 Schematic diagram of a combined Water heated, Close-Air Open-water HDH cycle and Heat pump……... 9

2.3 Schematic representation of general Multi-stage flash desalination process …… 10

2.4 Schematic diagram of Vapor compressor distillation/Mechanical vapor compression ……12

2.5 Schematic diagram of Multi-effect distillation ……... 13

2.6 Schematic of Electro-dialysis desalination process……. 14

2.7 (A) Schematic diagram of Capacitive deionization and (B) Membrane capacitive deionization ……..... 15

2.8 Schematic diagram of Membrane distillation ……. 17

2.9 The Schematic representation of Reverse Osmosis desalination process ……... 18

2.10a Total desalination unit capacity (worldwide) 1980-2015……..... 21

2.10b. Global installation capacity of desalination methods 2010-2018…… 21

2.11. Possible integration of renewable energy sources with desalination methods……. 27

2.12. Schematic diagram of concentrated solar power-reverse osmosis desalination…… 33

2.13. Schematic diagram of Photovoltaic-reverse osmosis desalination system…….34

2.14. World wild share distribution of installed indirect solar power desalination plant (2011) ….35

2.15. Classification of Optimization solution techniques……...37

2.16(a) Graph of Number of publications and (b) country of publications (1981-2019) ……48

2.17 (a) Network visualization and (b) Overlay visualization map of Optimization of RES desalination……51

3.1 Model's flowchart…….....62

3.2 Hourly solar irradiance …….....63

3.3 Hourly price of grid power ……...64

3.4 Hourly water demand ……...64

3.5 Case 1 hourly energy dispensed……....65

3.6 Case 2 hourly energy dispensed……66

3.7a Case 3 hourly energy dispensed……66

3.7b Case 3 hourly load curve with and without demand response program compare with hourly price of power……....67

3.8 Comparison of hourly freshwater production quantity……68

4.1 Case 1 hourly energy dispensed……....80

4.2 Case 2 hourly energy dispensed……80

4.3a Case 3 hourly energy dispensed……81

4.3b Case 3 hourly load curve with and without demand response program compare with hourly price of power……81

4.4 Comparison of hourly freshwater production quantity……82

4.5 Comparison of emission produced and the associated cost for the three Cases……84

5.1 Schematic diagram of a combine desalination and brine treatment process……90

5.2 Hourly wind speed…….....98

5.3 Hourly energy dispensed…….....99

5.4 Hourly freshwater dispensed……....99

5.5 Hourly freshwater, brine and salt produced……....100

6.1 Effect of increase in carbon tax on levelized cost of energy for the three cases with demand response……...……106

6.2 Effect of increase in carbon tax on cost of water for the three cases with demand response…107

6.3 Impacts of percentage increased on the annual cost of the system……108

6.4 Impacts of percentage increased on LCOE…….....109

6.5 Impacts of percentage increased on cost of water and salt……109

LIST OF TABLES

2.1: Summary of comparison of desalination methods……...22

2.2: Hybridization of RO and other methods of desalination……24

2.3: Simplified mathematical model of some performance indicators……39

2.4: Summary of sizing optimization of RES-desalination plants……...41

2.5: Summary of operational optimization of RES-desalination systems……...43

2.6: Summary of thermodynamic optimization of RES-desalination processes……46

3.1: Results of daily power supply……68

3.2: Summary results of optimized parameters……...69

4.1: Summary results of power output……82

4.2: Summary results of cost parameters……83

4.3: Summary of optimized results……83

5.1: Summary results of optimized parameters…… 100

6.1: Comparison of model results……...105

6.2: Summary results of cost parameters……108

LIST OF SYMBOLS/ABBREVIATIONS

Set	
t	Time (hr)
Parameters	
a, b	DG fuel cost coefficient
ρ_{air}	Air density (kg/m^3)
C_p	Power coefficient
α	Power law exponent
λ(t)	Locational marginal price ($/kWh)
ή	PV efficiency
I	Interest rate
r	Discount rate
AC_{CH}	Annual cost of RO treatment chemicals ($)
AC_{MR}	Annual cost of RO membrane replacement ($)
AMC_{PV}	Annual maintenance cost of PV ($)
AMC_{RO}	RO annual maintenance cost ($)
AMC_{WT}	Annual maintenance cost of the wind generator ($)
CRF	Capital recovery factor
$CGP_i(t)$	Cost of grid power imported ($)

$CGP_e(t)$	Cost of grid power exported ($)
CGP	Total cost of grid transferable power ($)
C_{PV}	PV panel cost ($/m^2)
C_{RO}	RO cost ($/m^3)
C_{WT}	Wind turbine cost ($)
CW_{TK}	Water tank cost ($/m^3)
FC(t)	DG fuel consumption
Fp	DG fuel price ($/m^3)
GP_i^{max}	Maximum imported grid power (kW)
GP_e^{max}	Maximum exported grid power (kW)
h	Projected height of wind turbine (m)
h_R	Reference height of wind turbine (m)
IC_{DG}	Initial capital cost of DG ($/unit)
IC_{PV}	Initial capital cost of PV ($)
IC_{RO}	Initial capital cost of RO Plant ($/m^3)
ICW_{TK}	Initial capital cost of the water tank ($)
IC_{WT}	Initial capital cost of the wind generator ($)
ΔL^{max}	Maximum allowable change in demand (kW)
ΔLC	Cost of demand response load curtails ($)

MC_{PV}	Cost of maintenance of a PV panel ($)
P(t)	Price of grid power($/kWh)
Pg^{min}	Minimum power of DG (kW)
Pg^{max}	Maximum power of DG (kW)
P_{ω}^{min}	Minimum power demand (kW)
P_{WD}^{max}	Maximum power demand (kW)
Q_B	Quantity of brine produced (m^3)
Q_F	Quantity of feed water (m^3)
Q_w	Quantity of freshwater produced (m^3)
QW^{min}	Minimum RO water produce (m^3)
QW^{max}	Maximum RO water produce (m^3)
RR	Freshwater recovery ratio
SEC	Specific energy consumption (kWh/m^3)
SI(t)	Solar irradiation (W/m^2)
TICC	Total initial capital cost of the System ($)
TMC	Total maintenance and operational cost ($)
TMC_{DG}	Maintenance cost of DG ($)
TMC_{PV}	Maintenance and operational cost of PV ($)
V(t)	Wind speed (m/h)

V_R	Reference wind speed (m/h)
WD(t)	Hourly water demand (m^3)
Variables	
ACS	Annualized cost of System ($)
APV	Area of PV (m^2)
AWT	Area of wind turbine (m^2)
CE_{DG}	DG carbon emission cost ($)
CE_g	Grid carbon emission cost ($)
COP	Cost of Products (water and salt) ($/m^3$)
C_{QW}	Cost of water ($)
FC_{DG}	Total DG fuel cost ($)
$GP_i(t)$	Grid power imported (kW)
$GP_e(t)$	Grid power exported (kW)
GWI	Global warming impact ($kgCO_{2\text{-}e}$)
LCOE	Levelized cost of energy ($/kWh)
$\Delta L(t)$	Demand response load curtails (kW)
$P_B(t)$	Hourly power demand for brine treatment (kW)
Pg(t)	Power output of DG (kW)
$P_{PV}(t)$	Hourly power output of PV (kW)

P_{WD} (t)	Hourly power demand by RO Plant (kW)
QW_{RO}(t)	RO hourly volume of water produce (m^3)
Saltp	Volume of salt produce (m^3)
SEF_{DG}	DG Specific Emission Factor (kg/L)
$SEF_{j,t}$	Grid Specific Emission Factor ($kgCO_{2\text{-}e}$/kWh)
TEC	Total carbon emission cost ($)
W_p(t)	Wind generator power output (kW)

ABBREVIATIONS

DG	Diesel Generator
DR	Demand Response
PV	Photovoltaic
RES	Renewable Energy Source
RO	Reverse Osmosis
TOU	Time of Use

CHAPTER 1
INTRODUCTION

1.1 Background

There is water everywhere, yet not enough water to drink, just as there are different sources of energy everywhere, yet not enough energy to power the world!

Energy and water are both essential commodities, vital for continuous human existence. Copious as the amounts in which they are to be found are, the amount available for use is inadequate. The earth sits on water, as it is estimated that two-thirds of the earth is covered by water, yet only 1% is suitable for domestic and industrial purposes [1]. At present, one-fifth of the world's population experience a water scarcity crisis [2]. One-fourth of the world's population have access to water sources but lack adequate purification facilities [2]. According to the United Nations World Assessment Program (UNESCO, Paris 2015) [3], up to 40% of the world's population will be affected by water scarcity by 2030. The major causes of inadequate freshwater resources are climate change and pollution [4]. With 97% of the total available water resources being saline water, the obvious solution for obtaining sustainable freshwater is via desalination and water reuse technologies [4] and [5].

In simple terms, desalination is a purification process for obtaining fresh or potable water from available saline (seawater or brackish) water. Desalination systems over the years have experienced constant advancement, leading to the availability of different methods, which can be classified as either membrane methods or thermal processes. Membrane desalination methods use membranes with unique chemical and physical properties, such as ion adsorption and desorption, ion selectivity and semi-permeability in methods such as capacitive deionization (CDI), electro-dialysis (ED) and reverse osmosis (RO) respectively [1]. Other membrane methods include

electro-dialysis reversal (EDR) and membrane distillation (MD). On the other hand, thermal desalination processes are based on change of state methods, such as humidification dehumidification (HDH), multi-stage flash distillation (MSF), vapor compressor distillation (VCD) and multi-effect distillation (MED). RO, MSF and MED are the most frequently used methods among the various desalination methods, with RO accounting for 65%, MSF for 21%, MED for 7%, ED for 3% and the others for 4% of global production capacity [1].

Considering the world's energy state, it is estimated that 18% of the global population lacks access to electricity [6]; [7]; [8]. According to the International Energy Agency, electricity statistics show that the global total electricity consumption as at 2016 amounted to 20 863 TWh and was then expected to increase by at least 3.2% annually, judging by the increment the previous year (2015). Of this figure, coal accounted for the highest supply with 38.3%, followed by natural gas with 23.1%, hydropower with 16.6% and nuclear power with 10.4%, while solar/wind/geothermal/tide supplied 5.6%, oil 3.7% and biofuel and waste 2.3% [9]. Of the total energy supply mix, only 34.9% was renewable, with hydropower having the highest percentage. Coal, which currently accounts for the highest percentage of the entire global energy supply mix, emits about twice as much CO_2 per generated kWh as natural gas, making both (coal and natural gas) major contributors to global warming [9].

Furthermore, usage statistics of generated electricity shows that about 40% is used for domestic purposes, 47% for industrial purposes and 13% is lost during power transmission [9]. Conventional energy sources from fossil fuel have negative impacts on the environment, causing greenhouse gas (GHG) emissions and pollution, leaving renewable energy sources (RES) as viable option for consideration [10] and [11]. RES on their part have considerable limitations, such as inconsistent solar irradiation and intermittent wind speed; these are usually addressed by hybridization.

The energy-water nexus concept describes the interconnection between both resources with the aim of maximizing synergy and addressing trade-offs between the two [12]. This concept has gained significant prominence in recent times owing to the overt importance of the two commodities (energy and water) to the human populace. As the population of the world continues to grow, the need and demand for both energy and freshwater continue to increase exponentially, putting pressure on the existing infrastructure designed for the supply of energy and freshwater [13]. Research in this area has also increased over the years, proffering solutions to different problems associated with the energy-water nexus. While the negative environmental impact of fossil power energy sources can be mitigated to a vast extent by the alternative use of RES that provide green energy without gas emissions and hence are more environmentally friendly, the problem of inadequate freshwater for human consumption has led to the advancement of water desalination systems as possible solutions. The trade-off between the integration of the two (energy and water) gives room for wide research. Authors [14] present a reference system architecture for an energy-water nexus detailing subsystem configurations. It also details different drivers on which the trend in the nexus studies has been based. These factors include, i) Increase in demand for both resources as a result of population growth; ii) Economic growth resulting in per capita growth; iii) Degradation of available freshwater due to climate change and concern for negative environmental factors, and iv) Electricity-intensive water and water-intensive electricity cum ageing infrastructure. These factors exert strain on the energy-water nexus.

1.2 Problem Statement

Continuous growth in population, constant water pollution and other water stress have made freshwater scarcity a major problem around the world [15]. Treatments such as water reuse and seawater desalination have become prominent in recent years owing to the abundant availability

of seawater around the world [16]. Desalination is a viable solution to meet water scarcity but is considered cost-intensive. The RO technique of desalination is commonly used because of its cost-effectiveness but is energy-intensive. Conventional fossil energy sources emit carbon gas, which has environmental and cost implications, while RES are limited by intermittency. Moreover, the byproduct of desalination is high concentration of salts (brine), which if indiscriminately disposed of has environmental consequences, hence necessitates proper management. The cost implications of emitted carbon gas and brine management are regarded as the external costs of desalination [17].

1.3 Aim and Objectives of Study

The aim of this study is to develop mathematical models suitable for an optimal energy schedule for a cost-effective desalination system with the following objectives:

- To present a mathematical model of an optimal energy mix that includes a demand response (DR) program for an efficient energy schedule to power an RO desalination unit at minimal levelized cost of energy (LCOE).
- To develop a mathematical optimization model that enhances effective techno-economic analysis of a RES-powered RO desalination system considering carbon emission and its cost while maximizing freshwater production.
- To design a techno-economic optimization model of a combined desalination and brine treatment unit for freshwater production and brine management.

1.4 Significance of Study

Energy and water are both essential commodities, vital for continuous human existence. The inadequacy, limitations and cost of these commodities are serious challenges that require critical solutions. This study presents mathematical optimization models that can be used to manage the

techno-economic effect of the integrated system effectively. The designed models are intended to minimize cost, complement technical and natural limitations and reduce negative environmental outcomes while increasing the availability of freshwater for both domestic and industrial use.

1.5 Research Methodology

This thesis uses a classical optimization approach to model different techno-economic optimization problems that consider economic factors such as components cost, the effect of a time-of-use (TOU) DR program and its cost, environmental factors such as carbon emission and its cost, and brine management. The metrological data from Stellenbosch University, Western Cape province of South Africa is used. The hourly solar irradiation and wind speed for the area were collected from the Southern African Universities Radiometric Network. Furthermore, the TOU energy price (in US $) for South Africa obtained from the Eskom schedule of standard prices for Eskom tariffs 2019/2020 [18] is implemented for the DR program. Other data used as parameters were those given in [19] and [20]. The multi-objective optimization problems formulated were solved with the CPLEX 12.10 solver of the Advanced Interactive Multidimensional Modelling Software (AIMMS).

1.6 Delimitation of Study

The focus of this study is the integration of grid and RES to power RO desalination systems considering TOU DR and environmental factors such as carbon emission and brine production. The study could not take into account all carbon emissions from the production of components to the production of freshwater and salt; only carbon emitted from the energy sources and cost implications were considered. The detailed production processes of the desalination and brine treatment are also beyond the scope of this study. Water storage, the transportation network and

cost are not considered, only the LCOE and unit cost of production. Furthermore, the treatment and economic value of salt produced are beyond the scope of this study; the study's focus is limited to the techno-economic analysis of freshwater production and brine management.

1.7 Organization of Work

The remainder of this thesis is organized such that:

Chapter 2 reports an extensive review of literature highlighting the different methods of desalination, the renewable energy sources considered to power desalination systems and the optimization approaches utilized for techno-economic analyses of desalination systems powered by renewable energy sources.

Chapter 3 presents a mathematical model to determine optimal energy mix for a reverse osmosis desalination unit considering demand response.

A techno-economic evaluation of reverse osmosis desalination system considering emission cost and demand response is detailed in Chapter 4.

Chapter 5 presents an optimal design and techno-economic evaluation of a renewable energy powered combined reverse osmosis desalination and brine treatment unit.

In Chapter 6, a comparison of results from the three models of Chapters 3, 4 and 5 and sensitivity analyses from models 2 and 3 are reported.

Chapter 7 concludes the study highlighting its contributions to knowledge and recommendation for future work.

CHAPTER 2
REVIEW OF LITERATURE

2.1 Desalination: Overview, Methods and Configurations

Desalination is a purification process of obtaining fresh or potable water from abundantly available saline (seawater or brackish) water. The desalination system has over the years experienced constant advancement, leading to the availability of different methods, which can be classified into two [1]: The membrane method and the thermal process. Figure 2.1 explicitly depicts the classification of the desalination process and various techniques.

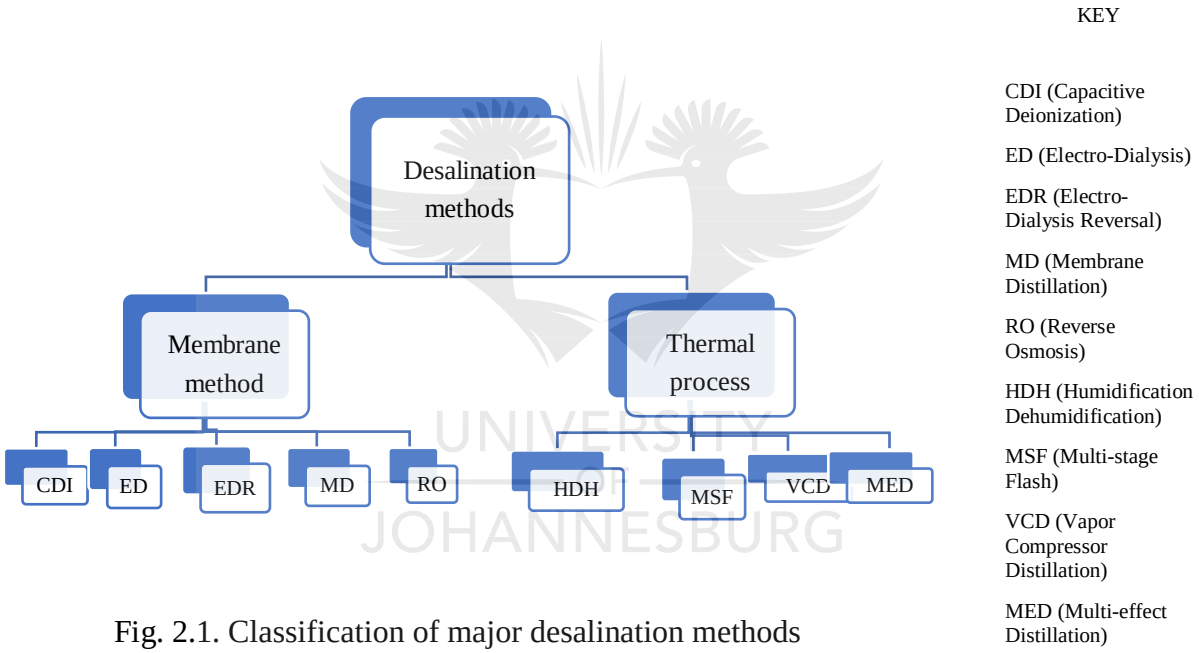

Fig. 2.1. Classification of major desalination methods

The operational principles of different desalination methods are presented in the following subsections.

2.1.1 Humidification Dehumidification Method of Desalination

The HDH desalination method is based on the principle of evaporation and condensation, as happens in a natural water cycle [21]. Saline water is heated, and the humidity of the ambient air is increased in the humidification tower or humidifier to the point of saturation, based on the

designed temperature specification, leading to the evaporation of water [22]. The air, by its increase in humidity, becomes the carrier of water from the humidifier to the dehumidifier, where the condenser is used to reduce the air temperature and consequently condense freshwater [23]. HDH is classified based on the cycle configuration as close-air open-water , close-water open-air and open-air open-water [24]. It could also be air-heated or water-heated [22]; [25]. This method of desalination requires relatively cheap materials for its simple arrangement and can use low-grade thermal energy to reduce the carbon footprint [22]. Its main limitation is the higher requirement for thermal energy per unit volume of freshwater produced compared to other desalination methods such as MED and MSF. The challenge of scaling up the energy requirement is another limitation [22]; [25]. Some improved HDH configurations have been proposed that are aimed at the reduction of specific energy consumption (SEC) as a result of air circulation carrying evaporated water or vapor from the humidifier to the dehumidifier. The multiple effect humidification method using innovative geometry was proposed by Muller-Hoist [26]; [27]. This configuration reduces and maintains the energy requirement at a deficient level by inserting parallel plates as high-performing film condensers, which enhances continuous temperature distribution and natural air circulation. Authors [21] present the inclusion of absorption beds to improve the close-water open-air cycle configuration of HDH to HDH adsorption (HDHA) configuration. This configuration allows the saturated air at the lowest temperature to be sent for dehydration in the absorption beds where the humidity is reduced by absorption and the dry air is sent to the humidifier. The drying of the saturated air at the bottom gives room to produce more distillate per cycle. Authors [28] develop an HDH cycle configuration model based on the first principle of thermodynamics, demonstrating heat and mass transfer in the HDH heat pump cycle. A heat pump is used as a source of heating and cooling for the HDH system to improve the output

ratio and energy recovery of the system. Figure 2.2 presents a schematic diagram of a combined water-heated close-air open-water HDH cycle and heat pump, where a, w and r represent air, water and refrigerant respectively, while 1, 2, 3 … are state points.

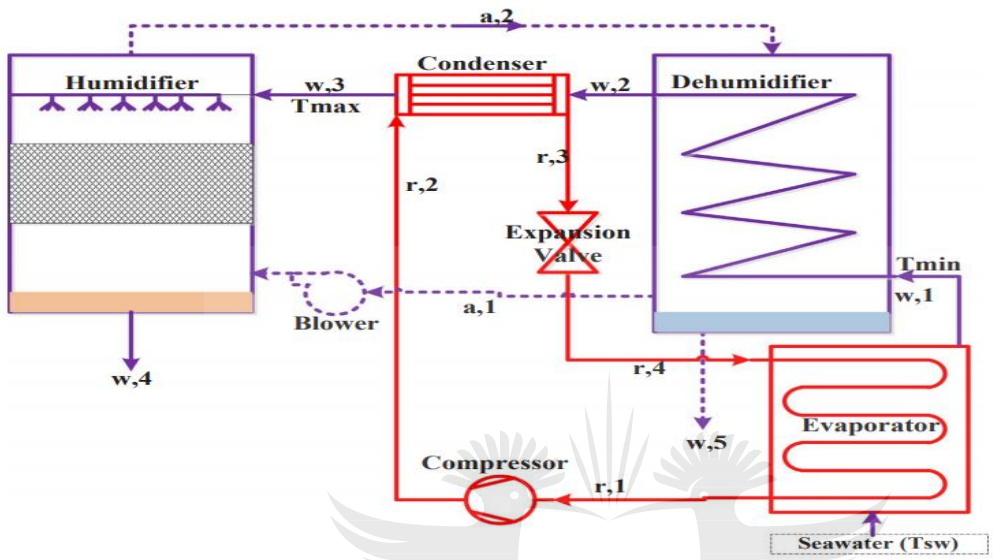

Fig. 2.2 Schematic diagram of a combined water-heated, close-air open-water Humidification dehumidification cycle and heat pump [28]

2.1.2 Multi-stage Flash Desalination Method

MSF plants are designed to have three sections: the brine heater, the heat rejection section and the heat recovery section. Desalination via MSF involves brine heating, flash distillation in multiple stages and finally, heat recovery [29]. Authors [30] explain that the hot brine is supplied to a liquid pool, where evaporation takes place. The vapor flashes from the pool towards the tube bundles and condenses on the surface because the tube's surface has a lower temperature than the vapor. The condensed vapor is collected as freshwater, while the hot brine flows into other stages. During this process, the condenser tubes circulate low-temperature seawater (brine) for the absorption of latent heat from vapor generated by the high-temperature brine pool. The heat recovery process

commences as the absorbed latent heat partially heats the circulating low-temperature brine, thereby saving energy and enhancing the system's performance. MSF has different design configurations, which are brine recirculation (MSF-BR), a once-through (MSF-OT) configuration and simple mixer (MSF-M); of these configurations, MSF-BR is the most efficient while MSF-OT has the simplest design [27]. Several studies have investigated the optimization of these MSF configurations. Authors [31], [32] and [33] detail the application of MSF-BR, [34] considers MSF-M, while MSF-OT is presented in [35]. A method of improvement of corrosion resistance in MSF desalination plants during an acid cleaning operation by cationic surfactant was presented in [36], whereas [37] examined the environmental and human health impact of different MSF plants using a life cycle assessment. Figure 2.3 depicts a general MSF process.

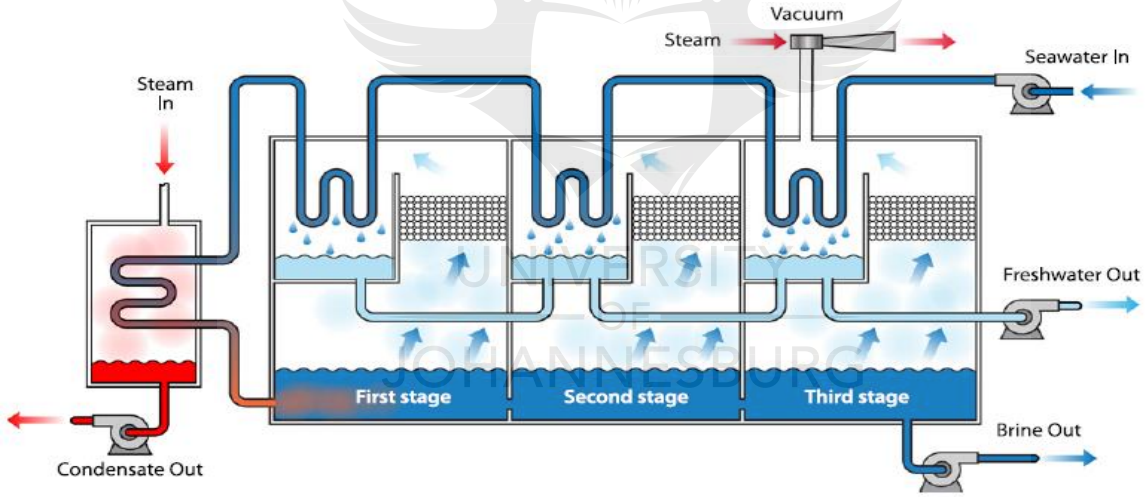

Fig. 2.3 Schematic representation of general Multi-stage flash desalination process. [38]

2.1.3 Vapor Compressor Distillation Method of Desalination

The VCD method is also frequently studied as a mechanical vapor compression/recompression (MVC/MVR) technology for water desalination [37]; [39]. This method of desalination does not depend on external sources of heat like other methods of desalination; it rather generates heat from

the compressor [40]; [41]. The working principle of VCD is that free resulting vapor from boiling saline water in the evaporator is compressed by an external mechanical compressor. Then, the compressed hot water vapor is channeled back into the evaporator where it is condensed outside the evaporator tubes as freshwater, leaving behind hot brine water and heat energy from the steam of distilled to boil the saline water [39]. The main configurations of the water vapor compressor include the twin-screw version discussed in [41]; [42], centrifugal [43]; [44], single-screw [45] and roots compressor versions [46]. Several studies done to analyze the operating performance of the VCD method used the thermodynamic behavior of the system [47]; [48]; [49]. Thermo-economic analysis of single-effect and forward-feed multi-effect mechanical vapor compression desalination is presented by references [50] and [51] respectively, whereas [52] considered the performance of MVC driven by an organic Rankine cycle (ORC). A study on a zero-emission system was done based on MVC by [53]. Figure 2.4 represents the schematic diagram of VCD/MVC.

2.1.4 Multi-effect Distillation

MED plants are designed with multiple airtight effects. A sequence of constant evaporation/condensation takes place at every effect in descending order of pressure and temperature. The external heat supplied boils the feed water as it enters the first effect, which has the highest pressure. The vapor generated inside the first effect is used as the energy source for the next effect and this continues successively along the series of effects. Therefore, on one side, the feed water is boiling and generating vapor, while on the other side, vapor is condensing as freshwater [54]. There are many configurations of MED based on an external heat source, hybridization with other methods, and a design arrangement of tubes: vertical and horizontal tubes [36]. Figure 2.5 depicts a schematic diagram of MED. In [55] MED is classified into four

configurations based on the feed water concentration supplied to the evaporators and the direction of flow of the vapor. These configurations are back-feed, parallel feed, Forward-Feed and parallel/cross-feed (PCF). These configurations were compared using the transient performance index of the MED system. It was concluded that PCF responds faster to applied disturbances than the others.

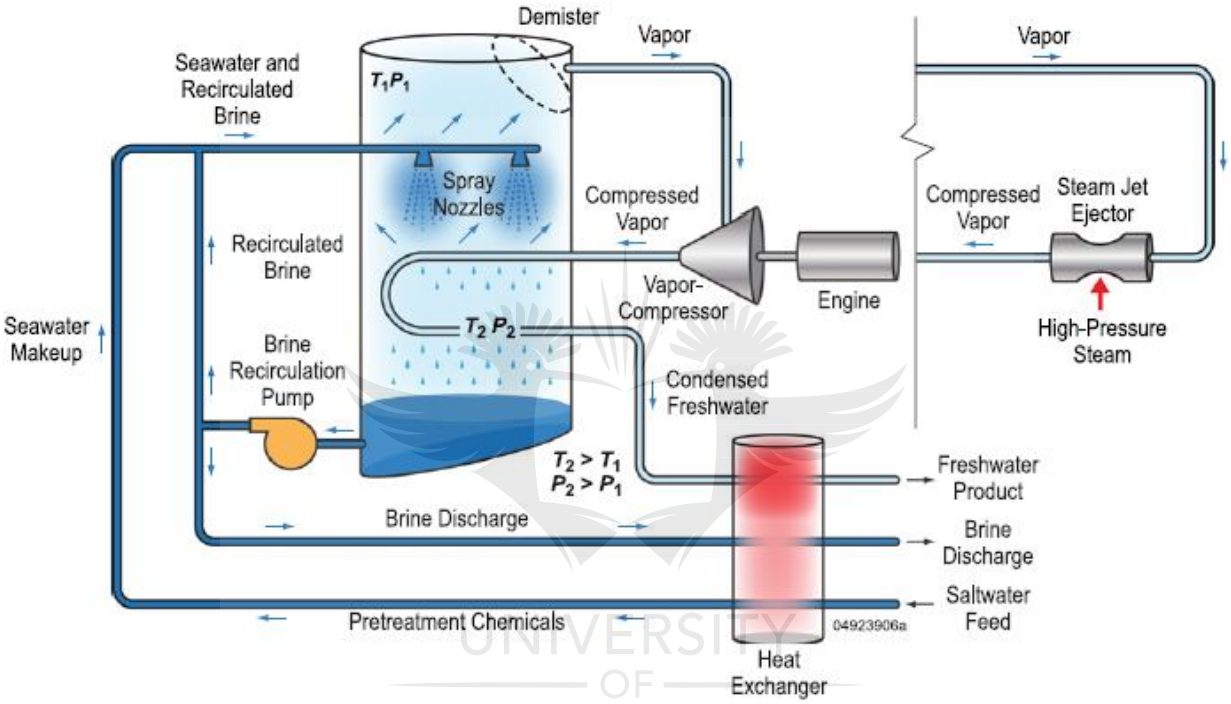

Fig. 2.4 Schematic diagram of Vapor compressor distillation/Mechanical vapor compression [38]

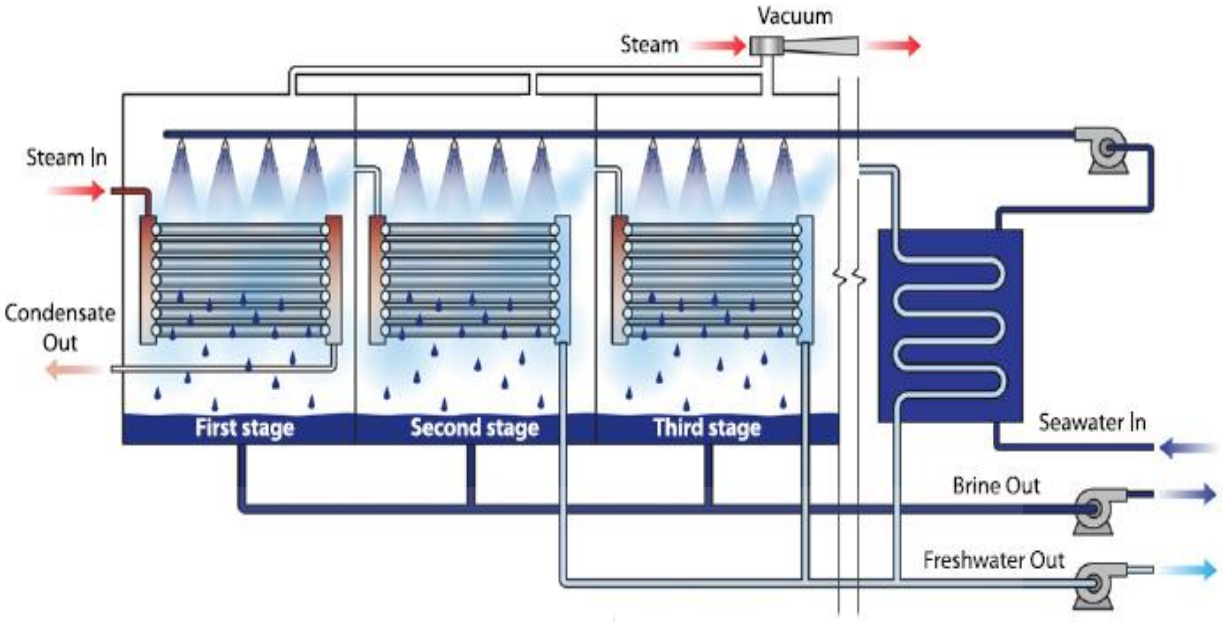

Fig. 2.5 Schematic diagram of Multi-effect distillation [38]

2.1.5 Electro-dialysis and Electro-dialysis Reversal Desalination Methods

ED is similar in principle to electrolysis except that in ED, different compartments are used for the positive and negative electrodes, unlike electrolysis where both electrodes are in the same compartment. Therefore, on this basis, the ED method of desalination implies that direct current from the external source is supplied through the electrodes in a solution of saline water containing ion-selective membranes, which are connected in parallel to form channels. As the electrodes are charged, the negative salt ions move through the anion permeable membrane towards the anode, whereas the positive salt ions move the other way through the cation permeable membrane to the cathode. These movements of ions create channels for concentrated brine leaving behind freshwater [36] and [56]. The continual use of membranes in the same direction leads to accumulation of precipitant on the concentrated side. EDR provides a solution to this by periodically alternating the polarity of the electrodes, reversing the flow of ions, therefore cleaning up both sides of the membrane and thus increasing its life span [36]. Figure 2.6 depicts the ED

desalination process schematically. The limitations of ED, such as the high cost of electrodes and membranes, short life span of membranes and need for high saline water recirculation to obtain the required freshwater, have led to limited interest and research in this method of desalination [57]; [58]. Authors [59] present an extensive study of the ED method of desalination, highlighting recent development and applications, one of which is reverse ED (RED). RED is used for energy generation from salinity gradients. This employs controlled mixing of two solutions of different salinity concentration, with the difference converted into electricity. This has sparked the development of new designs and new membranes with an optimized process for plant configuration suitable for operational processing of seawater with high salinity [60], [61] and [62].

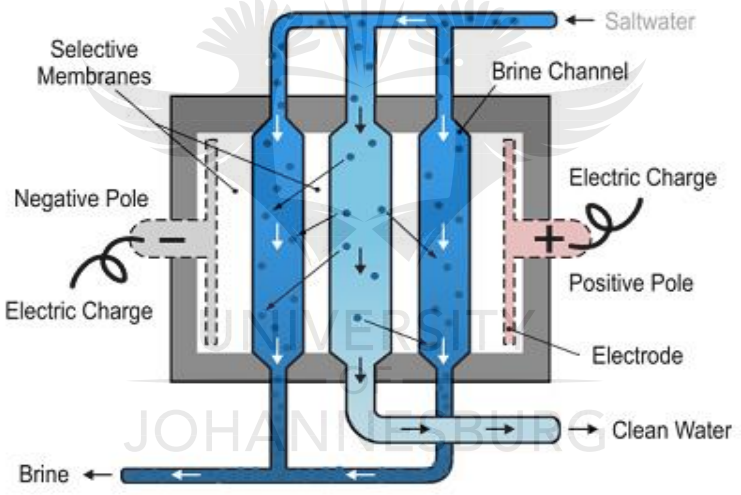

Fig. 2.6 Schematic of Electro-dialysis desalination process [38].

2.1.6 Capacitive Deionization Method

CDI is very similar to ED, as both involve the removal of salt ions from saline water, leaving freshwater. While in ED the ion-selective membrane is used as a channel for the removal of salt ions, CDI deploys carbon-coated electrodes as channel for the adsorption of salt ions [63]; [64]; [65]. Membrane capacitive deionization (MCDI), as an improved ED, on the other hand, employs

an ion exchange membrane for the separation of negative and positive ions before they are attracted towards the electrode with opposite polarity, which acts as the channel for adsorption [66]; [67]; [68]. The CDI process is such that when electrical potential is applied between the electrodes from an external source, salt ions are adsorbed by the surface of the charged electrodes from the feed solution, leaving behind freshwater. The electrodes, at some point, become saturated and then regenerated by reversing the electric potentials, thus desorbing ions back into the solution, producing brine [61]. The CDI can be designed with either a unipolar or bipolar configuration of electrodes. A comparison between the two connections is yet to be extensively reported in the context of desalination [69]; [70]; [71]. CDI requires only little maintenance compared to other methods of desalination. It does not require the use of chemicals or a pressure pump. Electrodes are stable and less fouled compared to membranes. Moreover, it has a high energy recovery rate, depending on the condition of operation [72]; [73]; [74]. Figure 2.7 depicts CDI and MCDI.

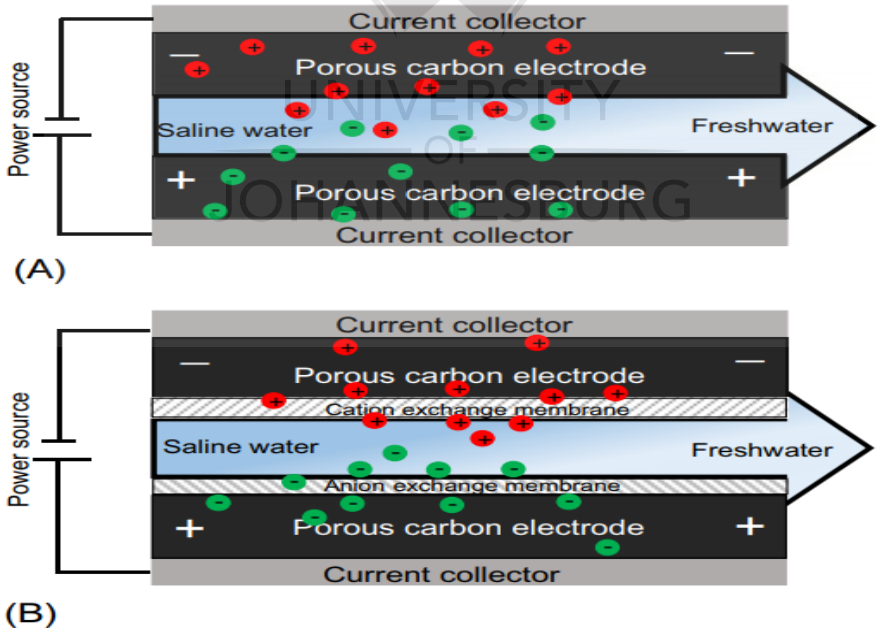

Fig. 2.7 (A) Schematic diagram of Capacitive deionization and (B) Membrane capacitive deionization [72]

2.1.7 Membrane Distillation

MD is a hybrid method of desalination, combining both thermal and membrane processes. It involves the separation of volatile solutes from feed water via a microporous hydrophobic membrane. A vapor pressure difference of the component being separated exists as a result of temperature differences on either side of the membrane [75]. The vapor pressure difference and the membrane temperature difference act as the driving force for the separation. Vapor from the heated feed passes via the membrane pores from the hot side to the cold side of the membrane surface, where condensation takes place. Desalination is, therefore, partly due to vapor/liquid equilibrium at the membrane and partly to diffusion. Some of the salient characteristics of MD are (i) 100% non-volatile solute rejection, thus guaranteeing 100% purity [76]; [77], (ii) The process not being affected by salinity of the feed water [74]; [76]; [77], and (iii) Low operating pressure and temperature [78]; [79]. MD is classified into four configurations based on methods of collection of water vapor on the condensed side of the membrane [77] and [80]. There is direct contact membrane distillation, air-gap membrane distillation, vacuum membrane distillation and sweep gas membrane distillation. A schematic diagram of MD is represented in Figure 2.8.

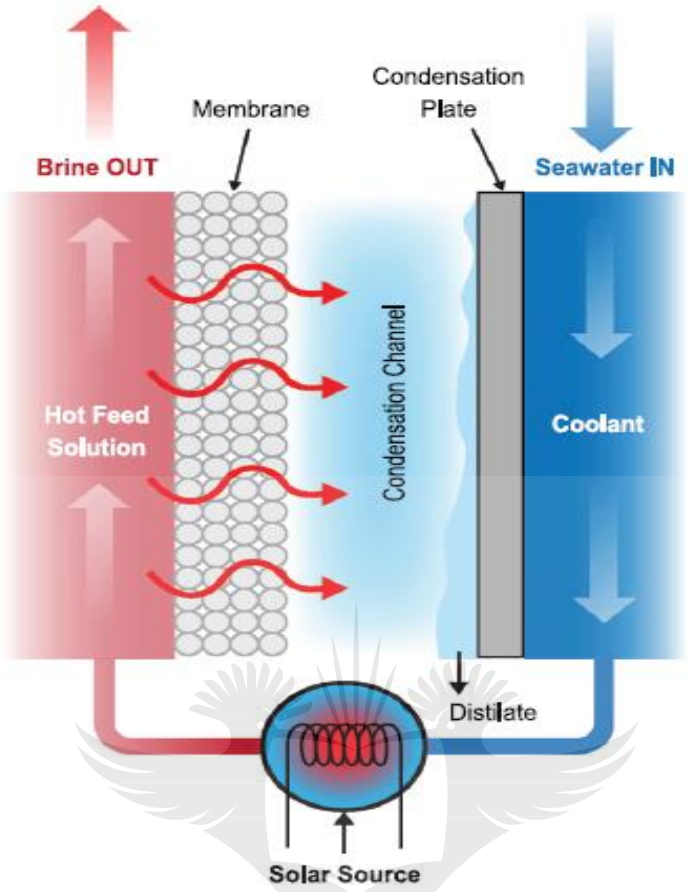

Fig. 2.8 Schematic diagram of Membrane distillation [38].

2.1.8 Reverse Osmosis Method of Desalination

The basic principle of osmosis is that water moves from a less concentrated to a more concentrated aqueous solution via a semi-permeable membrane, hence diluting the concentrated solution until an equilibrium concentration is reached. This process does not require a pressure difference larger than osmotic pressure (a threshold differential pressure for both the concentrated and dilute solution). RO, on the other hand, as the name implies, is the reverse process of osmosis in which water diffuses from the more concentrated to the less concentrated aqueous solution, enhanced by a pressure difference larger than osmotic pressure across the semi-permeable membrane [81]. The membrane, on its part, characterizes a significant pressure differential to the flow of freshwater

[82]. The high amount of energy required to sustain the pressurization requirement of the RO method is its obvious limitation; otherwise RO is the most frequently used desalination method because of its efficiency and overall cost-effectiveness. RO also has the ability of not permitting almost all colloidal or solute from passing through the membrane; hence it assures high quality freshwater. According to [36], RO desalination has four subsystems: (i) Pre-treatment section, which involves some form of percolation and sterilization to reduce scaling and fouling by addition of useful chemicals, (ii) A high-pressure pump used for the creation of the required pressure differential necessary to push water across the membrane, (iii) A membrane for the separation of freshwater from concentrated feed water, and (iv) Post-treatment with chemicals to guarantee high-quality freshwater. Figure 2.9 depicts the schematic representation of RO.

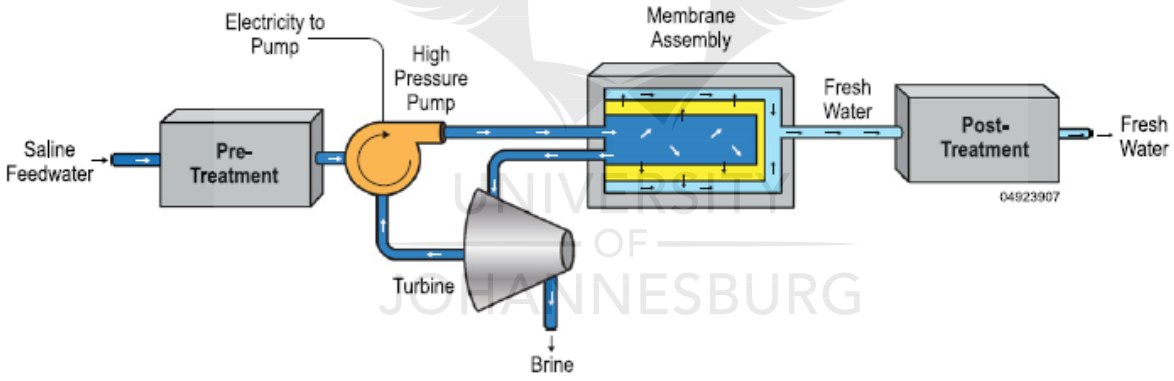

Fig. 2.9 Schematic representation of Reverse Osmosis desalination process [38].

The RO system's operational design was described and classified into three main configurations: (i) Single-stage RO, (ii) Two-stage RO, and (iii) Close-circuit RO by [83]. The comparison of these configurations was made considering the relationship between SEC and average water flux of the RO system. It was concluded that, based on average water flux and SEC, which were the main factors analyzed, a two-stage RO configuration might be considered the ideal choice. However, it is capital-intensive when compared to the other two configurations.

2.1.9 Other Desalination Methods

There are several other methods of desalination, usually an appendage or hybridization of the major techniques. In some cases, there are new innovative methods that are yet to be explored extensively and implemented compared to the major desalination methods. This category includes forward osmosis (FO), nano-filtration (NF), freeze desalination (FD) and hybrid approaches.

2.1.9.1 Forward osmosis

FO can be regarded as the direct opposite process of RO. It uses the basic principle of osmosis, which depends on the natural osmotic pressure difference across the membrane to draw water from the less concentrated side (salty feed water) of the membrane to the more concentrated solute (draw solute), balancing the concentration level by diluting the draw solute. According to [84], the process of desalination when using FO is completed only with the addition of a freshwater recovery unit. Hence FO is best used as a pre-treatment unit for other desalination methods such as RO. The hybrid method is more suitable than standalone methods [85]. Whereas the hybrid FO system is ideal for the desalination of high-salinity feed water, RO is not. The FO hybrid system also consumes less energy than RO. Other advantages of FO over RO include high water recovery and minimal fouling [86][87]. The major limitations of FO are the high energy requirement when used as a standalone method of desalination and the limited choice of draw solute [88].

2.1.9.2 Nano-filtration

NF is used as a desalination method for the removal of scaling divalent ion, which implies that the separation process is based on the solute charge and molecular size of uncharged solute. It is a membrane-based desalination process with the membrane having pore sizes of less than 0.002 µm [89]. NF membrane rejects solute selectively based on charge and size, unlike RO that rejects all solute. This method also requires lower operating pressure than RO. It is not adequate for seawater

desalination, but should rather be used as a pre-treatment unit in a hybrid method [90]. NF has two forms of configuration based on the flow pattern through the membrane, namely (i) Crossflow with concentrate recycle, otherwise known as tangential flow or dynamic filtration, and (ii) A dead-end flow system (dead-end filtration or static filtration) [86]. Research trends in this area increasingly focus on the development and improvement of the nanomaterials [91].

2.1.9.3 Freeze desalination

The working principle of the FD method is based on phase change, from liquid to solid (solidification). The feed water (saline water) is subjected to a freezing process using a refrigerant to form ice crystals mainly composed of freshwater, leaving behind concentrated liquid as brine. The ice slurries are then separated from the brine and melted to obtain freshwater as the final product [92]. The FD process, therefore, has three stages: precooling, crystallization and separation [89]; [93]. FD configurations are of two types, based on refrigerant position. These are direct FD and indirect FD [89]. As the names imply, in the direct FD configuration the refrigerant is in direct contact with the feed water, which absorbs heat from the water while it is vaporized. On the other hand, indirect FD has a crystallizer wall separating the feed water and the refrigerant. While direct FD is considered more efficient than indirect FD because of its large surface area, high heat transfer coefficient and economic viability, the limitations are the probability of hydrate formation and contamination of the water by refrigerant [89].

Figure 2.10 depicts the global installation capacities of desalination methods over different periods, while Table 2.1 is a summary of a comparison of desalination methods.

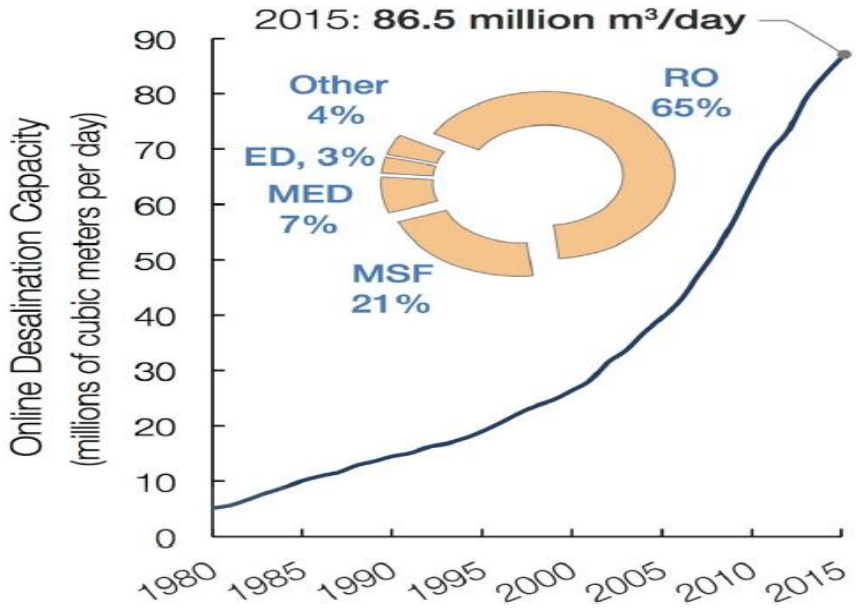

Fig. 2.10a Total desalination unit capacity (worldwide) 1980-2015 [1].

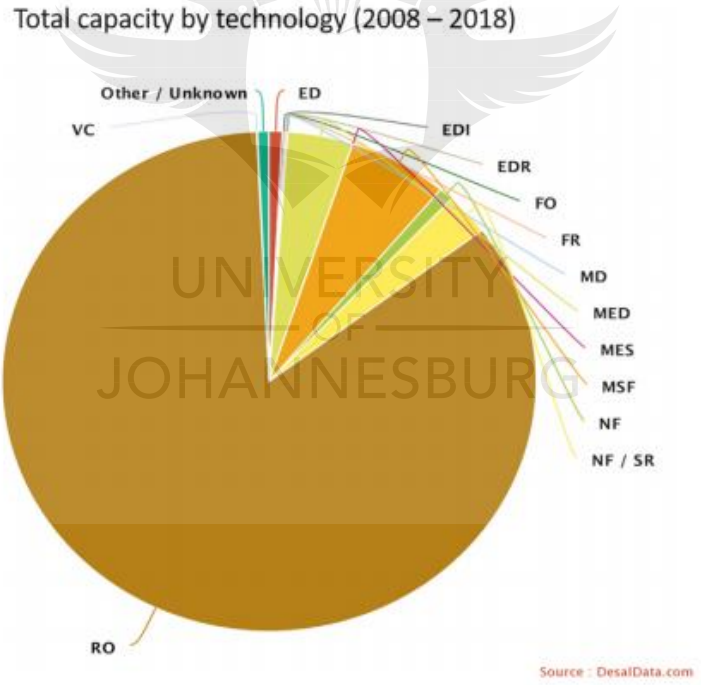

Fig. 2.10b. Global installation capacity of desalination methods 2010-2018 [94].

Table 2.1: Summary of comparison of desalination methods [31,58]

Desalination processes	Methods of desalination	Energy consumption	Merits	Demerits	Ref.
Thermal Processes	HDH		➢ It requires relatively cheap materials for its simple arrangement and can use low-grade thermal energy to reduce the carbon footprint.	➢ It has a higher requirement than the MED, MSF and membrane methods. ➢ Challenges in scaling up the energy requirement.	[24] [25]
	MSF	19.58-27.25 kWh/m^3	➢ More efficient than RO for high total dissolved solids. ➢ Simple operation and management.	➢ Higher energy requirement than membrane methods and MED. ➢ Lower water recovery than RO. Operation is usually less than 60% of capacity. ➢ Releases hot brine into the environment.	[95] [96] [97]
	VCD	7-12 kWh/m^3 for MVC and 16.26 kWh/m^3 for thermal vapor compressor	➢ It generates required heat from the compressor. ➢ Less energy required compared to MFS and MED.	➢ Less cost-effective compared to MFS and MED as VCD capacity is quite small. Hence, best used as a hybrid with other methods.	[39] [92]
	FD		➢ Low operating pressure and maintenance cost. ➢ High values of water flux, permeate flux and water recovery rate.	➢ Probability of hydrate formation and water contamination by the refrigerant.	[89] [90]
	MED	14.45-21.35 kWh/m^3	➢ More efficient than RO for high total dissolved solids. ➢ Effective for utilization of waste heat.	➢ Higher energy requirement and lower water recovery than membrane methods. ➢ Releases hot brine into the environment.	[92] [93] [94]
Membrane Processes	ED	2.64-5.5, 0.7-2.5 kWh/m^3 at low TDS	➢ Compared to thermal methods, ED has a lower energy requirement and capital cost. ➢ Compared to RO: no external pressure is required other than electrical potential deference. ➢ Higher water recovery and less membrane fouling and scaling due to RED.	➢ Cost-effective only for brackish water. High cost and short electrode life span due to corrosion. ➢ Removal of charge solute only. High saline water recirculation to obtain required freshwater	[54] [55] [58]
	CDI		➢ It requires only little maintenance compared to other methods of desalination. ➢ It does not require use of chemicals or pressure-pump. Electrodes are stable and less fouled compared to membranes.	➢ High cost and short electrode life span due to corrosion. ➢ Removal of charge solute only.	[65] [69] [72]

			➢ It has a high energy rate recovery depending on the condition of operation.		
	MD		➢ Can treat feed water with high total dissolved solids close to 200 000 mg/l. ➢ It has less membrane fouling than RO and a simple plant design. ➢ It has a high rejection rate and can use waste heat	➢ Low water recovery and water flux with a probability of membrane wetting. ➢ Lack of specific membrane. ➢ It requires both electrical and thermal energy.	[73] [74] [78]
	RO	4-6 kWh/m^3 for SWRO and 1.5-2.5 kWh/m^3 for BWRO	➢ Compared to thermal methods, it has low energy requirement, high water recovery, low capital and operating cost and no thermal pollution. ➢ Compared to other membrane methods, RO has a low-price membrane.	➢ High external pressure, membrane scaling and fouling. ➢ Brine contains used chemicals that can have a negative impact on the environment.	[79] [93] [94]
	FO		➢ No external pressure required, only osmotic pressure difference and flow resistance in the membrane module. ➢ Lower energy requirement, membrane fouling and higher water recovery than RO and thermal methods. ➢ High rejection of the different types of contaminants.	➢ The flow rate is lower than RO. ➢ It requires a concentrated draw solution, which requires easy separation. ➢ High cost as a result of freshwater extraction and draw solution regeneration and control system to prevent cross-contamination between feed and draw solution.	[85] [98]
	NF	3.35 kWh/m^3	➢ It requires lower operating pressure than RO. High water recovery, permeate flow rate with a large volume of feed handling in a continuous manner. ➢ No heating, cooling, or mechanical stirring of feed is required. ➢ Preferably, it can be used as a pre-treatment unit in a hybrid method	➢ Rejects solute selectively based on charge and size, unlike RO, that rejects all solutes. ➢ Short membrane life span. ➢ It is not adequate for seawater desalination.	[86] [88]

Table 2.2: Hybridization of RO and other methods of desalination

Hybrid Methods	Performance indicators	Limitations	Ref
HDH-RO	Improvement of brine recirculation temperature to be higher than the system make-up temperature. Reduction of energy requirement by HDH standalone.	17.5% increase in the total investment cost of the RO unit.	[99] [100] [101]
MSF-RO	Generation of electrical energy and freshwater using co-generation power desalting plants.	Complexity of operation	[33][102] [103][104]
TVC-RO	Improvement of SEC and production ratio.	Possible limited distribution ratio as a result of inadequate supply of feed water by TVC to RO unit.	[46]
MED-RO	Quality water production, high recovery ratio, minimization of energy consumption and RO brine treatment.	Dependent on the quality of steam used. Scale formation on heat exchanger surface	[105] [106][107]
RO-ED	Brine minimization and salt production	Priority may shift to salt production	[108][109]
RO-CDI	High-quality water production	Time of charge and discharge of the CDI cell.	[110]
RO-MD	Treatment of brine	Fouling and membrane wetting are critical problems resulting in reduced flux.	[104][111] [112][113]
FO-RO	Treatment of brine and wastewater for reuse	Difficulty in the recovery of draw solute after FO treatment of the RO brine.	[104] [114]
RO-NA	Enhancement of water quality, reduction of RO pressure and energy requirement.	Increased complexity and cost with the use of more membrane.	[79][115]
RO-FD	Brine treatment and management.	Nucleation control within FD unit.	[89][116]

2.2 Renewable Energy Sources for Desalination

The high energy requirement of the thermal process of desalination and the consequent environmental impact of the conventional energy sources used to power the thermal methods have made the membrane process powered by RES more dominant and prevalent. However, it is not quite easy to determine the most appropriate RES for a desalination method considering the efficiency and varieties of both RES and desalination methods. According to [1], the choice of RES for desalination is a function of several variables, such as desalination plant size, location, feed pressure and characteristics and expected cost of production of freshwater. The limitations of the use of RES are the inherent characteristics of low intensity and intermittency of some of the RES. These challenges can be minimized or even eliminated by integration into the grid, hybridization and usage of energy storage systems or batteries. Figure 2.11 depicts the possible integration of RES with desalination methods, as presented by reference [1].

Some of the RES available and considered for integration with the desalination system are discussed in the next subsection.

2.2.1 Geothermal Energy

Geothermal energy is the heat source from beneath the earth's surface, either in the form of hot water or steam or even a mixture of both. This form of RES is categorized based on the temperature range; in other words, the enthalpy range: (i) Low temperature (range below 150^{o}c), and (ii) High temperature (higher than 150^{o}c) [38]. It is one of the most stable and environmentally friendly RES. It provides consistent heat flux, making it very reliable. It does not depend on weather variations and its operating cost is quite low. These attributes justify the merit of geothermal energy, making it very suitable for desalination. The major limitation is the high cost of power

plants. It is also constrained by limited location for its activity [1]. The direct supply of heat energy from the geothermal plants makes it more applicable to thermal desalination processes. The application of geothermal energy to power HDH and MD in Tunisia was reported in [117] and [118], respectively. Energy can also be converted to mechanical and electrical power for use in membrane desalination processes. In RO, for instance, the mechanical energy is used in the pressure pump, which generates the pressure required to get the feed water across the membrane. The lower the temperature of the feed water, the more the viscosity and the more pressure is needed for the RO process and, consequently, the more energy it consumed. With RO having temperature tolerance ranging from 20-35^{o}C, geothermal waters with appropriate high salinity and temperature can serve as feed water to produce freshwater. This can help augment the mechanical energy required to pump cold water during winter [119]. A techno-economic analysis to compare the production cost of freshwater using geothermal energy with MED and RO methods of desalination was presented by [120]. It was concluded that the RO method is relatively more cost-effective than MED for seawater desalination in Gulf countries.

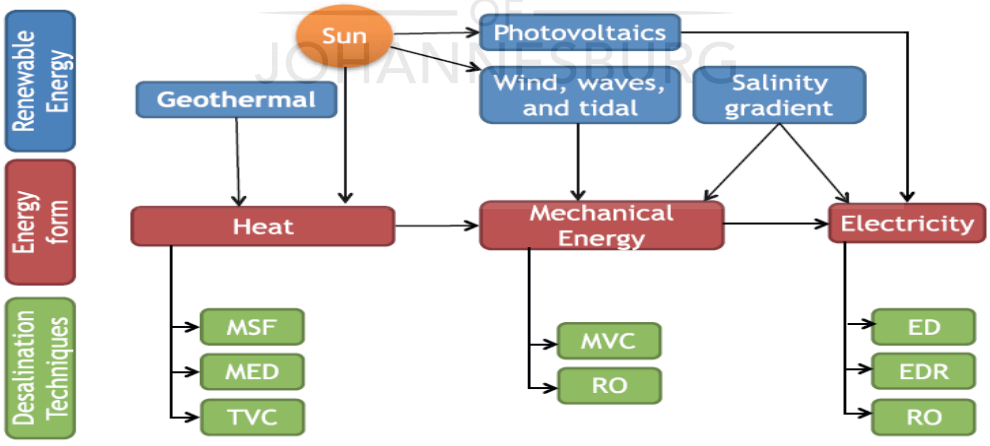

Fig. 2.11. Possible integration of renewable energy sources with desalination methods [1].

2.2.2 Ocean Energy

Ocean energy involves the harnessing of energy from the ocean in thermal, mechanical, or chemical form. It is considered a more stable RES compared to wind and solar energy because of its higher energy density and lower intermittency [121]. The commonly used ocean energy is the mechanical energy of a wave, tide or current, mainly converted to electrical energy by using energy converters [122].

2.2.2.1 Ocean thermal energy

Ocean thermal energy involves the sourcing of heat energy already absorbed from the sun by the ocean and stored on its surface. The thermal energy from the ocean is then a result of the temperature difference between the deeper levels and the surface of the ocean heated by the sun. According to [123], D'Arsonaval, a French physicist, first proposed the harnessing of ocean thermal energy in 1881. This form of ocean energy can be sourced by the ocean thermal energy conversion (OTEC) cycle. According to [124], the application of a thermal form of ocean energy is more straightforward using the thermal process of desalination but is still at the research and development phase, with the limitations of high up-front capital cost and the requirement of a large seawater pump and piping system. The experimental design of a desalination process to produce freshwater from brackish water using ocean thermal energy was reported by [125]. The result shows an adequate increase in freshwater production. Authors [126] analyzed dual-use open-cycle OTEC to determine the performance of the system in power generation and seawater desalination. It was concluded that the low water feed rate determined the pumping costs and production rates. Using ocean thermal energy, [127] performed an exergy analysis of a system of siphon ash

evaporation desalination. The experimental result deduced that lower surface seawater, higher deep seawater and higher ash achieved enough efficiency.

2.2.2.2 Ocean mechanical energy (wave, tidal and current energy)

Ocean mechanical energy is subdivided into wave, tidal and current energy. Similar to wind energy generation, hydrokinetic devices such as turbines are used for harnessing ocean mechanical energy. The pressure created by this form of ocean energy can be directly applied to pressure-driven desalination processes. This will minimize the cost and energy requirements of such a desalination process. Several researchers support ocean mechanical energy applications to the RO desalination method, since it is easy to use both mechanical and electrical energy to drive the RO process. In [128], ocean mechanical energy was deployed to the RO system for co-generation of electricity and desalination.

Wave energy is generated by energy transfer from the wind that blows across the surface of the ocean, causing a ripple movement of the surface water. Authors [116] and [129] evaluate the techno-economic analysis of wave-powered RO desalination, employing a water hammer and hydro-ram, respectively. The systems show the feasibility of applying direct pressure adequate to drive the RO desalination process and offer cheaper alternatives to the conventional RO system. Moreover, [130] presented an independent wave-powered RO desalination system for energy recovery.

Tidal energy is generated by a swift rise and fall of water bodies creating a pressure difference, which in turn generates mechanical energy that can be converted to electrical energy. The swift rise and fall of water bodies is influenced by the gravitational force of attraction between the earth, moon and sun and the rotation of the earth and that of the moon around the earth. Authors [131] proposed an RO desalination system using tidal energy, with the result indicating a 31-41.7%

reduction in water production cost and 40% water recovery rate compared to traditional RO systems. The tidal-RO feed pressure influences the cost reduction. The decline in cost is also expected to appreciate over the life span of the plant.

Current energy is generated by the movement of water bodies in a specific direction, usually influenced by the topography of the ocean, temperature and salinity difference of the water. This form of ocean energy is yet to be extensively explored in terms of research and application to water desalination. The possible application of ocean energy to RO desalination in South Africa was estimated by [132]. It was concluded that the RO plant powered by ocean current energy cannot always supply enough freshwater as a unit to meet the demand of the population. This is a result of deficient water speed at specific periods.

2.2.2.3 Ocean chemical energy (salinity gradient energy)

One of the biggest challenges with the deployment of either thermal or mechanical ocean energy to the desalination process is the requirement for redesigning the desalination plants, especially the feed inlet section of the plants [133]. This modification increases capital costs. The chemical energy (blue energy) for seawater desalination does not require any form of modification to the conventional desalination process. This form of ocean energy is harvested from the mixture of two sources of water, usually seawater (high saline water) and river-water (low saline or freshwater) with different salinity gradients under controlled conditions [134]. According to [134] and [135], an estimated 2.4 to 2.6 TW of salinity gradient energy is available globally, which almost equals global electricity consumption. The salinity gradient of the two forms of water supply creates an osmotic pressure difference between them, which serves as the driving force for the membrane desalination process. The extraction of salinity gradient energy in the form of electrical energy for desalination can be obtained in RED and in the form of mechanical energy, it is extracted in

pressure retarded osmosis (PRO) [61] and [136]. The application of ocean chemical energy to the RO desalination system is still to be extensively explored. Details of the developmental status of ocean energy are reported in [123], [137] and [138].

2.2.3 Wind Energy

Wind energy involves the harvesting of the kinetic energy of air movement by using wind turbines and converting such kinetic energy into mechanical and subsequently to electrical energy. Wind energy is relatively cheap and highly environmentally friendly. The major limitation of wind energy is its intermittent nature, which affects the consistent production of power. To mitigate this challenge, options such as its integration with storage systems, the grid, or hybridization with another RES have been suggested and implemented [139]. Wind energy is one of the most commonly used RES to power desalination, second only to solar energy. The use of wind energy to power desalination cuts across different methods of desalination and, in some cases, involves hybridization of desalination methods or with another RES. The most common method of desalination power by wind energy remains the RO method.

The technical and economic feasibility of wind-powered RO and MVC desalination was confirmed in [140], while [129] evaluated the effects of wind intermittency and fluctuation on the RO system and proffered three possible solutions: integration of energy storage, a hybrid energy system, or matching of RO capacity with transient energy supply. Authors [141] presents a techno-economic investigation of RO systems for a strategic aquifer storage and subsequent recovery (ASR) scheme as a measure to reduce the cost of water desalination for the Gulf Council Cooperation countries. An ASR project in the United Arab Emirates was used as a case study. The feasibility of the scheme was confirmed but avoiding shut-down of variable load by RO plant mitigate the effective use of unstable wind power, leading to plant capital cost. A wind-powered RO system for the

Canary Islands with the aim to quantify the unit cost of freshwater as well as analyzing the exergy efficiency of the system was presented in [142]. The result shows the unit cost of freshwater to be 76 c€/m^3 and the exergy efficiency of RO to be higher than that of wind power. Authors [143] discussed the economic analysis of the RO system powered by wind compared to conventional energy sources using the levelized cost of freshwater as the main parameter. Wind-powered RO shows lower levelized cost of freshwater production.

2.2.4 Solar Energy

Solar energy involves the harvesting of energy from the sun using either solar collectors or semiconductors present in photovoltaic (PV) cells. The sun provides heat and light, which can be harnessed to generate thermal energy and electrical energy, respectively. Therefore, solar energy can be classified into solar thermal (ST) and PV [144]. Both forms of solar energy can be used to power a desalination process either as stand-alone method or in hybrid use with another RES. Like wind energy, the major limitation of solar energy is its intermittent nature, which can also be minimized or dealt with through hybridization and storage systems.

2.2.4.1 Solar thermal-powered desalination

The solar thermal system consists of a solar collector that is used to collect or absorb radiation from the sun. In the absorber of the solar collector, the solar energy received is converted into heat energy, which is then transferred to fluid passing through the absorber [139]. This heat energy can be applied directly to power thermal desalination processes or otherwise applied indirectly to power membrane processes by converting from heat energy to either mechanical or electrical energy. An assessment of critical determinants of market opportunities for solar thermal-power desalination shows that a dish concentrator integrated with micro-gas-turbines is a viable and

promising alternative to PV-RO in the case of limited water demand [145]. Developments in the use of solar energy and advancement in its design for application with water desalination revealed that, despite many design enhancements for improving productivity, available designs are yet to be made suitable for large-scale production of freshwater [146]; [147]; [148].

The application of concentrated solar power (CSP) to power RO is a form of indirect application of the solar thermal system to the desalination process, which has become a suitable option. CSP technology involves using the steam ORC, dish-Stirling and other types of turbine and engine to convert high temperature heat extracted by a controlled concentration of solar radiation on a glass mirror to either mechanical or electrical energy [149]. CSP technologies are classified into four [38], namely dish engine, Fresnel mirror reflector, power tower and parabolic trough, which is the most efficient of the four. MED and RO are the most suitable desalination methods powered by CSP [38]. Figure 2.12 depicts the CSP-RO system. The major drawback of the application of the solar thermal system to desalination is the cost of the energy conversion unit, its installation and operation [94].

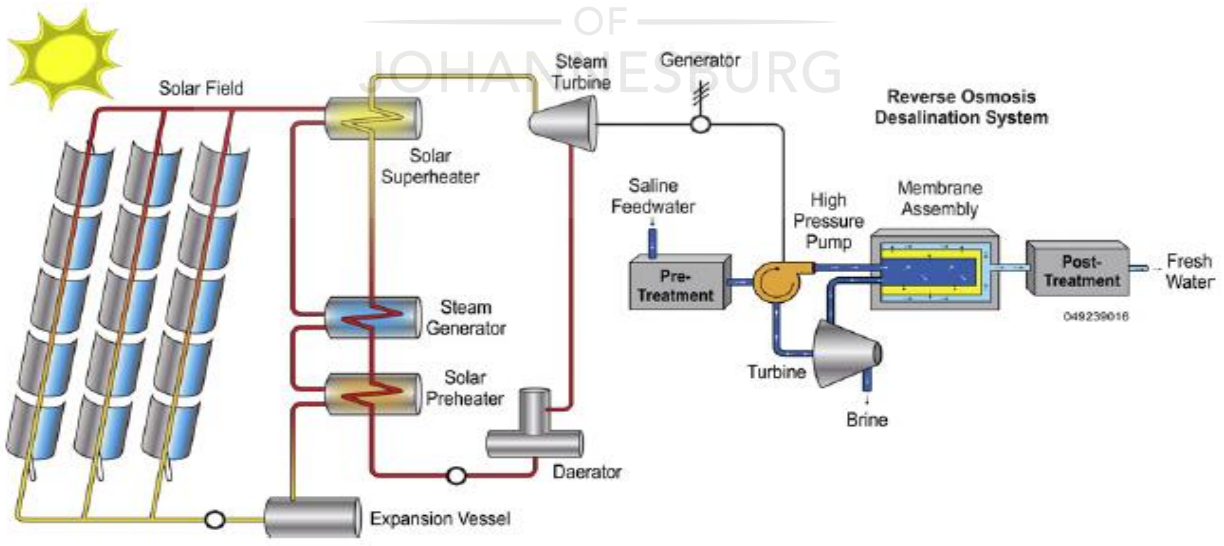

Fig. 2.12. Schematic diagram of concentrated solar power-reverse osmosis desalination [38]

2.2.4.2 Photovoltaic-powered desalination

A solar PV energy system is built on the principle of conversion of sun radiation or light to electricity via apparatus with a 'PV effect.' The PV effect is the indication of voltage difference as a result of light shining on systematically arranged electrodes with a solid or liquid between them [150]. A solar PV system, therefore, involves the use of solar panels of various layers to capture photons, which provides enough energy to activate the release of electrons from atoms in the semiconductor [144]. This process generates electric current as electrons flow from positive to negative electrodes. Based on the intermittent nature of solar irradiation, batteries are usually used for storage in the PV system. Figure 2.13 represents a schematic representation of the PV-RO desalination system.

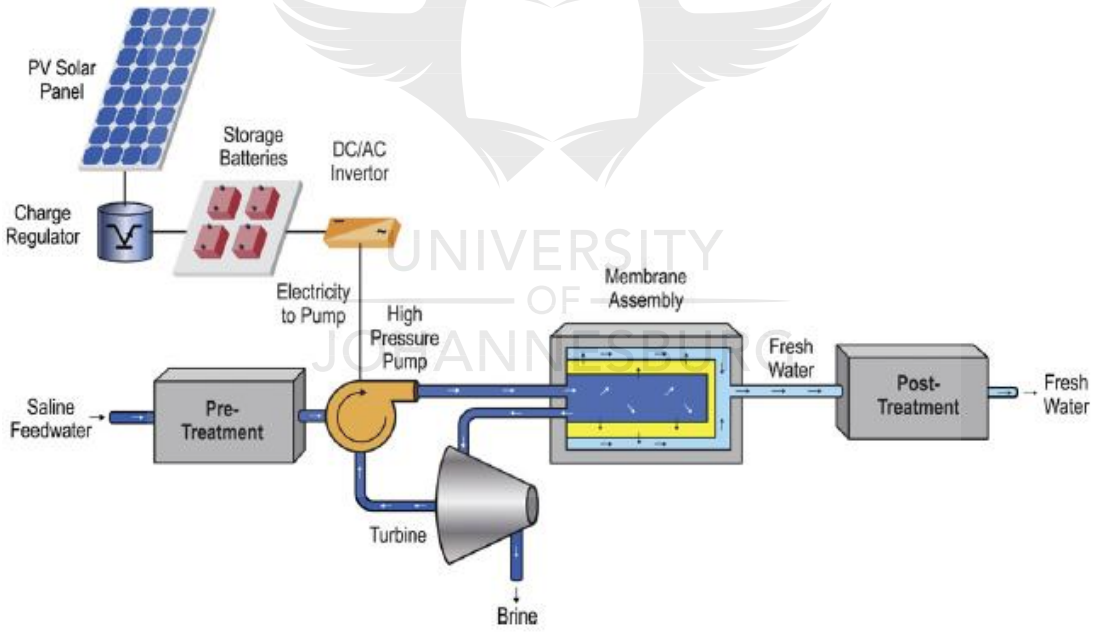

Fig. 2.13. Schematic diagram of Photovoltaic-reverse osmosis desalination system [38]

Research and application of PV energy to desalination have been focused more strongly on the RO method, since RO requires electrical energy to drive it and has become the most dominant method of desalination. This, interestingly, has made PV-RO the most investigated and installed RES

indirect solar-powered desalination method, as depicted in Figure 2.14 [151]. Authors [152] categorized publications on PV-RO based on the main concept of reviewed papers into four: effect of parameters on PV-RO system performance, economic evaluation of the PV-RO unit, modification of the PV-RO system and hybridization of PV-RO with another RES or a desalination method. An extensive summary of studies on PV-RO was made. The main aims of most reports on the effect of parameters on PV-RO system performance are to investigate areas of parameter modification for economic efficiency and adaptability to the minimized limitation of location [153] and [154]. PV-RO modification aims at the improved performance of the system to produce sufficient freshwater at a low cost [155]. The hybridization of PV-RO with other RES or desalination methods eradicates the limitation of both PV and RO [156]; [157]. Authors [158] and[159] report an economic evaluation of PV-RO with the aim of reducing freshwater production cost.

2.2.5 Hybrid RES for Desalination

To eradicate limitations of different RES, several studies have suggested the implementation of hybrid RES. The hybrid system improves reliability, as each RES compensates for the weakness of the other, thus improving the economic efficiency and environmental impact of the system [160]. When a conventional energy source is hybridized with RES such as wind and solar, the conventional energy source compensates for the intermittency and high cost of the RES. At the same time, the RES reduces the negative impact of conventional energy sources on the environment [19]; [161]. On the other hand, different RES can be hybridized for cost-effectiveness and effective performance of the system, based on the location and availability of RES [100]; [105]; [110]. RES can also be combined with energy storage systems such as capacitors, batteries and hydrogen storage to mitigate intermittent and variable irradiation [162]; [163]; [164].

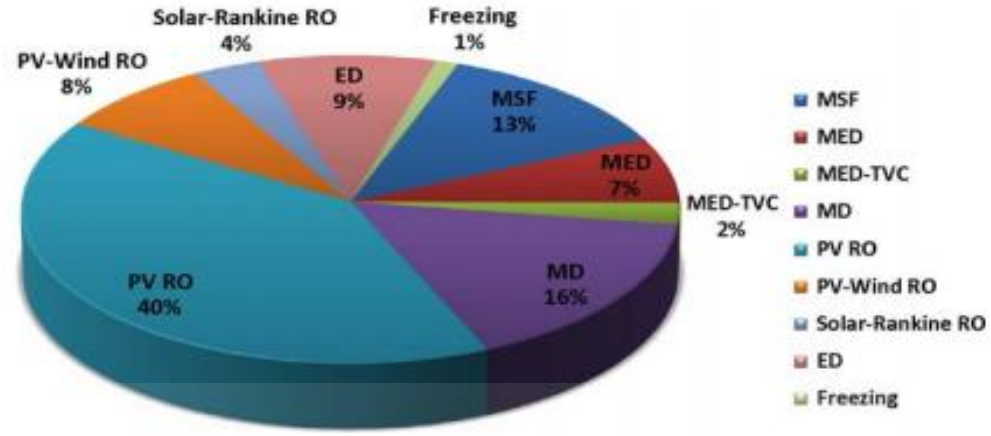

Fig. 2.14. Worldwide share distribution of installed indirect solar-power desalination plant (2011) [151].

2.3 Optimization of RES-RO Desalination System

System optimization is the minimization or maximization of certain system parameters to enhance the overall system performance by the selection of the best possible variable that satisfies the system constraints. Optimization problems are classified based on (i) The nature of design variables: static or dynamic (parameter or trajectory), (ii) Existence of constraints: constrained or unconstrained, (iii) Physical structure of the problem: optimal control or non-optimal control, (iv) The type of equation formulated: linear programming (LP), nonlinear programming (NLP), quadratic programming (QP) or geometric programming, (v) Permissible values of design variables: integer programming (IP) or non-integer programming, (vi) Separability of functions: separable or non-separable programming, (vii) Deterministic nature of variables: stochastic (with no certain variables) or deterministic (with known parameters or variables), and (viii) Number of objective functions: single or multi-objective problems [165]. Optimization of RES-powered desalination is mostly a combination of different optimization problems, usually constrained,

deterministic, nonlinear and optimal control. The complex nature of the combination of these optimization problems requires careful selection of the appropriate optimization techniques as a tool for solving the problems. Optimization solution techniques can be classified as in Figure 2.15, into mathematical, also known as classical or analytical optimization techniques, and artificial intelligence (AI) techniques, which are either heuristic or meta-heuristic techniques [166].

The classical techniques use selected mathematical approaches, such as gradient information of functions, to solve optimization problems. These methods are well known for their ability to obtain the exact solution of a linear or convex optimization problem. However, it is difficult to obtain an optimal solution to nonlinear or nonconvex problems. On the other hand, AI techniques have become very prominent in solving optimization problems. AI algorithms are integrated into computer-aided heuristic solvers, which provide an optimal solution using the iterative approach. Metaheuristic techniques thus have the advantage of fast computation, but solutions are approximate and not exact [167].

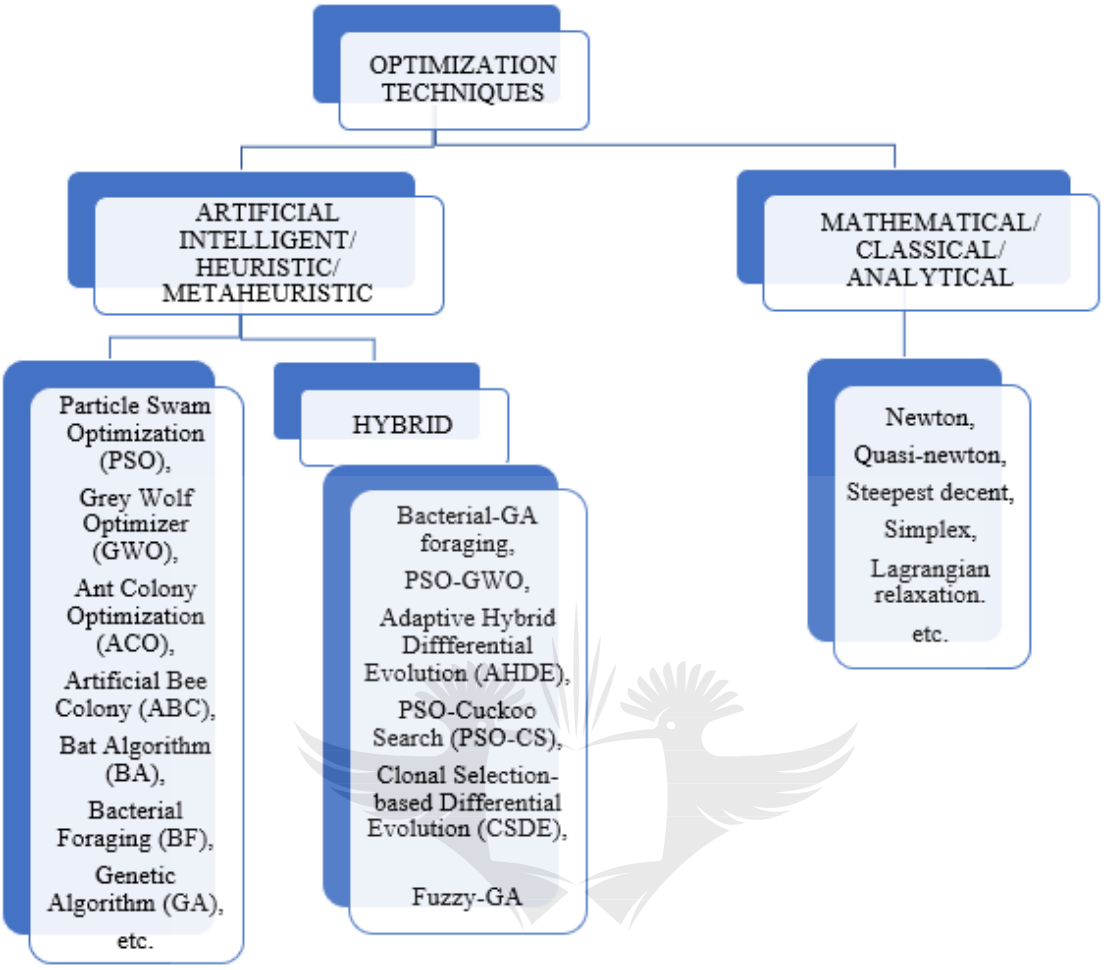

Fig. 2.15. Classification of optimization solution techniques

Every optimization problem has an objective function. The achievement of an objective is ascertained and evaluated by some performance indicators. The performance indicators, therefore, determine the formation of an appropriate optimization problem. In the case of RES-powered desalination optimization problems, the performance indicators mostly used in the formation of objective functions are (i) Energy requirement and consumption by the desalination process, (ii) Cost of production of freshwater using different cost matrices, (iii) Permeate flux rate, (iv) Volume of the freshwater output, (v) Brine handling and treatment, (vi) Environmental impacts of both energy sources and the desalination process, (ii) System reliability, and (viii) The life span of the system to be optimized. Therefore, the best optimal desalination system will be one with very low

energy requirements and consumption, a high permeate flux rate, a large volume of freshwater production, low risk of environmental impact, a long life span and minimal cost of production. In practical application, achieving the best of all these performance evaluations in a system simultaneously might be difficult, given some physical and technical constraints. However, optimizing a desalination system to achieve one of the performance indicators will be solving a single objective optimization problem. In the case of a combination of more than one performance indicator, a multi-objective optimization problem will be formulated and solved. In any case, the system is expected to yield better performance within its physical and technical constraints. The stochastic nature of some RES is of great concern, hence the need for reliability checks for adequate performance in a RES-RO desalination system. Reliability indicators such as loss of power probability, loss of load probability and expected energy not supplied can be used to evaluate the system reliability [168], while different cost matrices are used to assess the economic viability of a RES-RO desalination system. Some of the applied cost matrices are system total cost, total annualized cost of the system (ACS), LCOE, net present cost, and total life cycle cost. Table 2.3 contains the mathematical representation of performance indicators, including different cost matrices and reliability indicators.

Table 2.3: Simplified mathematical model of some performance indicators

Performance indicators	Cost matrices	Mathematical equations	Ref.
Economic indicators	Capital Recovery Factor	$CRF = \left[\frac{i(i+1)^n}{(i+1)^n - 1}\right]$	[169] [170]
	System Total Cost	$STC = C_{capital} + C_{operation} + C_{maintenance} + C_{installation} + C_{replacement}$	[168] [171]
	Total Annualized Cost of the System	$ACS = C_{capital}(CRF) + C_{replacement}(CRF) + C_{maintenance}$	[168] [172]
	Levelized Cost of Energy	$LCOE = \frac{ACS + energy\ consumption\ cost}{annual\ energy\ production}$	[173] [174]
	Net Present Value	$NPV = \sum_{n=1}^{N} \frac{investment\ in\ year\ n\ Q_n}{(1 + return\ rate\ r)^n} - 1$	[6][168]
	Life Cycle Cost	$LCC = \sum_{n=1\ldots N}^{N} NPV$	[6][175] [176]
	Cost of Water Production	$COW\left(\frac{\$}{m^3}\right) = \frac{\left(\frac{Investment\ cost}{CCRF}\right) + Cost\ of\ opration\ \&\ man}{volume\ of\ water\ /year}$	[17] [169]
	Gas Emission Cost	$GEC\left(\frac{\$}{m^3}\right) = Electricity\ requirement\left(\frac{kWh}{m^3}\right) \times Emission\ factor\left(\frac{kgCO_{2-e}}{kWh}\right) \times Carbon\ tax\left(\frac{\$}{kgCO_{2-e}}\right)$	[17]
Reliability indicators	Specific Energy Consumption	$SEC = \frac{power\ consumed\ by\ pump\ (W_{pump})}{permeat\ flux\ rate}$	[177] [178]
	Loss of Power Supply Probability	$LPSP = \frac{\sum_{t=1}^{T} power\ not\ supplied\ (t)}{\sum_{t=1}^{T} E_{load}\ (t)}$	[168] [176]
	Loss of Load Probability	$LLP = \frac{\sum_{t=1}^{T} \begin{cases} 0, L(t) > P(t) \\ 1, L(t) \leq P(t) \end{cases}}{T}$	[168]

Recent studies have presented some application of optimization models to improve the RO desalination process. The review of some of these studies will be based on three optimization approaches, namely system sizing, operational optimization and thermodynamic optimization. These three optimization approaches are based on the main concepts as gleaned from reviewed literature. The next subsections detail some of the applications of the three optimization approaches to RES-RO systems.

2.3.1 System Sizing Optimization

System sizing involves the optimal design of considerable system capacity within the constraints of the system components' limitations. Authors [8] designed and modeled the sizing of six grid-independent hybrid renewable systems: solar-battery, solar-hydrogen, wind-battery, wind-hydrogen, solar-wind-battery and solar-wind-hydrogen, to power RO desalination systems, each with the objective of minimizing total life cycle cost using an improved bee algorithm and compared with a harmony search algorithm. It was concluded that the hybridization with battery energy storage is more cost-effective than hydrogen energy storage, while the solar-battery power RO unit proved to be the most cost-effective energy system of the six. A grid-connected RES-RO desalination plant in New Borg El-Arab city of Alexandria, Egypt, was optimized by minimizing total investment cost and CO_2 using a hybrid of particle swarm optimization and the Grey Wolf optimizer (PSO-GWO) [19]. The result also shows that battery storage is more cost-effective than the hydrogen storage system and the hybrid PSO-GWO proved to be more effective than either PSO or GWO. Authors [171] designed an optimal desalination model powered by PV and wind energy for a small community and a residential household to determine the optimal number and type of system units at minimal total cost using a genetic algorithm (GA). Table 2.4 contains a summary of sizing optimization models under review.

Table 2.4: Summary of sizing optimization models of RES desalination plants.

Objective function	Constraints	Optimization techniques	Outlook	Ref.
Minimization of total life cycle cost	Inequality constraints: bound limit of area of PV, area of wind turbine, number of hydrogen and battery storage systems, energy stored and battery state of charge. Equality constraint: Loss of power supply.	Improved bee algorithm compared with harmony search (HS) algorithm	The hybridization of a solar power, battery and RO system is considered the most cost-effective system compared to five other configurations.	[176]
Minimization of total life cycle cost	Inequality constraints: bound limit of area of PV, area of wind turbine, number of hydrogen and battery storages, energy stored and battery state of charge. Equality constraint: Loss of power supply.	HS algorithm and HS-based chaotic search (HSBCS)	Proposed HSBCS yields a better result than HS algorithm	[6]
Minimization of total life cycle cost	Inequality constraints: bound limit of area of PV, area of wind turbine, number of hydrogen and battery storage systems, energy stored and battery state of charge. Equality constraint: loss of power supply.	Artificial bee swarm optimization (ABSO)	ABSO proves effective. The hybrid system led to a cost-effective system for different maximum loss of power supply probability (0-100%).	[7]
Minimization of total life cycle cost with loss of power probability as reliability index.	Inequality constraints: bound limit of area of PV, area of wind turbine, number of hydrogen and battery storage systems, energy stored and battery state of charge. Equality constraint: loss of power supply.	PSO, ABSO, simulated annealing (SA) HS, chaotic search (CS), Tabu search algorithm.	The hybrid metaheuristic improved harmony search-based chaotic simulated annealing yielded a better result than eight other metaheuristic algorithms, while ABSO yielded the worst performance.	[175]
Minimization of total investment cost and CO_2 emissions.	Inequality constraints: bound limit of numbers of PV arrays, wind turbines, hydrogen tank and battery storages, electrolyzer, inverters, fuel cell and capacity of RO plant and water tank. All are ≥ 0. Renewable factor (FR) $\geq$ 70%. Limit of diesel output power generation.	Hybrid PSO-GWO	The result also shows that battery storage is more cost-effective than the hydrogen storage system and the hybrid PSO-GWO proved more effective than either PSO or GWO.	[179]

Determination of the optimal configurations of the hybrid system at a minimal cost.	Inequality constraints: the state of charge of hydrogen storage. Equality constraints: power balance and water flow balance equations.	A new optimization iterative algorithm was formulated using MATLAB software	The formulated method can be applied to any desalination method. The result shows improvement in energy supply reliability and reduced energy storage requirements and consequently reduced system installation cost.	[180]
Determination of the optimal number and type of system unit at minimal total system cost.	Inequality constraints: bound limit of numbers of PV modules, wind power generation blocks, battery storage systems, RO plant and PV tilt angle.	GA	The overall configuration is profoundly affected by the capital cost. The hybrid of PV and wind generator is more cost-effective than PV or wind standalone.	[171]
Minimization of excess energy at minimal cost	Operating reserve of 10, 15 and 25% of the load demands, output wind and solar power, respectively.	An optimization algorithm was developed to select the best combination of hybrid RES.	The impact of the optimization method on the unit cost of energy and, consequently, the unit cost of desalinated water was demonstrated.	[181]
Minimization of total capital cost (capital + operational cost)	Daily state of tank and maximum permeable depth of battery discharge.	GA	Only an economic estimation of power provided by RES was presented using HOMER. The hybrid of PV, wind and battery shows significant improvement of the system.	[182]

2.3.2 Operational Optimization

The RO desalination system can be optimized by reconfiguration or adjustment of some components of the system to achieve optimal performance. In most cases, operational optimization studies are based mainly on performance analysis of the system without much consideration of the size. The levelized unit cost of water and electricity for a wind-powered seawater RO system in Gokceada Island, Turkey, was evaluated in [174]. A reverse osmosis system analysis (ROSA) model was used to predict an optimal levelized cost for the system, determine the energy requirement and analyze emission reduction. The result shows the predicted levelized cost of water to be between 2.96 $/m^3 and US $6.457 $/m^3 for the system's energy requirement with a capacity

range of 6 kW to 30 kW and 0.077 $/kWh to 0.155 $/kWh for the levelized cost of electricity using a 30 kW wind turbine at 8% discount rate based on the turbine's specific cost. With a 30 kW wind turbine for RO, the result predicted 80.028 tons of CO_2 emission reduction annually. The feasibility of using water and hydrogen as double storage for a continuous supply of energy and water from a PV-wind powered RO system at a minimal cost was evaluated in [183]. The system optimization was performed using the hybrid optimization model for electric renewables (HOMER) and ROSA. The technical feasibility and reliability of the system were confirmed, and a significant reduction in CO_2 was also achieved. Using formulated mixed integral linear programming (MILP), [184] presents the hybridization of PV and CSP-ORC to power MED-RO with the objective of minimization of unit operational cost. A rolling horizon approach coupled with a 24-h unit commitment problem formulated as MILP shows accuracy and speed. The hybrid system improves reliability and sustainability. More operational optimization of RES-RO systems is summarized in Table 2.5.

Table 2.5: Summary of operational optimization of RES-desalination systems.

Objective function	Constraints	Optimization techniques	Outlook	Ref.
Evaluation of economic analysis of the system using a levelized cost matrix and determination of energy requirement.	Physical properties of the system components and year of consideration.	HOMER and ROSA	Seven hybrid RES configurations were evaluated; wind-PV-diesel was considered a better option.	[170]
Evaluation of the levelized unit cost of electricity and water (LCOE and LCOW), determination of energy requirement and emission reduction.	Physical properties of the system components and year of consideration.	ROSA	Significant reduction of emission.	[174]

Minimization of critical excess of electricity production (CEEP) and the highest possible share of RES in the mix	Inequality constraints: storage capacity and allowable RES. Equality constraints: power balance equation.	An optimization algorithm was developed to select the best combination of hybrid RES.	Increasing the optimization horizon from 1 to 24 h can reduce the CEEP by 80%.	[185]
Determination of feasibility of supplying both energy and water from RES at a minimal cost	Power balance equations.	HOMER and ROSA	The technical feasibility and reliability of the system were confirmed, and CO_2 was reduced.	[183]
Minimization of total system cost (cost of power generation + cost of desalination)	Inequality constraints: power and desalination limits. Equality constraints: power balance equation.	Proposed MILP	Significant economic saving. The flexibility of the desalination unit can be advanced by the addition of DR programs, making room for frequency regulation or spinning reserve products.	[186]
Minimization of energy cost in water supply network.	Inequality constraints: pressure head, water tank capacity limits. Equality constraints: water flow balance equation and mass conservation equation.	Formulated an optimal water flow model	Adaption of proposed optimization model and integration with metaheuristic techniques are recommended for implementation in water network with demand uncertainty, considering DRs.	[187]
Minimization of total annualized production cost while maximizing the percentage of RES in the total power production and minimizing wind power curtailed.	Inequality constraints: water reservoir capacity limits. Equality constraints: water flow balance and power balance equations.	Direct multi-search	Increased penetration of RES and reduction of emission at a minimal cost.	[172]
Minimization of unit operation cost	Technical limits of components, spinning reserve requirements and efficiency curves at part load operation.	Formulated MILP	Fast and accurate solution to the formulated MILP problem.	[184]
Minimization of freshwater cost of hybrid MED and RO system	Operational parameters of RO unit, seawater salinity of MED and freshwater salinity of RO-MED	Sensitivity analysis	The optimal feed pressure and feed flow rate of RO and stem flow rate along temperature of MED were regarded as continuous variables of optimization. RO-MED proved cost-effective.	[169]

Minimization of SEC, total dissolved solids of permeate (D_{TDS}) and maximization of permeate production rate.	Limits of trans-membrane pressure and total dissolved solids of permeate.	GA	The multi-objective optimization shows the practical benefit of hybrid RES with a jointly controlled module.	[178]
Maximization of permeate production rate.	Limits of trans-membrane pressure and total dissolved solids of permeate.	GA	The two-dimensional GA produced maximum permeate rate even as the proportional integral derivative failed.	[154]

2.3.3 Thermodynamic Optimization

Heat and electrical energy transfer and their relationship to temperature and mass of water flow in RO desalination system power by RES can be used as parameters and variables for optimization of the system. The thermodynamic optimization approach often involves thermodynamic and economic analysis of the system considering energy transfer, exergy destruction and cost of freshwater production. Authors [188] investigated the exergy analysis of a 725 m^3/d RO desalination system in California. The exergy across the main components of the system was evaluated to determine the total exergy destruction of the entire system compared to that of an optimal alternative unit. The exergy analysis of the existing plant showed that more exergy destruction occurred in the membrane modules (74.07% of total exergy input) and less in the mixing chamber (0.67% of the total exergy input). In comparison, the second law of efficiency of the plant was calculated to be 4.3%, whereas the second law of efficiency of the alternative unit was increased to 4.9% by the addition of a pressure exchanger with two throttling valves on the brine stream. This optimized the system by minimizing the pump energy requirement of the input saline water and hence saved 19.8 kW of electricity. The effect of irreversibility and cost of solar ORC-RO desalination was examined with different energy recovery configurations such as basic, Pelton wheel turbine and pressure exchanger. These energy recovery devices, coupled with the

Shann El-Shiekh RO unit, show that a pressure exchanger is more economical than the basic and Pelton wheel turbine versions, with minimum exergy destruction. Reference [189] used different adaptations of the non-dominated sorting GA (NSGA-II, NSGA-II-jumping gene and NSGA-II-adapted jumping gene [NSGA-II-aJG]) to find an optimal solution to multi-objective optimization of RO desalination units. The objective functions were to minimize system cost, permeate throughput and permeate concentration with decision variables of different operating pressure, active area of membrane, type of membrane and module. The NSGA-II-aJG converges more rapidly than NSGA-II and NSGA-II-JG. Table 2.6 contains a summary of the thermodynamic optimization approach.

Table 2.6: Summary of thermodynamic optimization of RES-desalination processes.

Ref.	Objective function	Constraints	Optimization techniques	Outlook
[189]	Minimization of permeate throughput cost of desalination and permeate concentration.	Inequality constraints: permeability of membrane and permeate concentration bounds. Equality constraints: component properties and mass conservation equation.	NSGA-II, NSGA-II-JG, NSGA-II-aJG,	At highest permeability of water and salt, the maximum permeate throughput is achieved with constrained permeate concentration. The NSGA-II-aJG converges more rapidly than NSGA-II and NSGA-II-JG
[190]	Maximization of energy efficiency, exergy efficiency, desalination output, VAR cooling output and total output.	Inequality constraints: turbine pressure and steam extraction limit and desalination heated feedwater temperature. Equality constraints: energy and mass balance equations.	GA	The polygeneration system is cost-effective, efficient and considered a very good option to satisfy energy demand in the global energy transition.
[191]	Maximization of net output power and freshwater of the system using an energy recovery system for wastewater and heat.	Inequality constraints: turbine pressure and steam extraction limit, boiler outlet temperature limit and temperature difference of heat exchanger. Equality constraints: energy and mass balance equations.	GA	Heat recovery from boiler blowdown stream increased power production of a steam turbine. The water recovery unit increased freshwater production. Exergy analysis shows high exergy destruction in the boiler unit, hence requires improvement. Economic analysis indicates adequate payback time. The optimization process improves the overall performance of the system by

				improving the net power output.
[192]	Maximization of permeate volumetric flow rate.	Permeate concentration limits and allowable pressure across the membrane.	Genetic algorithm reverse osmosis (GARO)	GARO shows approximate linearity between permeate volumetric flow rate and pressure difference across the membrane. Permeate concentration decreased as the permeate volumetric flow rate and pressure difference across the membrane increased.

2.4 Research Output and Trend

The research output and trend in the area of optimization of RES-powered desalination were investigated with the aid of VOSviewer software applied to data collected from the ISI Web of Science database. The choice of this database as a source of data extraction is in consideration of it being one of the oldest databases and its broad focus on science-based research [193]. Moreover, it is observed that a significant overlap exists between Web of Science and Scopus (an equally popular science database) in the area in context, thus it is necessary to settle for either of the two. In searching, three keywords, "optimization," "renewable-energy-sources," AND "desalination" were used. The search criteria included the period from 1981 to 2019 across all fields of study, considering only published journal articles and proceedings. The result is represented in Figures 2.16 (a), 2.16(b), 2.17(a) and 2.17(b) as number of publication graphs, country of publication graph, network visualization map and overlay visualization map, respectively. The graph in Figure 2.16a shows the exponential growth in the number of publications over the last decades. The increase reflects increased research interest in the area of optimization of the RES-RO desalination system. The number of publications in the field of optimization of RES-RO desalination from different countries around the world, considering only countries with at least two publications, is depicted in Figure 2.16b, with the USA registering most.

Furthermore, the literature search revealed 94 publications with a total of 606 keywords. However, at five co-occurrences, a total of 41 keywords were derived. Figure 2.17a shows the network visualization map indicating the link between keywords and common words at five co-occurrences in the 94 papers used for this analysis. Five clusters were formed to indicate strong relationships, hence the focus areas in the publications.

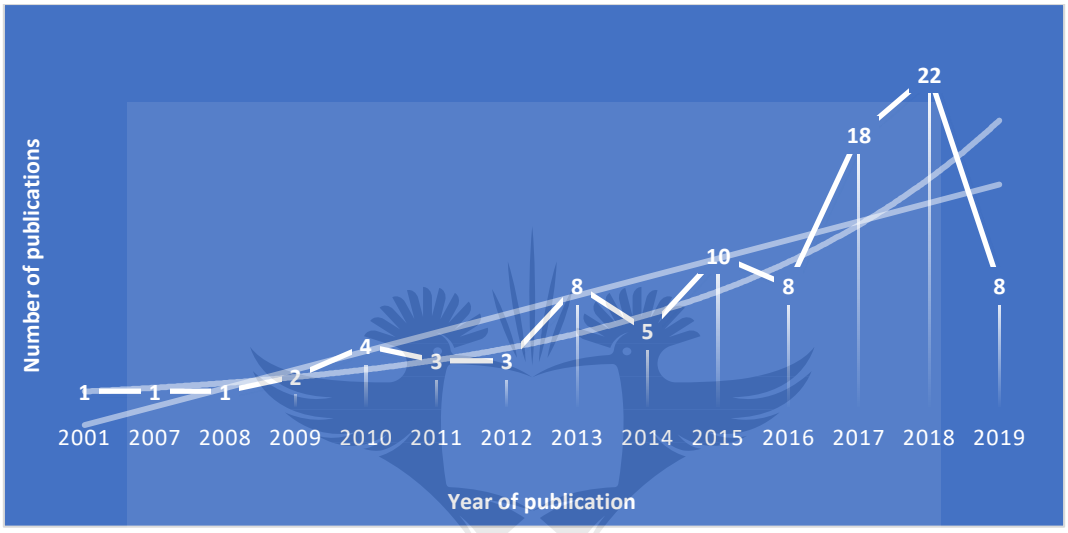

(a)

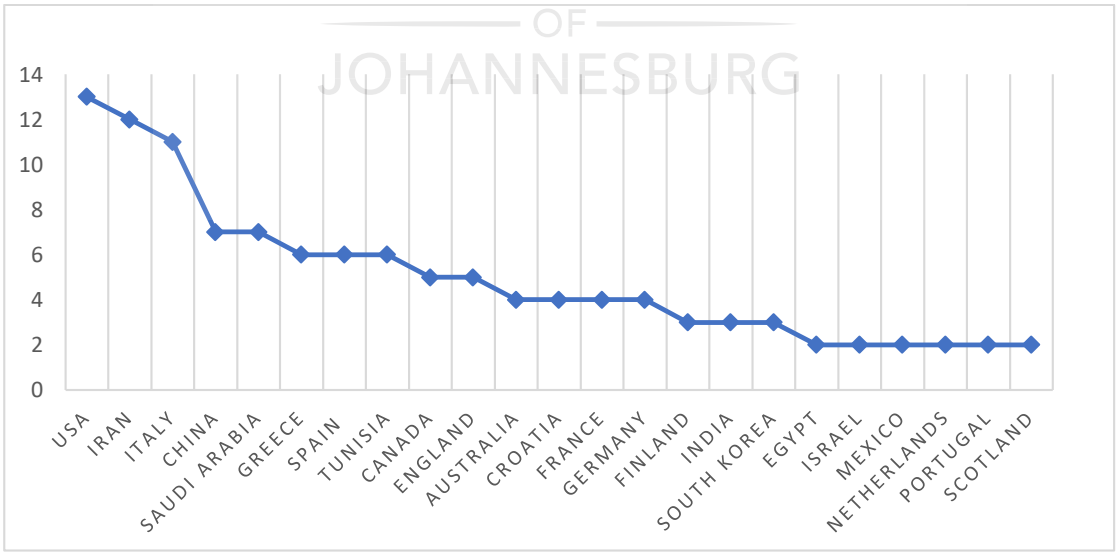

(b)

Fig. 2.16(a) Graph of number of publications and (b) country of publications (1981-2019)

2.4.1 Cluster 1 (Red): Economic Feasibility of RES Integration with Desalination

This cluster contains 12 items: cost, desalination, economics, feasibility, integration, power-generation, renewable energy, RES, solar, storage, system and wind. Desalination and renewable energy have the strongest link. Other item links in the cluster indicate the research focus of publications in this cluster to be on the economic evolution of a RES desalination system, as presented in [194], [181], [140] and [195].

2.4.2 Cluster 2 (Green): Simulation of RES-powered RO Seawater Desalination Plant

Cluster 2 contains nine items: plant, power, RES, RO, seawater desalination, simulation, systems, waste heat and water desalination. The most definite link in this cluster is renewable energy sources and water desalination. Considering the pattern of the cluster with other common items, their links show that the direction of research focus in this cluster is towards RES integration with seawater RO desalination, as discussed in [155] and [157].

2.4.3 Cluster 3 (Blue): Economic Analysis of PV-RO Technologies

This cluster contains seven items: economic analysis, PV, remote areas, renewable energies, RO, solar energy and technologies, with PV and RO having the most definite link, hence the research focus of publication in this cluster is the economic analysis of PV-RO in remote areas, as presented by [82] and [156].

2.4.4 Cluster 4 (Yellow): Design and Exergy Analysis of Solar-powered Desalination Unit

Cluster 4 contains seven items: energy, exergy analysis, performance, solar, desalination, unit and water. The strongest links are between design, energy and water; thus the focus of research in this

cluster is on performance and energy analysis of designed solar-powered desalination units as presented by [196] and [197].

2.4.5 Cluster 5 (Purple): Optimization of PV-RO Desalination Plant

This last cluster contains six items: generation, membrane distillation, optimization, PVs, plant and RO desalination. The most robust links are between optimization, renewable energy and RO. Therefore, the research focus of publications in this cluster is on optimization of RES-RO desalination, such as presented by [182] and [159].

Figure 2.17b depicts the overlay visualization map showing the trend of research focus. The purple cluster houses the research focus of publications around 2013 to 2015. The 2015 to 2016 research focus was on areas in the green cluster, which include optimization of desalination systems, while from mid-2016 to 2017 the research focus was on the yellow cluster, which mostly contains performance analyses of RES with energy storage systems to power desalination units.

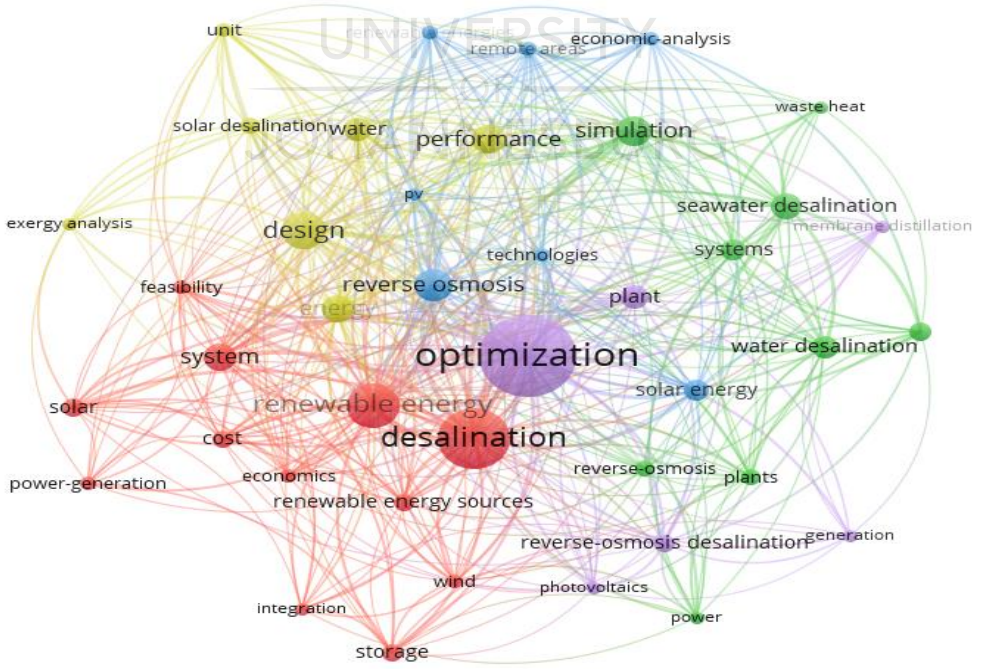

(a)

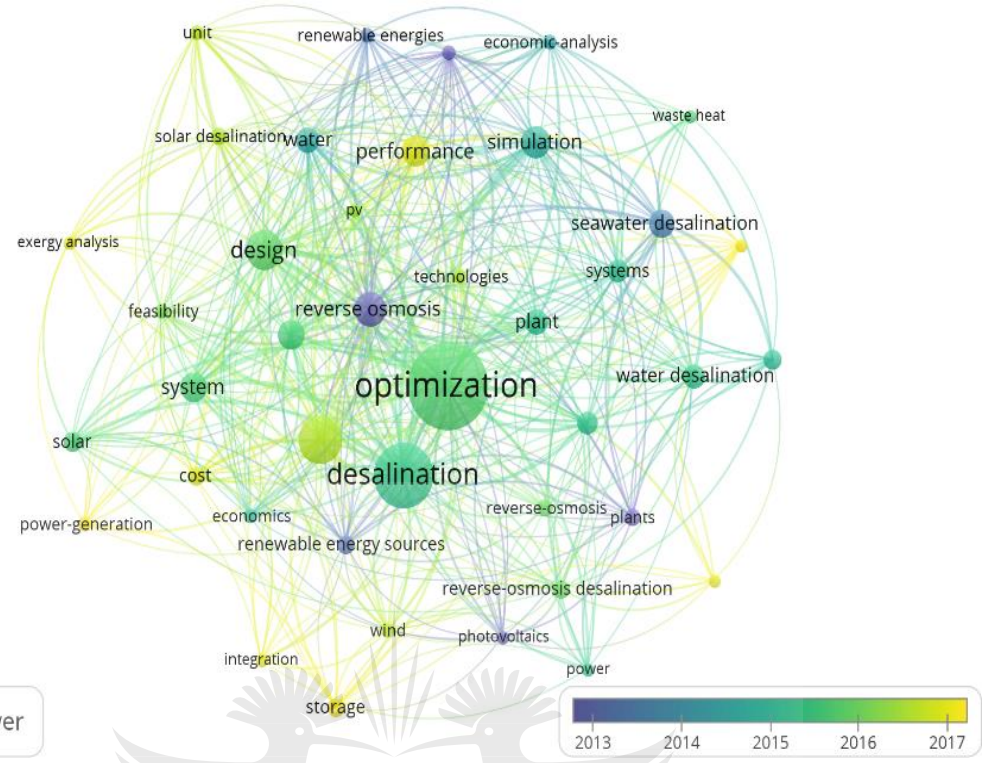

(b)

Fig. 2.17 (a) Network visualization and (b) Overlay visualization map of optimization of RES desalination

2.5 Findings and Conclusions from the Review of Literature

In this chapter, an extensive review of the optimization of the RES-RO desalination system was presented and discussed, based on optimal system sizing, optimal system operation and optimal thermodynamic analysis. RES such as geothermal, ocean, wind, solar and hybrid forms of these were considered, along with desalination methods other than the RO method. Important finds of the review have been summarized below. Also, knowledge gaps are identified and justification of this thesis methodology outlined.

In the area of sizing optimization of RES-RO desalination, PV-RO desalination plants are promising technologies for freshwater production in remote areas with no access to the electrical grid, but hybridization with other available RES or energy storage systems will yield more optimal

output. Although a standalone PV-RO system is more cost-effective than a hybrid system, the hybrid system provides more consistent optimal production of freshwater, considering the limitation of PV systems to daylight hours. As a result of this finding, Chapter 5 of this thesis implores hybridization of PV and wind RES compare to Chapter 3 and 4 with only PV as the renewable energy source utilized.

The hybridization of RO with other methods of desalination will produce more optimal results in terms of quality of freshwater production, minimization of energy consumption and the environmental impact of desalination systems. For instance, the use of nano-filtration as pre-treatment in an NF-RO desalination system enhances freshwater production, while FO and FD are promising options for post-treatment of brine. This helps to minimize the environmental impact of an RO desalination system. Furthermore, the MED-RO system enhances a high recovery ratio, quality water production, minimization of energy consumption and RO brine treatment. This finding led to the consideration of the propose model of Chapter 5 which combine RO, ED and crystallization method of desalination for optimal water production and zero brine discharge.

The operation of the RES-RO system can be optimized by first evaluating the performance of an individual component of the system and then making an appropriate adjustment. Modification of the pressure valve of an RO system can reduce the energy requirement of the system. Improvement of the RO membrane to enhance permselectivity has become a trend in research focus in 2019. The use of nanomaterials for designing membranes reduces RO pressure; as fouling resistance increases, permeability also increases. Therefore, specific energy consumption and cost of operation are minimized.

Techno-economic analysis of RES-RO desalination has become a central research focus, but the optimization of thermodynamic parameters such as exergy destruction and specific energy

consumption has not been extensively explored. It is therefore recommended that in future, more work should be done that applies optimization techniques to thermodynamic analysis of the RES-RO desalination system.

Furthermore, DR programs can be introduced to RES-RO systems for demand side management. This has the potential of minimizing system costs while maximizing the production of freshwater. This is another major identified gap from the literature review that this thesis intends to fill.

For more extensive optimization and analysis of RES-RO systems, a combined optimization approach should be considered, taking into account sizing, operation and the thermodynamic effect of the system. Furthermore, with the trend in the application of different metaheuristic optimization techniques, attention has shifted away from mathematical techniques. However, for accurate results, mathematical techniques are still very promising, especially with the availability of different computer software solvers. More metaheuristic optimization techniques can still be explored; thus far, only very few have been used in this area. Optimization objectives in this area have also been concentrated more strongly on economic performance indicators. In the future, more extensive work should incorporate both the economic and reliability index in the formation of objective functions. In general, there is still much work to be done in this area of optimization of RES-RO systems, especially the exploration of RES such as geothermal and ocean energy and salinity gradient energy. It is therefore, in these regards that this thesis proposes optimization models that incorporate the different identified gaps for optimal performance of desalination systems.

CHAPTER 3

OPTIMAL ENERGY MIX FOR A REVERSE OSMOSIS DESALINATION UNIT CONSIDERING DEMAND RESPONSE

3.1 Introduction

All desalination processes need a form of energy to power the system for operation. Conventional energy sources have several limitations, such as high cost and negative environmental impacts, predominantly GHG emission and pollution, hence the current trend in several studies favors the use of RES as a viable option for powering desalination. Different methods of desalination and possible configurations with RES have been studied, considering different drivers such as cost minimization, reliability criteria, system sizing, operational optimization and thermodynamic analyses of the desalination system.

Extensive as the reviewed literature may be in terms of optimal sizing of RES and energy storage systems to power a desalination plant, no publication considered the sizing of the RO desalination unit for optimal freshwater production with the effect of DR and its cost on the unit cost of freshwater. The contribution of this chapter is, therefore, to evaluate the optimal cost of freshwater production considering different energy supply sources, optimize the production capacity of RO unit for maximum freshwater production and determine the impact of demand-side management on RO desalination systems. Thus, the remainder of this chapter is organized such that section 3.1 presents the modelling of the energy supply mix, RO desalination unit and TOU DR model; section 3.2 formulates the component cost models; section 3.3 details the optimization model, then section 3.4 presents a case study; while section 3.5 present the results and discussion of the results, and section 3.6 summarizes the Chapter.

3.2 Energy Supply and Demand Modeling

The energy supply mix includes grid power, a diesel generator (DG) and PV to supply an optimally sized RO desalination unit and in a case of excess supply of energy, the excess is sold back to the grid. Hence the primary demand to be satisfied by the energy supply mix is the hourly power demand of the RO desalination unit, which in turn is expected to produce freshwater at optimal capacity. Seawater desalination is energy-intensive. The amount of energy required by the desalination unit to produce water depends on the type of desalination method, plant design, temperature and salinity of the feed water [38]. The SEC in kWh/m^3, which is the energy required to produce 1 m^3 of freshwater, differs according to the method of desalination. MED requires between 14.45 and 21.35 kWh/m^3, MFS requires between 19.58 and 27.25 kWh/m^3, MVC uses between 7 and 12 kWh/m^3, TVC requires about 16.3 kWh/m^3 and ED requires between 0.7 and 5.5 kWh/m^3 [38]; [95]. RO requires 2-4 kWh to produce 1 m^3 of freshwater [7] [198]. The energy sources and their models are detailed in the next sections.

3.2.1 Grid Power Model

The power supply from the grid serves as back-up to complement the inconsistent supply from PV to meet the power demand of the desalination unit. When the power output from PV is in excess of the load demand, the extra energy is sold back to the grid. Therefore, the hourly power ($GP_i(t)$) imported from the grid and the hourly power ($GP_e(t)$) exported to the grid are optimized variables ranging from zero to maximum hourly load demand by the RO unit, as expressed in (3.1) and (3.2) respectively.

$$0 \leq GP_i(t) \leq GP_i^{max} \quad (3.1)$$

$$0 \leq GP_e(t) \leq GP_e^{max} \quad (3.2)$$

The maximum transferable power to and from the grid is assumed equal:

$$GP_i^{max} = GP_e^{max} \quad (3.3)$$

3.2.2 Diesel Generator Power Supply Model

The DG is used in this study as another back-up to make up for the inconsistency of RES. Its output power (*Pg(t)*) is an optimized variable that is a function of its maximum capacity, as expressed in (3.4).

$$Pg^{min} \leq Pg(t) \leq Pg^{max} \quad (3.4)$$

3.2.3 PV Power Supply Model

The hourly output power ($P_{PV}(t)$) supply by the PV array is given as [199] and [200].

$$P_{PV}(t) = APV * ή * SI(t) \quad (3.5)$$

where

APV is the area of PV array in m^2, *SI(t)* is hourly solar irradiation, and ή is the PV efficiency.

3.2.4 RO Desalination Plant Power Demand Model

The $P_{WD}(t)$ demand of the RO desalination unit depends on the *SEC* to produce 1 m^3 of freshwater, this value ranges from 3 to 4kWh/ m3 for RO [19] and according to [13]; [20];[180] and [198] it currently ranges from 2-5kWh/ m3 which in this study is 3 kwh/m^3 and the actual volume of water (*QW(t)*) produced per hour [6]; [7].

$$P_{WD}(t) = QW(t) * SEC \quad (3.6)$$

The daily water production capacity is given as:

$$DQW = \sum_{t=1}^{24} QW(t) \quad (3.7)$$

The water dispensation model and network are not considered in this study. Thus, the water tank capacity (W_{TK}) expressed in m^3 is assumed to be twice the daily water production capacity to make

enough space available for excess water production and in the event of water remaining from the previous day.

$$W_{TK} = DQW * 2 \quad (3.8)$$

3.2.5 Demand Response Load Model

The maximum allowable demand variation (increase/decrease) per hour is assumed to be 30% of total demand at that hour. The DR load is an optimized variable, as expressed in (3.9) [201][202].

$$-\Delta L^{max}(t) \leq \Delta L(t) \leq \Delta L^{max}(t) \quad (3.9)$$

where

$$\Delta L^{max}(t) = 0.3 * P_{WD}(t) \quad (3.10)$$

3.3 Component cost model

The economic impact of the components and different sections of the entire system is evaluated using an annualized system cost matrix to determine the unit cost of water.

3.3.1 Grid Power Cost

The cost of grid power is dependent on the energy price and the difference between imported power and exported power to the grid. It is assumed that the unit cost of purchasing power is equal to the unit cost of selling power back to the grid. Hence, excess energy production that is not needed by the desalination unit is sold back to the grid to compensate for the cost of imported power or at least reduce importation cost of energy from the grid.

$$CGP_i(t) = GP_i(t) * P(t) \quad (3.11)$$

$$CGP_e(t) = GP_e(t) * P(t) \quad (3.12)$$

$$CGP = \sum (CGP_i(t) * P(t) - GP_e(t) * P(t)) \quad (3.13)$$

$$\forall t = 1,2,3,\dots 8760$$

where:

P(t) is the hourly unit price of transferable grid power and *CGP* is the total annual cost of transferable grid power.

3.3.2 Diesel Generator Cost

The hourly fuel consumption of the DG, *FC(t)* (L/hr), is a function of its electrical power output [203].

$$FC(t) = a * Pg(t) + b * Pg^N \quad (3.14)$$

where:

a = 0.246L/kWh, the slope of fuel curve and b = 0.08145 L/kWh, the rated fuel curve intercept coefficient and Pg^N is the generator nominal power [19]; [20]. The DG's fuel cost, therefore, is the function of the unit price of fuel (*Fp*), which in this study is 1 $/L and the amount of fuel consumed to produce its output power. Hence, the total annual fuel cost is expressed as (3.15) [19]; [20].

$$FC_{DG} = \sum_{t=1}^{8760} FC(t) * Fp \quad (3.15)$$

The initial capital cost of the DG (IC_{DG}) and the maintenance cost (AMC_{DG}) are $7 495 and 0.3 $/hr, respectively [20].

3.3.3 PV cost

Evaluation of PV cost is based on the area of PV array, initial capital cost and maintenance cost over its lifetime, as expressed in (3.16) and (3.17) [20][204].

$$IC_{PV} = APV * C_{PV} \quad (3.16)$$

$$AMC_{PV} = APV * MC_{PV} \quad (3.17)$$

3.3.4 RO Desalination Cost Model

The RO desalination cost model includes the initial capital cost (IC_{RO}), annual maintenance and operational cost (AMC_{RO}), annual membrane replacement cost (AC_{MR}), annual treatment chemical cost (AC_{CH}) and water tank cost (CW_{TK}) as adopted by references [19] and [20].

$$IC_{RO} = C_{RO} * DQW \tag{3.18}$$

$$ICW_{TK} = CW_{TK} * W_{TK} \tag{3.19}$$

3.3.5 Demand Response Cost

The application of TOU DR optimally shifts loads from peak hours when the price of demand is highest to either standard or off-peak hours, yet allows the demand at every hour to be met. The cost of DR is the difference between the cost of power demand before and after TOU DR. It is expressed as [205]:

$$\Delta LC = \sum \left[P_{WD}(t) * \lambda(t) - \left(P_{WD}(t) - \Delta L(t)\right) * \lambda(t)\right] \tag{3.20}$$

3.3.6 Total System Cost

In this study, the annualized system cost matrix is used for the economic evaluation of the RO desalination system powered by the different energy sources to determine the cost of freshwater and the LCOE. The *ACS* involves the *CRF* and the total system cost, which includes total initial cost (*TICC*) and the total maintenance and operational cost (*TMC*) of all the components that make up the system [168], [206] and [207].

$$TICC = (IC_{PV} + IC_{DG} + IC_{RO} + ICW_{TK}) * dr \tag{3.21}$$

where

$dr = \frac{1}{(1+i)^{20}}$, the discount rate for 20 years' lifetime of the system.

$$TMC = AMC_{PV} + AMC_{DG} + AMC_{RO} \tag{3.22}$$

$$ACS = TICC * CRF + TMC + AC_{MR} * CRF + AC_{CH} + CGP + FC_{DG} + \Delta LC \tag{3.23}$$

where

$$CRF = \frac{i(1+i)^n}{(1+i)^n - 1} \qquad n = 1 \dots 19 \tag{3.24}$$

$$CQW = {}^{ACS}/_{\sum QW(t)} \tag{3.25}$$

$$LCOE = \frac{ACS + P_{WD}(t)}{\sum P_{PV}(t) + Pg(t) + GP_i(t)} \tag{3.26}$$

$$\forall t = 1,2,3 \dots 8760$$

3.4 Optimization Model

The optimization problem is formulated as a multi-objective linear programming problem as expressed in (3.27), with the objective of minimizing annualized system cost, which includes total initial capital cost, membrane replacement cost, maintenance cost, treatment chemical cost of the RO unit, grid transferable power cost, DG fuel cost and DR cost, subject to constraints expressed by (3.28) - (3.32). This multi-optimization problem is solved using the CPLEX solver of the AIMMS.

Objective Function

Min ACS **=**

$$min \sum (TICC + AC_{MR})\, CRF + TMC + AC_{CH} + CGP + FC_{DG} + \Delta LC \tag{3.27}$$

S.t.

$$P_{PV}(t) + Pg(t) + GP_i(t) = P_{WD}(t) + \Delta L(t) + GP_e(t) \tag{3.28}$$

$$QW(t) = WD(t) \tag{3.29}$$

$$QW^{min} \leq QW(t) \leq QW^{max} \quad (3.30)$$

$$P_{WD}{}^{min} \leq P_{WD}(t) \leq P_{WD}{}^{max} \quad (3.31)$$

$$\forall t = 1,2,3 \ldots 8760$$

$$APV \geq 0 \quad (3.32)$$

Constraint (3.28) expresses the power balance that ensures power supply from PV, the DG and the grid at any time *t*, equaling the total demand by the RO desalination unit and the power exported to the grid at the same time *t*. Constraint (3.29) is water balance that ensures the water produces at any hour *t* equals the water demand at that hour *t*, or in excess of it, while constraint (30) ensures water produced per hour remains within the required limits. Constraint (3.31) is the limit of power required to produce water at any time t and constraint (3.32) expresses the limit of the area of PV. Other constraints include (3.1), (3.2), (3.3), (3.4) and (3.9), which express the limit of grid imported power, limit of grid exported power, maximum allowable transfer power and limit of DR load respectively. Figure 3.1 represents the Model's flowchart.

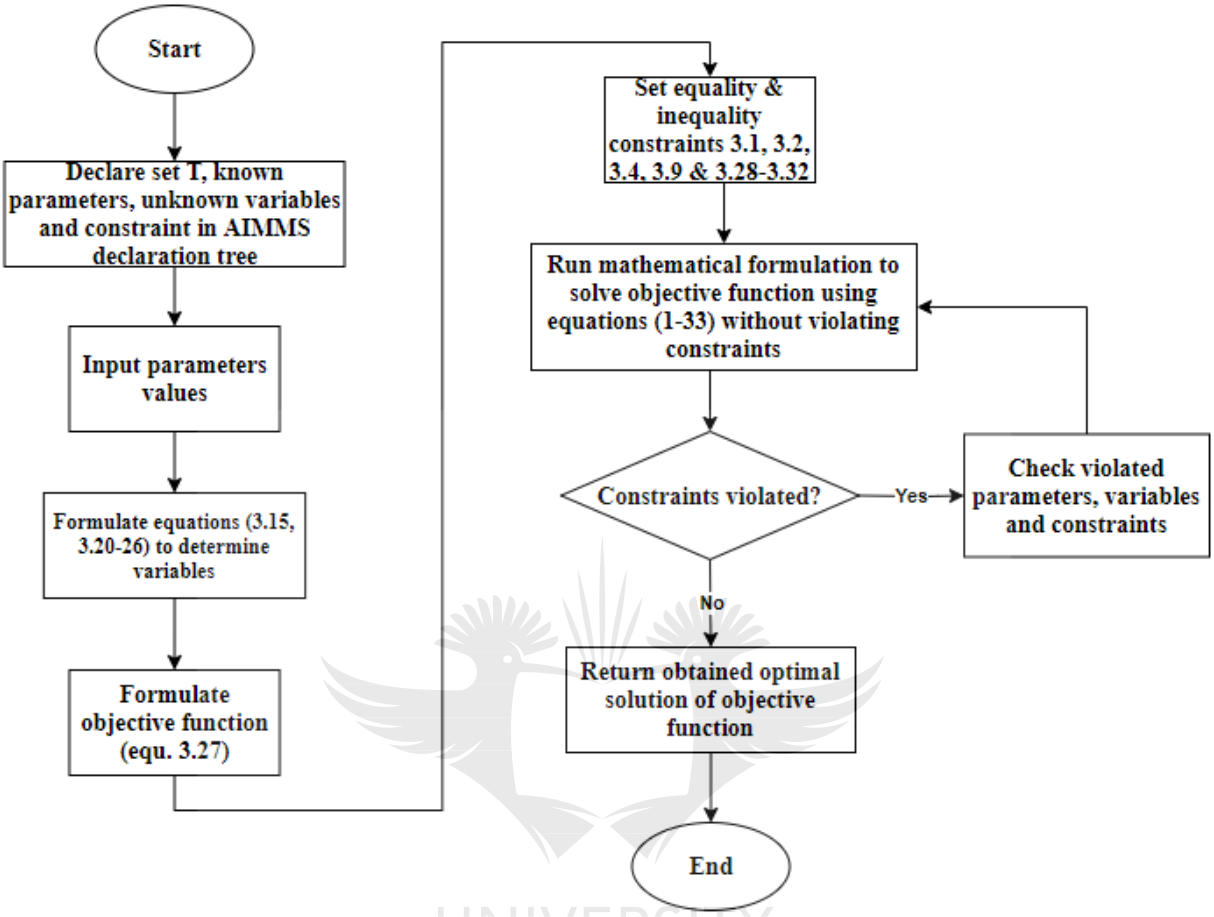

Fig. 3.1 Model's flowchart

3.5 Case Study

In this chapter, three case scenarios are implemented, and the results are presented and compared. Case 1 is an RO desalination system powered by the grid and a DG. This system is without RES and has no DR program. Case 2 is an RO desalination system with the incorporation of PV (a RES) in the energy supply mix of the grid and a DG, but also without a DR program, while Case 3 is an RO desalination system powered by the grid, a DG and PV, alongside the incorporation of a TOU DR program. The hourly solar irradiations were collected from the Southern African Universities Radiometric Network as depicted in Figure 3.2. Also, the TOU energy price (in US $) for South

Africa obtained from the Eskom schedule of standard prices for Eskom tariffs 2019/2020 [18] as shown in Figure 3.3 is implemented for the DR program. Whereas, an assumed hourly water demand curve based on expected behavioral water usage at different hour of the day as represented in figure 3.4 is used in this study.

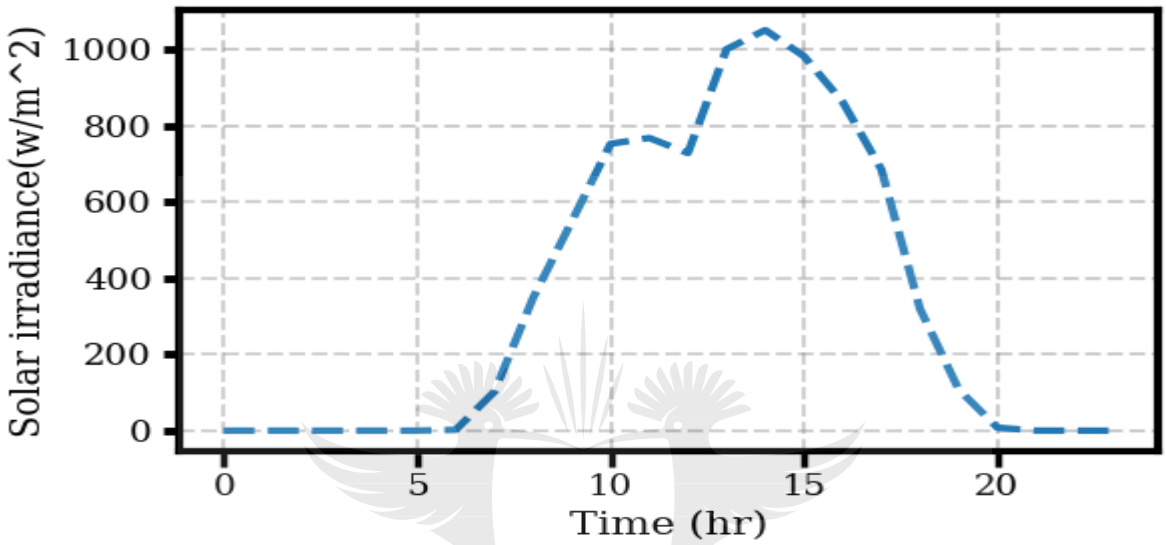

Fig. 3.2 Hourly solar irradiance

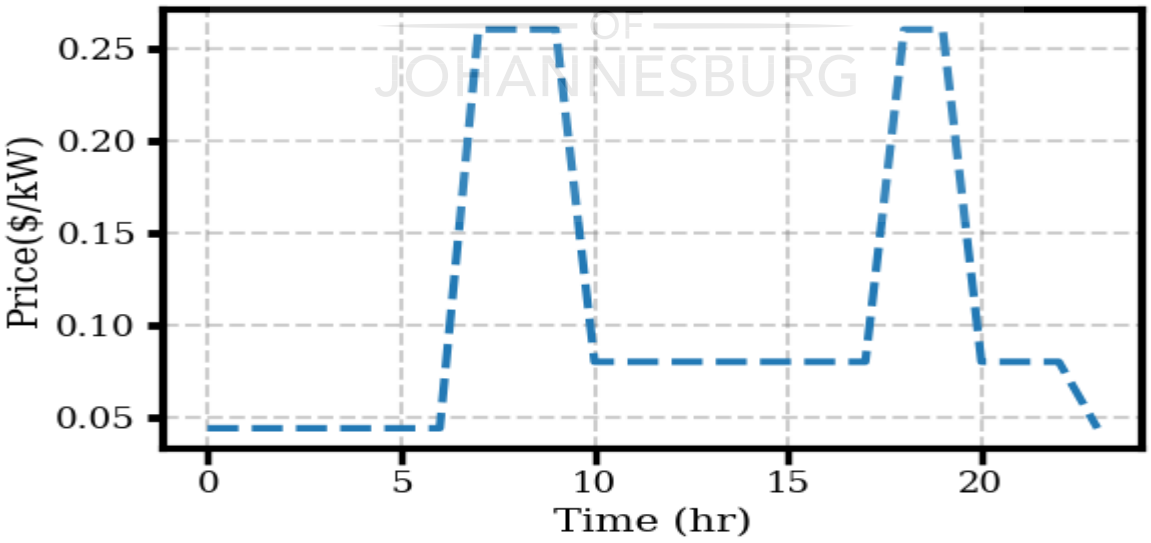

Fig. 3.3 Hourly price of grid power

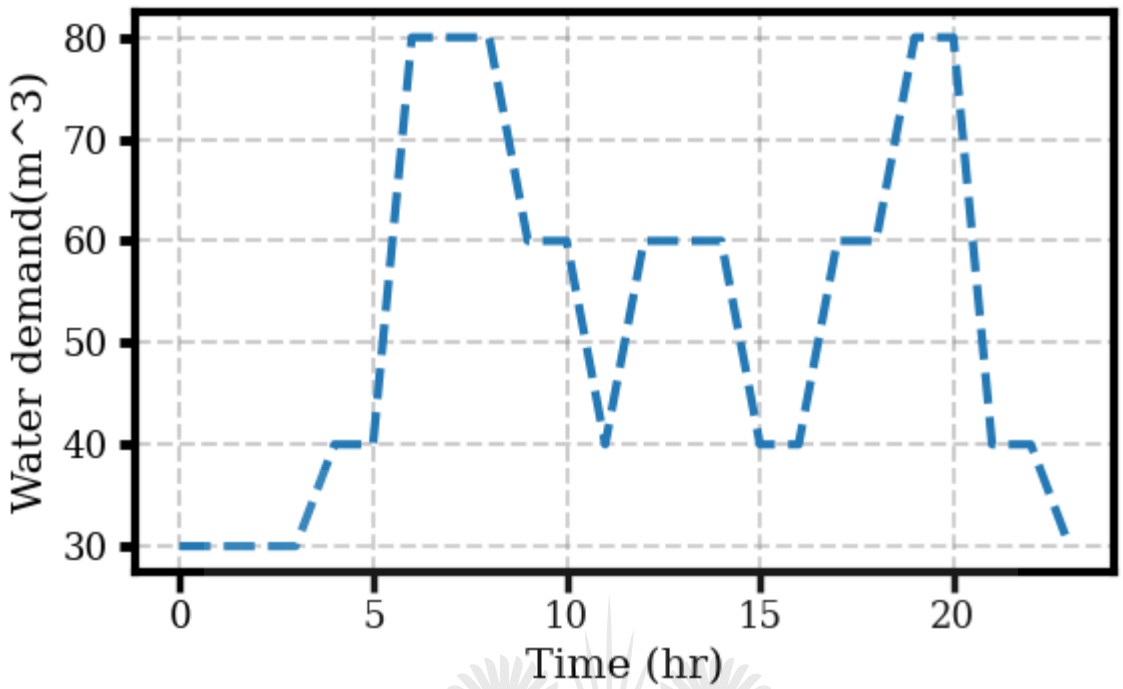

Fig. 3.4

Hourly water demand

3.6 Results and Discussion

3.6.1 Results

Figure 3.5 shows the hourly power supply from the grid and DG. An average daily simulation is used for purposes of clear comparison. Figure 3.6 depicts the hourly power output from the energy supply mix of Case 2, as well as the excess power exported to the grid. Figure 3.7a represents the hourly power supply mix for Case 3, while Figure 3.7b depicts the difference between the load curve before and after the application of the DR program. The volume of hourly water produced in each case is represented in Figure 3.8. While Table 3.1 is the summary of the results of daily power supply from the different mix of energy supply, Table 3.2 is the summary result of optimized parameters.

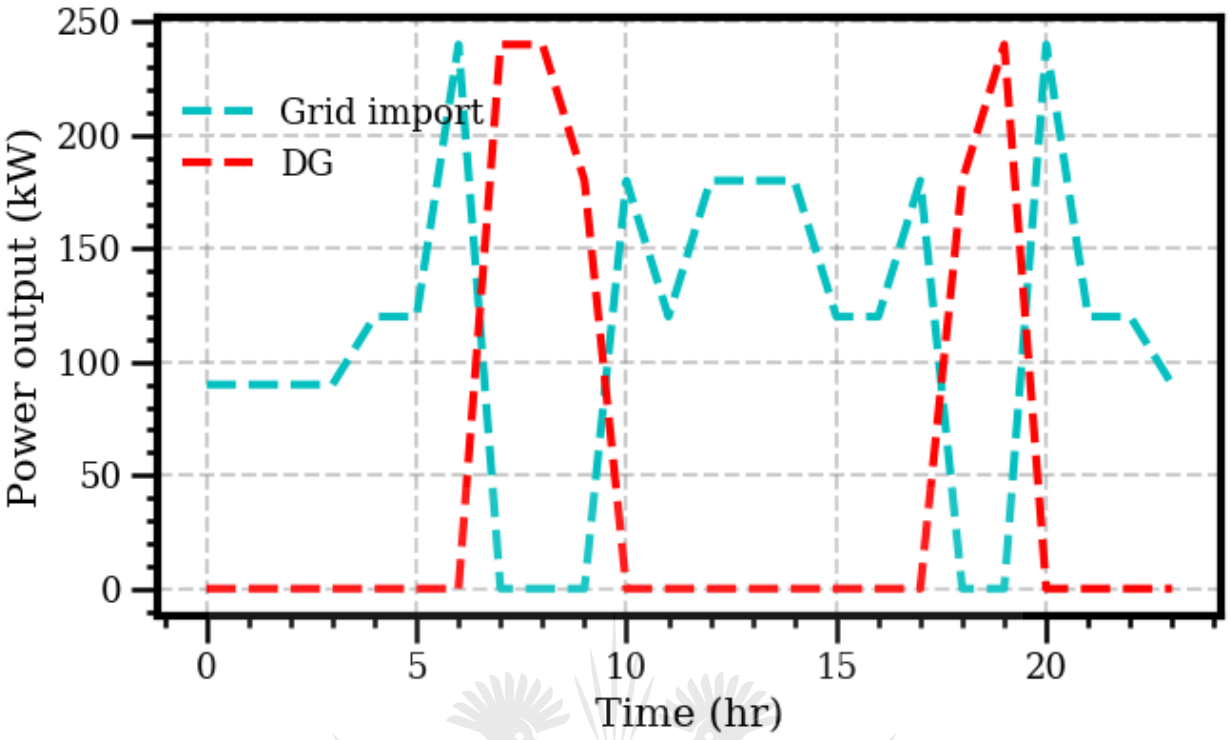

Fig. 3.5 Case 1 hourly energy dispensed.

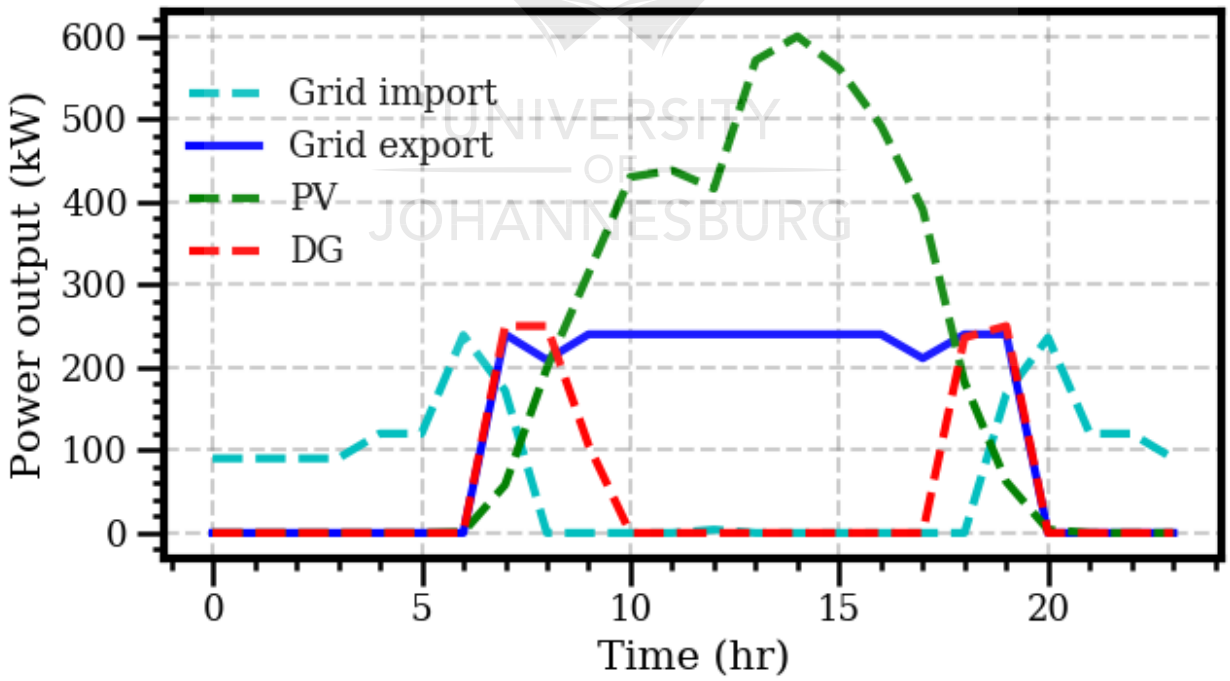

Fig. 3.6 Case 2 hourly energy dispensed

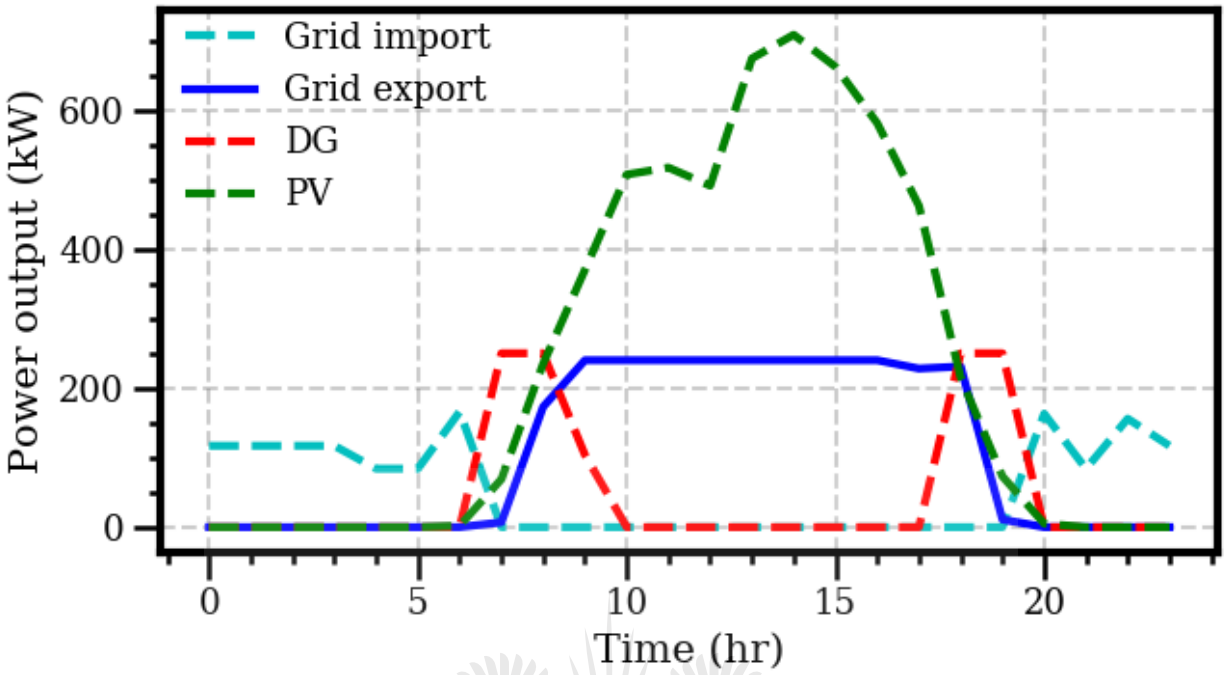

Fig. 3.7a Case 3 hourly energy dispensed

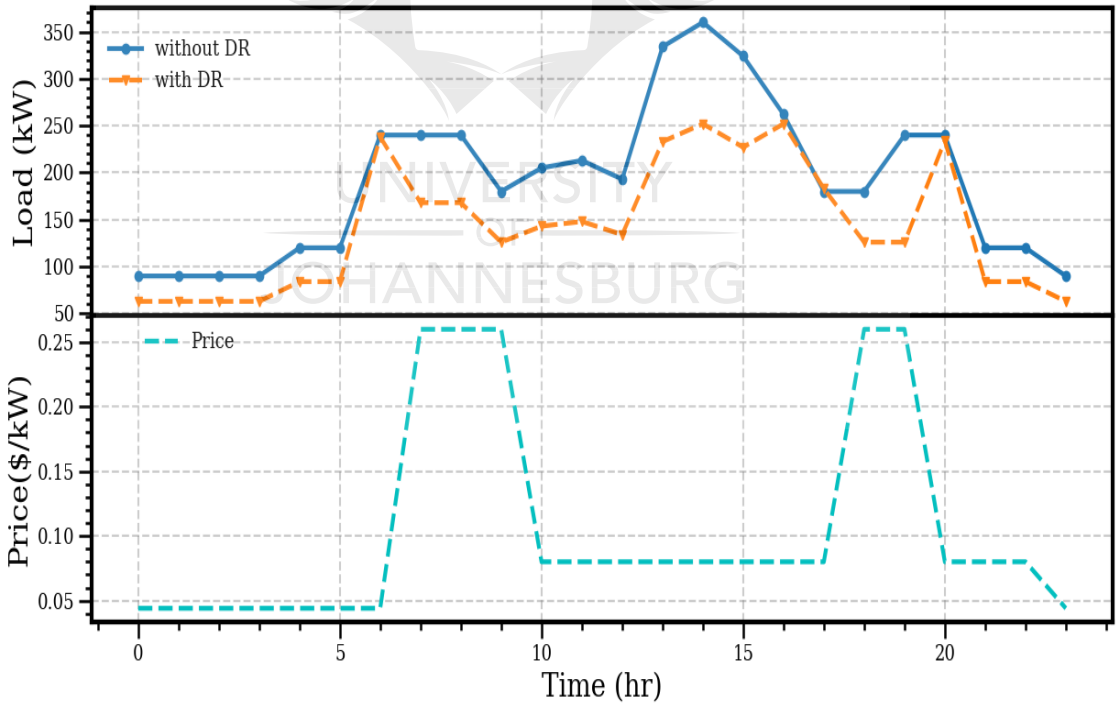

Fig. 3.7b Case 3 hourly load curve with and without DR program compared with hourly price of power

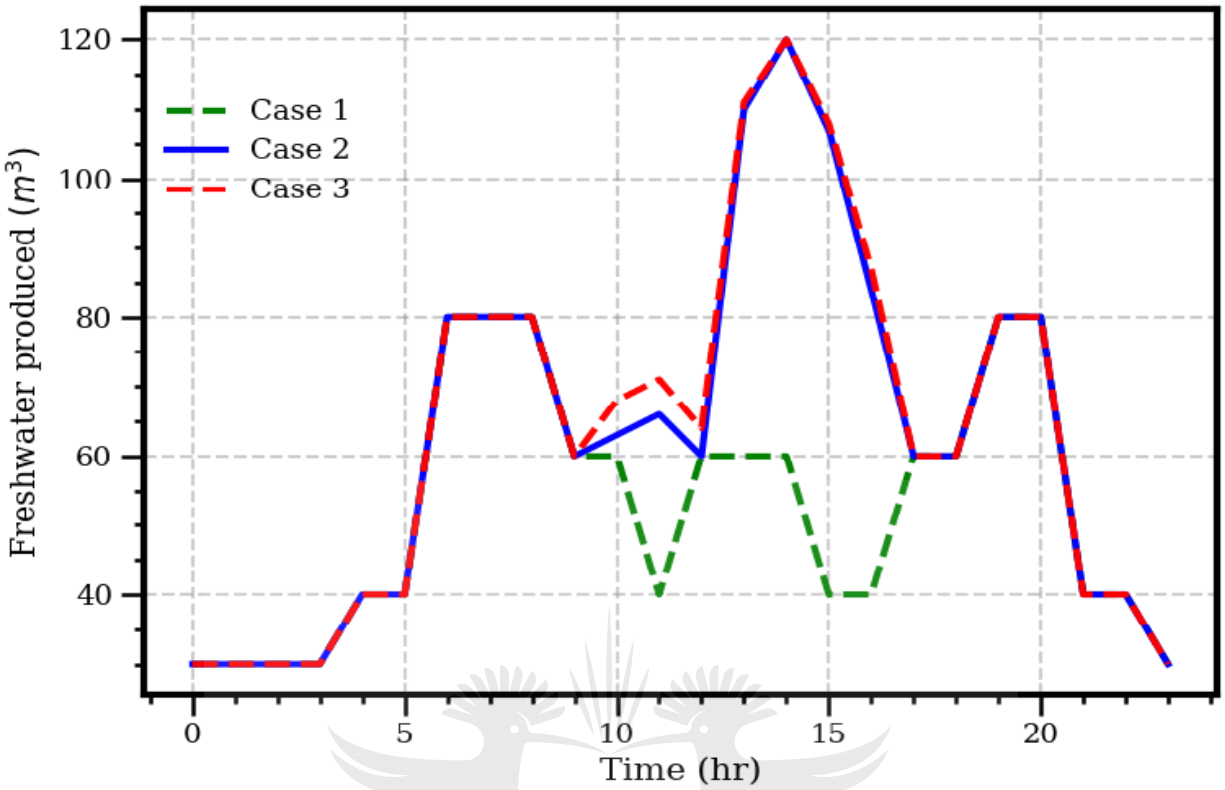

Fig. 3.8 Comparison of hourly freshwater production quantity

Table 3.1. Results of daily power supply

Optimized power output (kW)	Case 1: Without RES	Case 2: With RES	Case 3: With RES and DR
Grid import power	2670	1748	1322
Grid export power	---	3061	2570
DG output power	1080	1094	1104
PV output power	---	4721	5571

Table 3.2. Summary of results of optimized parameters

Optimized parameters	Case 1 Without RES	Case 2 With RES	Case 3 With RES and DR
Area of PV	---	3614	4264
Annual DG fuel cost ($)	275 940	276 594	277 486
Annual grid power imported cost ($)	65 744	61 172	26 522
Annual grid power exported cost ($)	---	16618	118 534
Annualized system cost ($)	764 802	728 008	752 353
Levelized cost of energy ($/kWh)	1.56	0.86	0.83
Daily freshwater produced (m^3/day)	1250	1 501	1 521
Unit cost of water ($/$m^3$)	1.68	1.33	1.36

3.6.2 Discussion

The results from Case 1 indicate that the RO unit was predominantly powered by the grid, with little back-up from the DG. In this case, there is no excess energy to sell back to the grid. This implies that even at peak hours, the RO unit depends on grid power and a DG to satisfy its load demand, resulting in high LCOE of 1.56 $/kWh. Case 1 also has the highest unit cost of freshwater produced with the lowest quantity of 1 250 m^3, as indicated in Figure 3.8 and Table 3.2.

Results from Case 2 are an improvement on those from Case 1, with a reduction in imported grid power cost from $65 744 of Case 1 to $61 172 of Case 2. This reduction is a result of the integration of PV (a RES) into the energy mix of Case 2. Furthermore, the impact of the integration of RES is reflected in the excess energy output that is sold back to the grid, which amounts to an annual cost of $16 618. There is also a reduction in LCOE in Case 2 (0.86 $/kWh) from

1.56 $/kWh of Case 1. Finally, Case 2, with a daily capacity of 1 501 m^3/day, produces more freshwater than Case 1 with a daily capacity of 1 250 m^3/day.

Case 3 is a system model formulated with the integration of the three energy sources (grid, DG and PV) as its energy mix to power the RO unit and with the incorporation of a TOU DR program. The results show the impact of the TOU DR program by the reduction of the demand curve in Figure 3.7b. Other optimized results are compared to Cases 1 and 2 in Table 3.2. Case 3 proves to produce more freshwater than Cases 1 and 2, with a daily capacity of 1 521 m^3/day at the low cost of 1.36 $/$m^3$. Furthermore, Case 3 has the lowest annual imported grid power cost of $26 522 and the highest export grid power cost of $118 534, reducing the transferable power cost and by extension, minimizing the LCOE to as low as 0.83 $/kWh against 1.56 $/kW/h and 0.86 $/kWh of Case 1 and Case 2 respectively. Hence, Case 3 proves to be the best option, considering its highest production capacity at lowest cost.

3.7 SUMMARY

In this chapter, a mathematical optimization approach is used to determine the optimal energy mix of three case scenarios: Case 1, which has grid power and a DG in its energy mix to supply an RO desalination unit without considering TOU DR; Case 2, which as has grid, DG and PV (a RES) power in its energy mix and does not consider TOU DR; and Case 3, which has the three energy sources in its energy mix and implements a TOU DR program on the demand side of the system. The objectives of these models are to maximize freshwater production at minimal cost and to determine the impact of DR and its cost on the quantity of water produced at different hours of the day and the unit cost of freshwater. The results show that Case 3 offers a significant increase in freshwater production at a considerably lower cost compared to the other two cases. Case 3 is therefore recommended as the ideal optimal sizing approach for the RO desalination system. The

cost of freshwater and the LCOE of Case 3 are also lower than those from similar cases in literature, such as 2.962 and 6.457 $/m^3 from [174], 1.08-1.5076 $/m^3 in [19] and 1.9452-2.0196 $/m^3 in [20].

CHAPTER 4

TECHNO-ECONOMIC EVALUATION OF REVERSE OSMOSIS DESALINATION SYSTEM CONSIDERING EMISSION COST AND DEMAND RESPONSE

4.1 Introduction

Most desalination plants around the world still largely depend on fossil energy sources, especially the grid. The direct consequence of this is high GHG, which also has cost implications alongside its environmental impacts. The cost implication of emitted carbon gas is regarded as one of the external costs of desalination, the other being brine management [17]. Hence, efficient energy supply management is key to gas emission reduction [208] and, by implication, reduction of the cost of desalination. The contribution of this study is, therefore, to (i) Evaluate the optimal cost of freshwater production considering carbon emission and DR cost, (ii) Determine the impact of carbon emission considering different energy supply sources, (iii) Optimize the production capacity of an RO unit for maximum freshwater production, and (iv) Determine the impact of demand side management on an RO desalination system.

Thus, the remainder of this chapter is organized such that section II presents the modeling of the power section; section III formulates the component cost models; section IV discusses the carbon emission cost and global warming impact (GWI) of the energy source; section V details the optimization model, while section VI presents a case study, section VII presents and discusses the results and section VIII summarizes the Chapter.

4.2 Energy Supply and Demand Models

4.2.1 Grid Power Model

The $GP_i(t)$ imported from the grid and the $GP_e(t)$ exported to the grid are optimized variables ranging from zero to maximum hourly load demand by the RO unit as expressed in (4.1) and (4.2) respectively.

$$0 \leq GP_i(t) \leq GP_i^{max} \quad (4.1)$$

$$0 \leq GP_e(t) \leq GP_e^{max} \quad (4.2)$$

The maximum transferable power to and from the grid is assumed equal:

$$GP_i^{max} = GP_e^{max} \quad (4.3)$$

4.2.2 Diesel Generator Power Supply Model

The output power ($Pg(t)$) of the DG is an optimized variable that is a function of its maximum capacity as expressed in (4.4).

$$Pg^{min} \leq Pg(t) \leq Pg^{max} \quad (4.4)$$

4.2.3 PV Power Supply Model

The $P_{PV}(t)$ supply by the PV array is given as [199] and [200]

$$P_{PV}(t) = APV * ή * SI(t) \quad (4.5)$$

where

APV is area of PV array in (m^2), $SI(t)$ is hourly solar irradiation and ή is the *PV* efficiency.

4.2.4 RO Desalination Plant Power Demand Model

The $P_{WD}(t)$ of the RO desalination unit depends on the *SEC* to produce 1 m^3 of freshwater, which in this study is 3 kwh/m^3 and the actual *QW(t)* produced per hour [16]; [6].

$$P_{WD}(t) = QW(t) * SEC(t) \tag{4.6}$$

The daily water production capacity is given as:

$$DQW = \sum_{t=1}^{24} QW(t) \tag{4.7}$$

The W_{TK} expressed in m^3 is assumed to be twice the daily water production capacity.

$$W_{TK} = DQW * 2 \tag{4.8}$$

4.2.5 Demand Response Load Model

The maximum allowable demand variation (increase/decrease) per hour is assumed to be 30% of total demand at that hour. The DR load is an optimized variable, as expressed in (4.9).

$$-\Delta L^{max}(t) \leq \Delta L(t) \leq \Delta L^{max}(t) \tag{4.9}$$

where

$$\Delta L^{max}(t) = 0.3 * P_{WD}(t) \tag{4.10}$$

Furthermore, for even distribution of load shift, the cut-off demand at certain hours of the day equals an increase in demand at other hours of the day, as expressed in (4.11).

$$\sum_{t=1}^{24} \Delta L(t) = 0 \tag{4.11}$$

4.3 Component Cost Model

The economic impact of the components and different sections of the entire system are evaluated using an annualized system cost matrix to determine the unit cost of water.

4.3.1 Grid Power Cost

The cost of grid power is a function of the difference between the cost of imported and exported power. Therefore, equation 4.14 depicts the total annual cost of transferable grid power.

$$CGP_i(t) = GP_i(t) * P(t) \quad (4.12)$$

$$CGP_e(t) = GP_e(t) * P(t) \quad (4.13)$$

$$CGP = \sum (CGP_i(t) * P(t) - GP_e(t) * P(t)) \quad (4.14)$$

$$\forall t = 1,2,3, \dots 8760$$

where

P(t) is the hourly unit price of transferable grid power.

4.3.2 Diesel Generator Cost

The DG's hourly fuel consumption FC(t) (L/hr) is a function of its electrical power output [203]. Total annual fuel cost is expressed as (4.15) [19]; [20].

$$FC(t) = a * Pg(t) + b * Pg^N \quad (4.15)$$

$$FC_{DG} = \sum_{t=1}^{8760} FC(t) * Fp \quad (4.16)$$

4.3.3 PV Cost

Evaluation of PV cost is based on the area of PV array, initial capital cost and maintenance cost over its lifetime, as expressed in (4.17) and (4.18)

$$IC_{PV} = APV * C_{PV} \quad (17)$$

$$TMC_{PV} = APV * MC_{PV} * r \quad (18)$$

4.3.4 RO Desalination Cost Model

The RO desalination cost model is determined by the summation of (IC_{RO}), (AMC_{RO}), (AC_{MR}), (AC_{CH}) and (CW_{TK}) [19] and [20].

$$IC_{RO} = C_{RO} * DQW \tag{4.19}$$

$$ICW_{TK} = CW_{TK} * W_{TK} \tag{4.20}$$

4.3.5 Demand Response Cost

The cost of DR is the difference between the cost of power demand before and after load variation due to DR. It is expressed as (4.21) [205].

$$\Delta LC = \sum \left[P_{WD}(t) * \lambda(t) - \left(P_{WD}(t) - \Delta L(t)\right) * \lambda(t)\right] \tag{4.21}$$

$$t = 1,2,3, \ldots 8760$$

4.4 Carbon Emission Cost and Global Warming Impact of Energy Source

The *GWI*, in other words, the carbon emission of the fossil-fuel energy source, could be due to construction or operation of the plant, with the impact due to operation exceeding that due to construction by multiple orders [208]. Thus, this study considered the impact due to operation as adopted by authors of reference [208]. The authors define *GWI* as the summation of input power $P_{j,t}$ of every fossil-fuel unit j in every time step $t \in T$ multiplied by specific operational emission factor $SEF_{j,t}$ and the period Δt_t of the time step as represented in (4.22).

$$GWI_g = \sum_{t \in T} \left[\Delta t_t \sum_j SEF_{j,t} * P_{j,t} \right] \tag{4.22}$$

where

$$SEF_{j,t} = \frac{emission\ due\ to\ electrical\ energ\ genarated}{electrical\ energ\ genarated} \tag{4.23}$$

The emission factor of DG (SEF_{DG}) depends on its characteristics and fuel consumption, with values ranging from 2.4-2.8 kg/L; in this study, 2.6 kg/L is used[19]. Therefore, DG carbon emission, in other words, the DG GWI, is given as:

$$GWI_{DG} = \sum_{t=1}^{8760} FC(t) * SEF_{DG} \tag{4.24}$$

In order to estimate the carbon emission cost, the formulated model given by references [17] and [209] was adopted, as shown in (4.25).

$$CE\ \left(\frac{\$}{m^3}\right) = Energy\ supply\ \left(\frac{kwh}{m^3}\right) * Emission\ factor\ \left(\frac{kgCO_{2-e}}{kwh}\right) *$$

$$Carbon\ tax\ \left(\frac{\$}{kgCO_{2-e}}\right) \tag{4.25}$$

For a system with grid and DG units, the total *GWI* and total carbon emission cost will amount to the sum of the emission from the two units and the sum of the associated cost from the units, as represented in (4.26) and (4.27) respectively.

$$GWI = GWI_g + GWI_{DG} \tag{4.26}$$

$$TEC = CE_g + CE_{DG} \tag{4.27}$$

The grid-specific emission factor and carbon tax depend on the country of location of the plant. This study adopted the calculated emission factor for South Africa given by reference [210]. The value of the emission factor is 1.069 $kgCO_2$/kwh. Recently the South African carbon tax rate ranged from R6-R48 ($0.40-$3.17)[211]. The lowest value of $0.40 is considered in this study.

4.5 Optimization Model

In this study, the annualized system cost matrix is used for the economic evaluation of the RO desalination system powered by the different energy sources to determine the cost of freshwater and the LCOE. The *ACS* involves the *CRF* and the total system cost, which includes total initial

cost (*TICC*) and total maintenance and operation cost (*TMC*) of all the components that make up the system [168]; [206]; [207]. Also included in the *ACS* are DR cost (*ΔLC*) and total carbon emission cost (*TEC*).

$$TICC = IC_{PV} + IC_{DG} + IC_{RO} + ICW_{TK} \quad (4.28)$$

$$TMC = AMC_{PV} + AMC_{DG} + AMC_{RO} \quad (4.29)$$

$$ACS = TICC * CRF + TMC + AC_{MR} * CRF + AC_{CH} + CGP + FC_{DG} + \Delta LC + TEC \quad (4.30)$$

where:

$$CRF = \frac{i(1+i)^n}{(1+i)^n - 1} \qquad n = 1 \dots 19 \quad (4.31)$$

$$CQW = {}^{ACS}/_{\sum QW(t)} \quad (4.32)$$

$$LCOE = \frac{ACS + P_{WD}(t)}{\sum P_{PV}(t) + Pg(t) + GP_i(t)} \quad (4.33)$$

$$\forall t = 1,2,3 \dots 8760$$

The optimization problem is formulated as a multi-objective linear programming problem as expressed in (4.34), with the objective of minimizing the ACS and carbon emission while maximizing the quantity of freshwater production subject to constraints expressed by (4.35) - (4.39). The weighting factors (w_1 = 0.3, w_2 = 0.5 and w_3 = 0.2) were allocated based on the preference of major concern, with the GWI of emission ranking highest, then ACS and quantity of water produced ranking lowest, since meeting water demand is more important than excess water production. This multi-optimization problem is solved using the CPLEX solver of AIMMS.

Objective Function

$$Min \left[w_1 * ACS + w_2 * \sum GWI - w_3 * \sum QW(t) \right] \quad (4.34)$$

S.t.

$$P_{PV}(t) + Pg(t) + GP_i(t) = P_{WD}(t) + \Delta L(t) + GP_e(t) \quad (4.35)$$

$$QW(t) \geq WD(t) \quad (4.36)$$

$$QW^{min} \leq QW(t) \leq QW^{max} \quad (4.37)$$

$$P_{WD}{}^{min} \leq P_{WD}(t) \leq P_{WD}{}^{max} \quad (4.38)$$

$$\forall t = 1,2,3 \ldots 8760$$

$$APV \geq 0 \quad (4.39)$$

Constraint (4.35) expresses the power balance that ensures that power supply from PV, a DG and the grid at any time, *t*, equals the total demand by the RO desalination unit and the power exported to the grid at the same time *t*. Constraint (4.36) is water balance that ensures that the water produced at any hour, t, equals or is in excess of water demand at that hour *t*, while constraint (4.37) ensures that water produced per hour remains within required limit. Constraint (4.38) is the limit of power required to produce water at any time t and constraint (4.39) expresses the limit of area of PV. Other constraints include (4.1), (4.2), (4.3), (4.4) and (4.9), which express the limit of grid imported power, limit of grid exported power, maximum allowable transfer power and limit of DR load respectively. Furthermore, constraint (4.11) ensures even distribution of load shift. Model's flowchart is similar to that of Figure 3.1.

4.6 Case Study

This chapter presents three case scenarios; Case 1 is an RO desalination system powered by conventional grid power source, Case 2 has grid and diesel generator whilst Case 3 combine grid, diesel generator and photovoltaic. The three Cases were model with and without TOU DR program incorporated.

4.7 Results and Discussion

4.7.1 Results

Figure 4.1 shows the hourly power supply from the grid with or without TOU DR, while Figure 4.2 represents the hourly power output from the energy supply mix of Case 2 and the excess power exported to the grid. Figure 4.3a represents the hourly power supply mix for Case 3, while Figure 4.3b depicts the difference between the load curve before and after the application of the DR program. The volume of hourly water produced by each case is as shown in Figure 4.4, while Table 4.1 is the summary of the results.

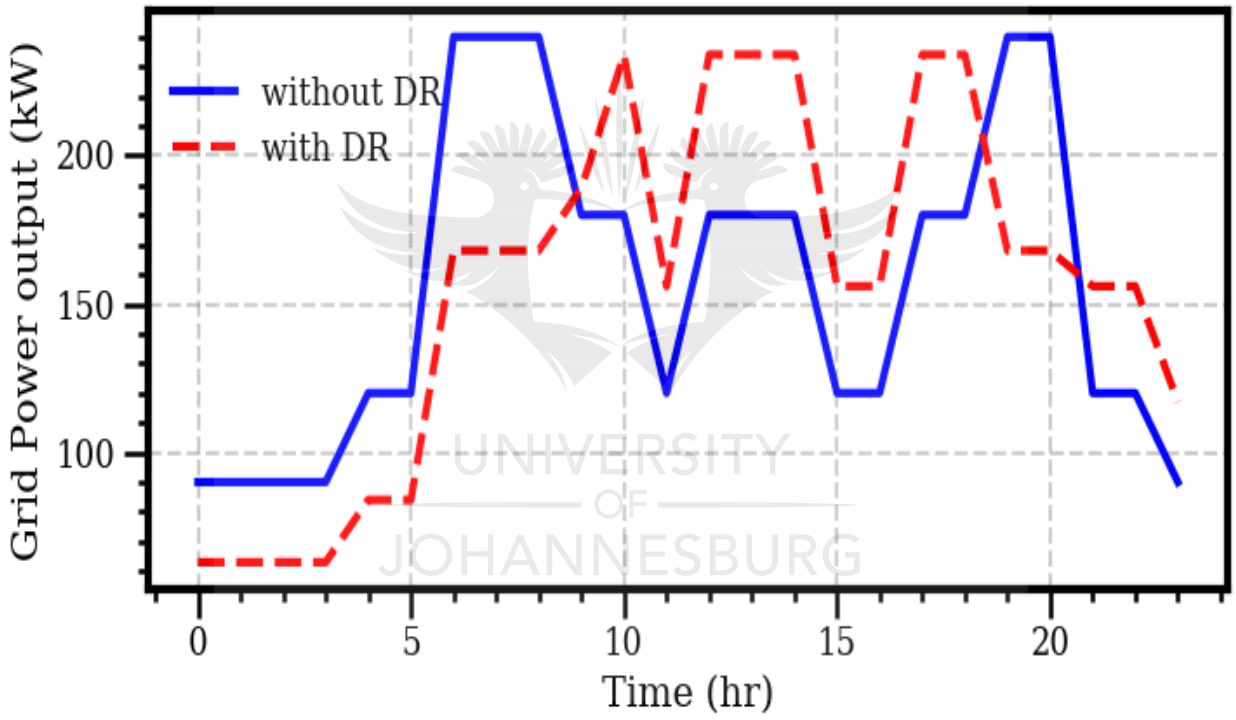

Fig. 4.1 Case 1 hourly energy dispensed

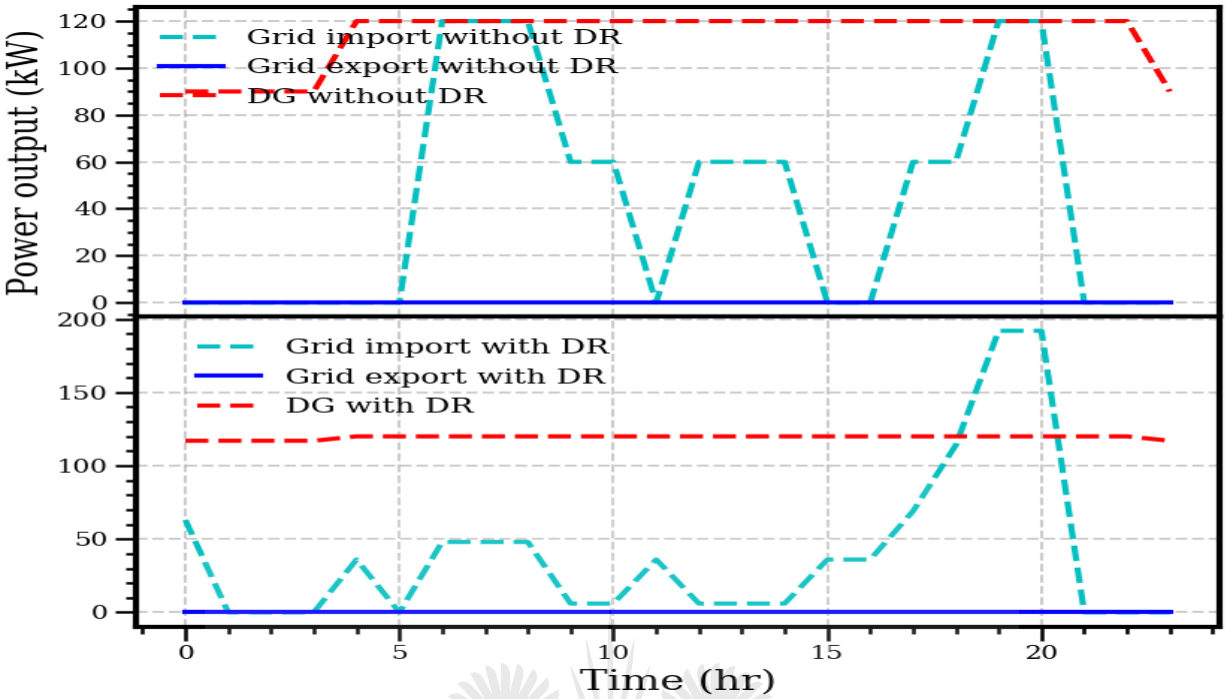

Fig. 4.2 Case 2 hourly energy dispensed

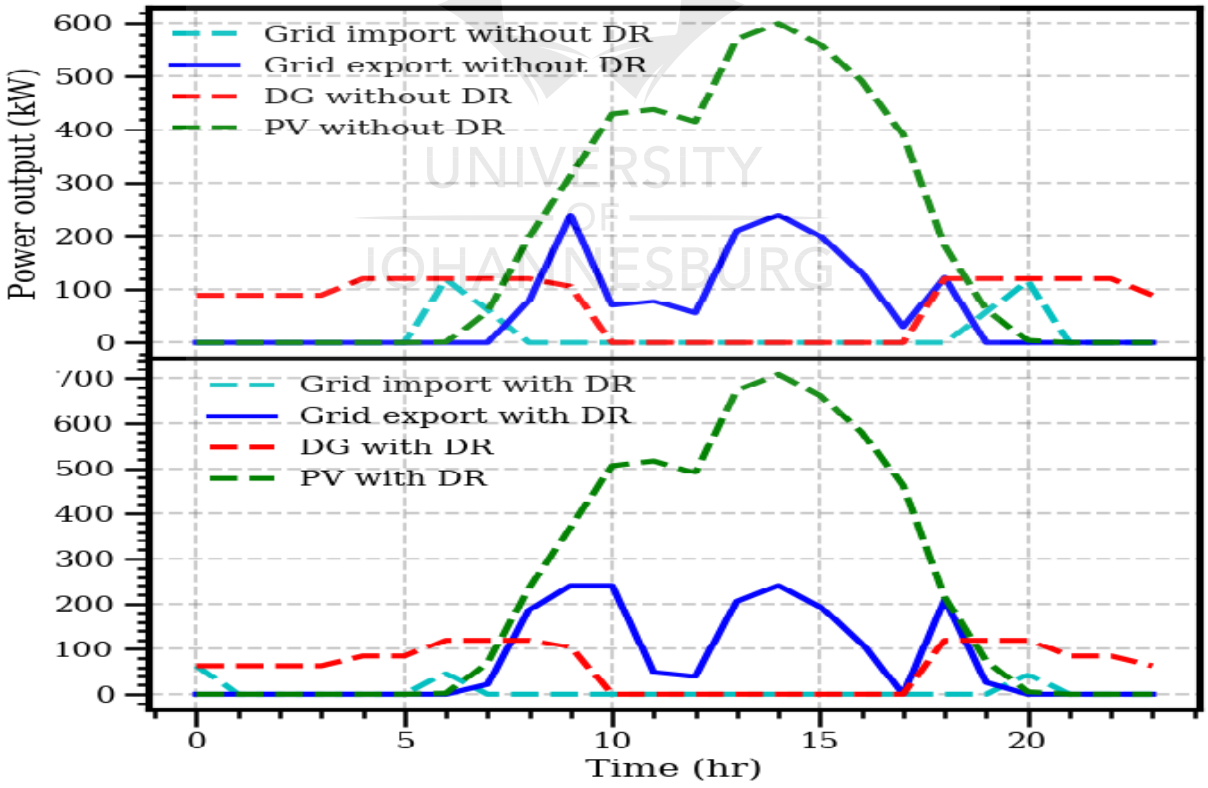

Fig. 4.3a Case 3 hourly energy dispensed

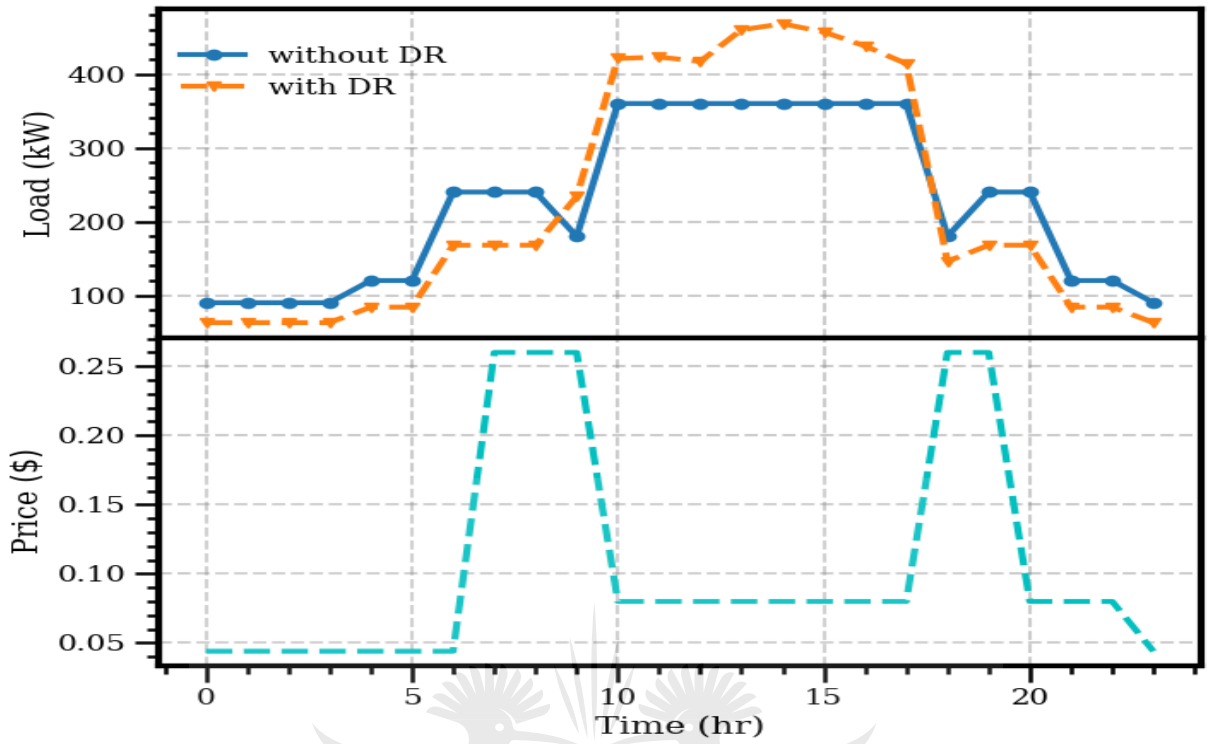

Fig. 4.3b Case 3 hourly load curve with and without DR program compared with hourly price of power

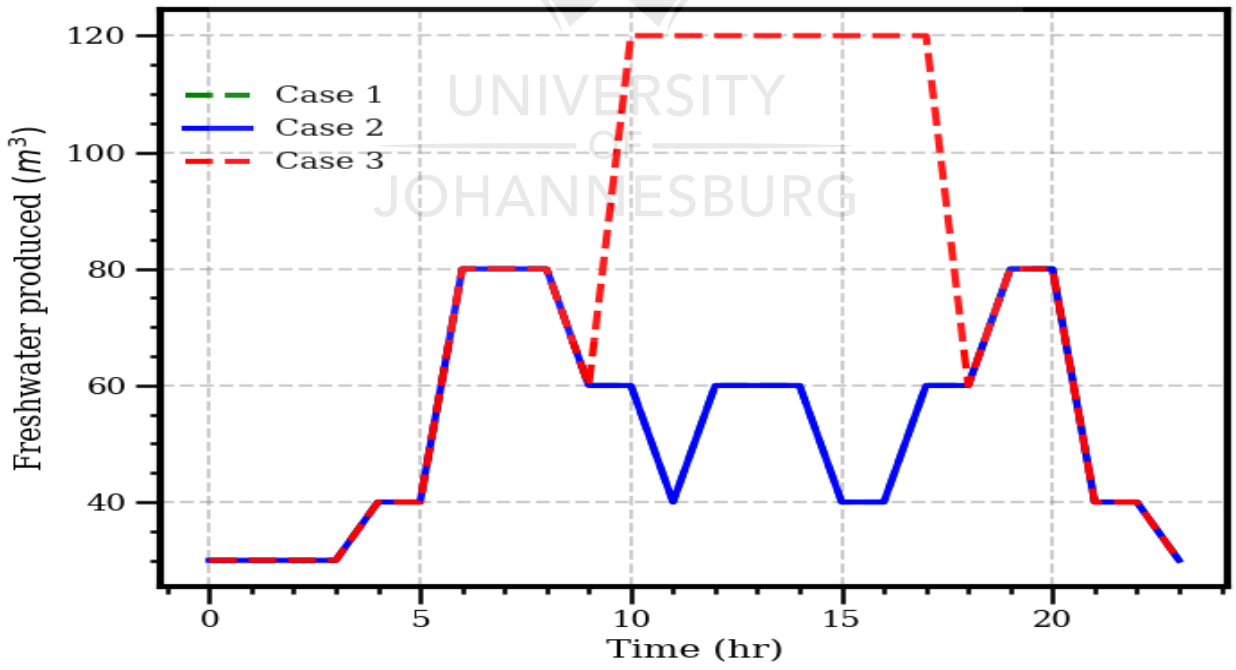

Fig. 4.4 Comparison of hourly freshwater production quantity

Table 4.1: Summary of power outputs

Optimized power output (kWh)	Case 1: Grid only		Case 2: Grid and DG		Case 3: Grid, DG and PV	
	Without DR	With DR	Without DR	With DR	Without DR	With DR
Grid import power	3750	3750	1020	885	354	89.2
Grid export power	-	-	-	-	1461	1765
DG output power	-	-	2730	2865	1756	1475
PV output power	-	-	-	-	4721	5571

Table 4.2: Summary results of cost parameters

Optimized Cost ($)	Case 1: Grid only		Case 2: Grid & DG		Case 3: Grid, DG & PV	
	Without DR	With DR	Without DR	With DR	Without DR	With DR
Grid import cost	168236	161140	59743	51544	16652	1993
Grid export cost	-	-	-	-	71677	96335
DG fuel cost	-	-	334260	346578	245398	219712
Grid emission cost	600471	600471	163328	141711	56691	14276
DG emission cost	-	-	342616	342616	251533	251533
Total emission cost	600471	600471	505944	493019	308224	265809

Table 4.3: Summary of optimized results

Optimized parameters	Case 1: Grid only	Case 2: Grid and DG	Case 3: Grid, DG and PV

	Without DR	With DR	Without DR	With DR	Without DR	With DR
ACS ($)	1203524	1203524	1337972	1326506	1255694	1158801
Emission ($kgCO_{2-e}$)	1464563	1464562	1234010	1181286	751766	648315
Daily water produced (m^3)	1250	1250	1250	1250	1790	1790
LCOE ($/kWh)	1.88	1.88	1.98	1.97	1.29	1.20
Cost of water ($/$m^3$)	2.64	2.64	2.93	2.91	1.92	1.77

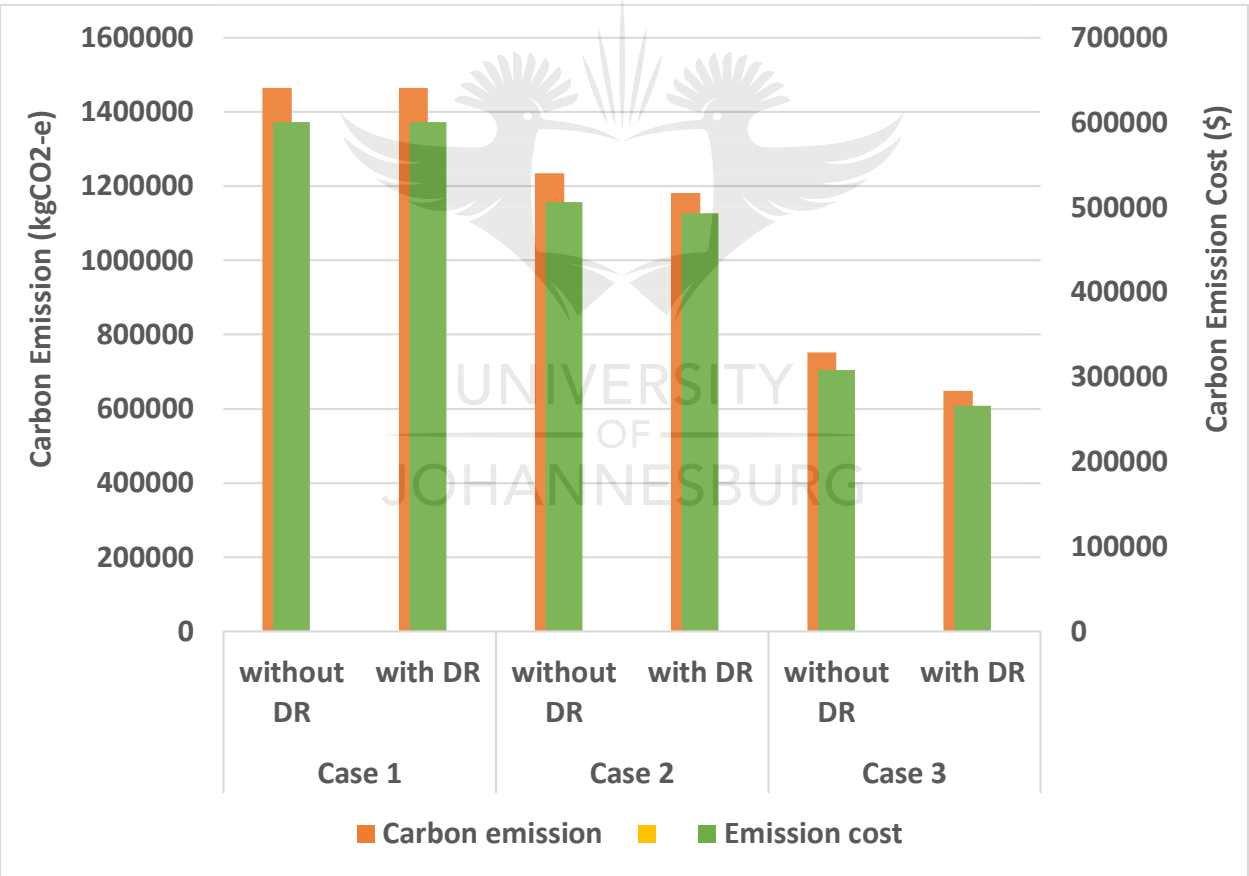

Fig. 4.5 Comparison of emission produced and the associated cost for the three cases

4.7.2 Discussion of Results

The results from Case 1, depicted as Figure 4.1, show the impact of TOU DRs in shifting load from peak hour to off-peak hour, thus reducing the cost of power imported from the grid. The grid power imported cost is reduced from $168 236 to $161 140, as shown in Table 4.2. Compared to Case 2, Case 1 has lower ACS, LCOE and lower cost of water production, since it depends on only the grid power supply, but the high carbon emission of 146 562 $kgCO_{2\text{-}e}$ and its associated cost of $600 471as reflected in Figure 4.5 are discouraging.

Results from Case 2 show a significant reduction of grid imported power compared to Case 1 in Figure 4.2 and Table 4.1. This reduction is a result of power distribution between the grid and DG. Further reduction is achieved with the TOU DR program. DR, therefore, optimally reschedules power supply from the grid and DG to minimize carbon emission and cost. Case 2, therefore, with its highest ACS, LCOE and cost of water production, has lower carbon emission and emission cost of 1 234 010 $kgCO_{2\text{-}e}$ and $505 944, respectively, compared to those of Case 1. These values are further reduced by DR to 1 181 286 $kgCO_{2\text{-}e}$ and $493 019, as shown in Figure 4.5 and Table 4.3 and 4.2.

Case 3, which is an RO desalination system powered by the grid, DG and RES (PV), shows very significant improvement in the reduction of carbon emission and total system cost. The power output from Case 3, as represented in Figure 4.3a, shows a large reduction in grid-imported power to only two hours a day, with a total output of 354 kW and a further reduction by DR to 89.2 kW. Furthermore, there is a reduction in the output power from DG when comparing Case 3 to Case 2. These reductions in grid imported power and DG power output are a result of the integration of a RES (PV), which tends to have a high power output at certain hours of the day. This has also led to excess total power output, which is sold back to the grid.

Other than the reduction of power supply from the grid and DG as a result of the integration of a RES and TOU DR in Case 3, the impact of the DR program is shown in the reduction of carbon emission and its cost, as reflected in Figure 4.5. The demand curve in Figure 4.3b also shows load shift from peak hours to off-peak hours and the subsequent optimized result compared to Case 1 and 2 is shown in Tables 2 and 3. Case 3 proves to produce more freshwater than Cases 1 and 2, producing, on average, a daily volume of 1 790 m^3 at a minimal unit cost of 1.92 $/$m^3$ without DR and 1.77 $/$m^3$ with DR incorporated. Furthermore, Table 4.2 shows that Case 3 has the lowest annual DG fuel cost, lowest annual grid power imported and is the only case with exported grid power cost, hence lowest ACS. Therefore, the LCOE and cost of water produced in Case 3 are lower than those of Cases 1 and 2; consequently, Case 3 produces more freshwater at a lower cost than Case 1 and Case 2, as shown in Table 4.3.

4.8 SUMMARY

In this study, a mathematical optimization model is formulated using a conventional grid and DG in comparison with a system that integrates PV, a RES, to power an RO desalination unit. The model is formulated to include a balance between power supply and demand, water demand and water production, cost functions and the TOU DR program. The cost functions include carbon emission cost, DR cost and the cost of components. The objective of the optimization model is to minimize the ACS and carbon emissions while maximizing the quantity of freshwater production subject to different economic and system reliability constraints. The model is implemented on three case scenarios: Case 1 is a system with only the grid as the energy source, Case 2 has the grid and a DG, while Case 3 combines the grid, a DG and PV. The economic impact of the integration of RES and a DR program was examined. The techno-economic analysis of the three cases was performed using LCOE, COW and ACS cost matrices and the results were compared.

The results showed that Case 3 offered a very significant improvement in the reduction of carbon emission and the total system cost. Case 3 is therefore recommended as the ideal optimization model for the RO desalination system, having proven that more freshwater can be produced at minimal cost. This submission gives credence to RES as viable alternatives to fossil fuel power sources. On the other hand, the inclusion of the DR program enhances the optimal schedule of energy supply to satisfy the demand of the desalination unit while minimizing cost and carbon emission and maximizing freshwater production.

CHAPTER 5

OPTIMAL DESIGN AND TECHNO-ECONOMIC EVALUATION OF A RENEWABLE ENERGY POWERED COMBINED REVERSE OSMOSIS DESALINATION AND BRINE TREATMENT UNIT

5.1 Introduction

Continuous growth in the population, constant water pollution and other water stress have made freshwater scarcity a serious problem around the world [15]. Treatments such as water reuse and seawater desalination have become prominent in recent years owing to the abundant availability of seawater around the world [16]. Seawater usually contains a large deposit of salt, making it difficult and unhealthy to drink. Desalination is the separation of freshwater from seawater (in other cases, brackish water), leaving behind more concentrated saline water known as brine. Indiscriminate brine disposal is harmful to the environment. Furthermore, most desalination plants around the world still largely depend on fossil energy sources, especially convectional grid generators. The direct consequence of this is high GHG emission, which has cost implications alongside its environmental impacts. The cost implications of emitted carbon gas and brine management are considered the external costs of desalination [17]. Therefore, the main challenges of seawater desalination are energy requirements and brine management. These challenges make seawater desalination quite expensive, both in terms of cost and the environmental impact of the energy supply source and brine disposal. Hence, efficient energy supply and brine management are crucial to carbon emission reduction [208] and cost evaluation of desalination.

To deal with these challenges, RES have been highly exploited and integrated into desalination systems to cut down the cost and gas emission of conventional fossil energy supply [181]; [171].

The thermal process of desalination is more energy- and cost-intensive than the membrane process, hence the predominant use of the RO technique. One major limitation of the RO method is the volume of brine (concentrate) produced during the desalination process [212]. Different brine management approaches have been proposed, and some have been implemented [15]; [212]; [213]. Most available brine treatment technologies such as desalination technologies are thermal-based or membrane-based. Most often, the same techniques are used in a specific combination for both desalination and brine treatment. In this study, RO is used for desalination while ED and crystallizer (CRY) are used for further treatment of the concentrate. ED, being a membrane technology, is cost-effective for brine treatment, as it uses ion selectivity to separate freshwater further from the concentrate. This process does not entirely convert the brine to potable water and salt. Its performance is limited by scaling soluble salt on the membrane. Therefore, further treatment of the highly concentrated brine is required. The crystallization of the remaining volume of brine can lead to zero brine discharge, as the resulting product will be crystals of salt and evaporated freshwater, which can be condensed and collected for drinking. The feasibility of RO-ED-CRY was presented by reference [108], and a framework for a cost and energy needs model was established. A comparison of RO-ED-CRY and the same system that includes a two-stage high-pressure RO (HPRO) was made; the results show that adding HPRO is uneconomical.

For sustainability and environmental friendliness, when considering seawater desalination, the cost and proper management of energy supply and brine production must be taken into consideration[214]. The contribution of this chapter is, therefore to (i) Evaluate the optimal cost of the freshwater output considering carbon emission, DR and brine treatment cost, (ii) Minimize the impact of carbon emission; (iii) Maximize freshwater production, and (iv) Minimized the brine discharged. Thus, the remainder of this chapter is organized such that section II details system

models; section III presents a case study; section IV presents and discusses the results, while section V Summarizes the Chapter.

5.2 System Models

5.2.1 System Architecture

Figure 5.1 describes the system design, which has two basic sections: (i) The power section, which integrates the RES of wind and PV with grid power, and (ii) The desalination and brine treatment section, which integrates the RO, ED and CRY units. The power sources are optimally scheduled with TOU DR and consider carbon emission to achieve minimal LCOE, whereas the desalination and brine treatment section is designed such that the RO unit desalinates 40% of the feedwater (seawater) to freshwater, leaving 60% as brine on the bases of equation 5.19-5.21 adopted from [16] and [213]. This brine is passed into the ED, which further desalinates 20% of the feedwater into freshwater (i.e., 33.3333% of the brine passed into ED), leaving a more concentrated brine in the CRY unit. The crystallization unit evaporates 10% of the feed water (16.6667% of the original brine from RO), which is condensed and collected as additional freshwater. The remaining 30% of the feedwater (which is 50% of the original brine from RO) forms crystals of salt, leaving zero discharge.

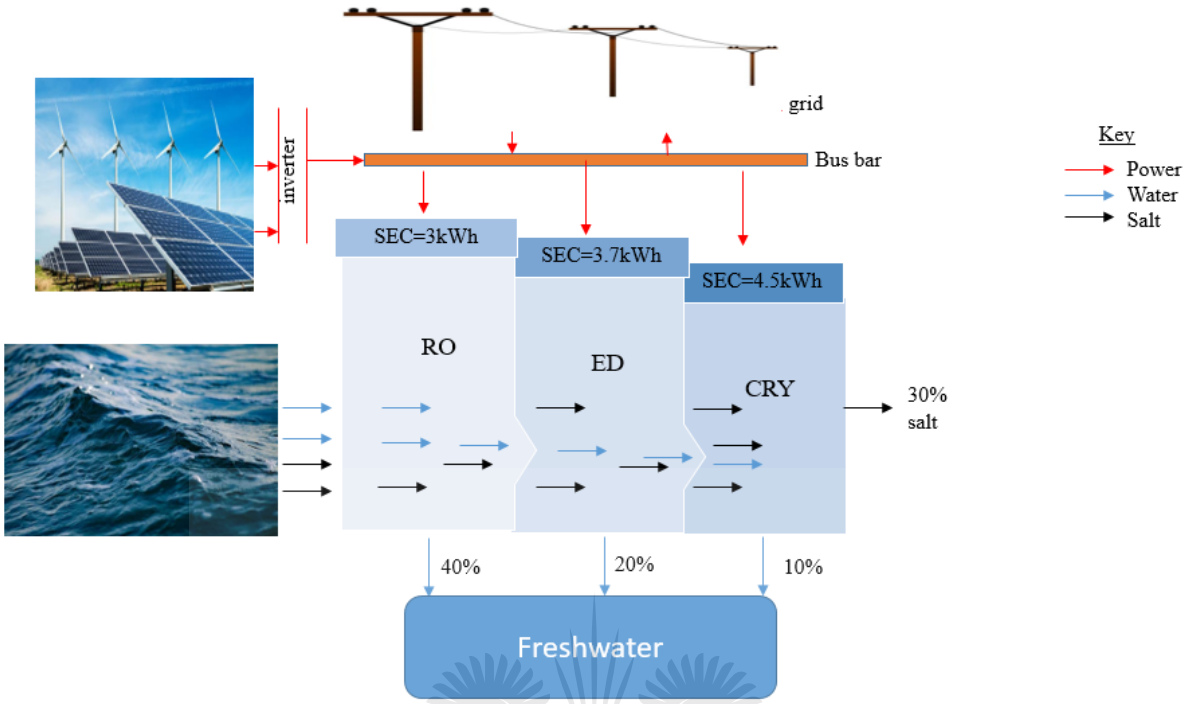

Fig. 5.1 Schematic diagram of combined desalination and brine treatment process

5.2.2 Grid Power and Cost Model

The $GP_i(t)$ imported from the grid and the $GP_e(t)$ exported to the grid are optimized variables ranging from zero to maximum hourly load demand by the RO unit, as expressed in (5.1) and (5.2) respectively.

$$0 \leq GP_i(t) \leq GP_i^{max} \tag{5.1}$$

$$0 \leq GP_e(t) \leq GP_e^{max} \tag{5.2}$$

The maximum transferable power to and from the grid is assumed equal:

$$GP_i^{max} = GP_e^{max} \tag{5.3}$$

The cost of grid power is the function of the difference between grid imported cost and grid exported cost.

$$CGP_i(t) = GP_i(t) * P(t) \quad (5.4)$$

$$CGP_e(t) = GP_e(t) * P(t) \quad (5.5)$$

$$CGP = \sum(CGP_i(t) * P(t) - GP_e(t) * P(t)) \quad (5.6)$$

$$\forall t = 1,2,3, \dots 8760$$

where:

P(t) is the hourly unit price of transferable grid power and *CGP* is the total annual cost of transferable grid power.

5.2.3 Renewable Energy Sources and Cost Model

5.2.3.1 PV power and cost model

The hourly output power ($P_{PV}(t)$) supply by the PV array is given as [199]; [200]

$$P_{PV}(t) = APV * \acute{\eta} * SI(t) \quad (5.7)$$

The initial capital cost and annual maintenance cost of PV are expressed as:

$$IC_{PV} = APV * C_{PV} \quad (5.8)$$

$$AMC_{PV} = APV * MC_{PV} * r \quad (5.9)$$

5.2.3.2 Wind power and cost model

The hourly power output of the wind generator ($W_p(t)$) is given as [199].

$$W_p(t) = \frac{1}{2} * \acute{\eta}_w * \rho_{air} * C_p * AWT * V(t)^3 \quad (5.10)$$

where $\acute{\eta}_w$ is the efficiency of the wind generator, ρ_{air} is the air density; C_p is the power coefficient, *AWT* is the swept area of the wind turbine and *V(t)* is the hourly wind speed given as [215]:

$$V(t) = V_R * \left[\frac{h}{h_R}\right]^{\propto} \quad (5.11)$$

where V(t) is the hourly speed at projected height (h), V_R is the hourly speed at reference height (h_R) and α is the power law exponent equivalent to 1/7.

The economics of using wind power for desalination is similar to those of PV and in this study these are analyzed based on the initial capital cost (IC_{WT}) and total maintenance cost (TMC_{WT}), depending on the area of the wind turbine, as follows:

$$IC_{WT} = AWT * C_{WT} \quad (5.12)$$

$$AMC_{WT} = AWT * MC_{WT} * r\,. \quad (5.13)$$

5.2.4 RO Desalination Plant Power Demand and Cost Model

The $P_{WD}(t)$ of the RO desalination unit is expressed as:

$$P_{WD}(t) = QW_{RO}(t) * SEC \quad (5.14)$$

The daily water production capacity is given as:

$$DQW = \sum_{t=1}^{24} QW_{RO}(t) \quad (5.15)$$

The W_{TK} is formulated as:

$$W_{TK} = DQW * 2 \quad (5.16)$$

The RO desalination initial capital cost (IC_{RO}), and water tank cost (CW_{TK}) are expressed as;

$$IC_{RO} = C_{RO} * DQW \quad (5.17)$$

$$ICW_{TK} = CW_{TK} * W_{TK} \quad (5.18)$$

5.2.5 Brine Treatment Power Demand Model

The brine treatment section includes the ED and crystallization units. The volumetric quantity of brine produced (*QB*) from the RO plant depends on its water production capacity and water recovery ratio (*RR*), expressed as [16]:

$$DQB = \frac{DQW}{RR} * (1 - RR) \tag{5.19}$$

where RR is the percentage of volume freshwater produced by the RO desalination to the volume of saline feed water (*QF*) [213]; it is assumed to be 40% in this study.

$$RR = \frac{QW}{QF} * 100 \tag{5.20}$$

This implies that QB can also be calculated as [213]:

$$QB = QF - QW \tag{5.21}$$

Equation (5.19) is modified to consider hourly brine production as:

$$QB(t) = \frac{QW_{RO}(t)}{RR} * (1 - RR) \tag{5.22}$$

Therefore, the hourly power demand ($P_B(t)$) of the brine treatment unit depends on the sum of SEC by ED and the crystallization unit, which in this study are adapted from [108] and [216] as 3.7 kwh/m^3 and 4.5 kwh/m^3 respectively. Hence,

$$P_B(t) = QB(t) * SEC \tag{5.23}$$

For a zero brine discharge, the brine from the RO unit, when passed through the ED unit, produces some quantities of freshwater (20% of the brine, in this study) and a more concentrated brine, which is further passed into the crystallizer. This also produced some quantities of freshwater (in this case, 10% of the total brine from the RO unit), and the remaining amounts of brine are

crystallized salt and other compounds. Thus, the total freshwater produced from the combine RO-ED-CRY system is given as:

$$TQW(t) = QW_{RO}(t) + QW_{ED}(t) + QW_{CRY}(t) \quad (5.24)$$

5.2.6 TOU Demand Response Load and Cost Model

The maximum allowable demand variation (increase/decrease) per hour is assumed to be 30% of total demand at that hour. The DR load is an optimized variable expressed as:

$$-\Delta L^{max}(t) \leq \Delta L(t) \leq \Delta L^{max}(t) \quad (5.25)$$

where:

$$\Delta L^{max}(t) = 0.3 * [P_{WD}(t) + P_B(t)] \quad (5.26)$$

Furthermore, for even distribution of load shift, cut-off demand at certain hours of the day equals an increase in demand at other hours of the day, expressed as:

$$\sum_{t=1}^{24} \Delta L(t) = 0 \quad (5.27)$$

The cost of DR is the difference between the cost of power demand before and after load variation due to DR. It is expressed as [205]

$$\Delta LC = \sum \left[(P_{WD}(t) + P_B(t)) * \lambda(t) - \left((P_{WD}(t) + P_B(t)) - \Delta L(t) \right) * \lambda(t) \right] \quad (5.28)$$

$$t = 1,2,3, \ldots 8760$$

5.2.7 Carbon Emission Cost and Global Warming Impact of Energy Source

The *GWI*, in other words, carbon emission of fossil-fuel energy source, could be due to construction or operation of the plant, with the impact due to operation exceeding that due to

construction by multiple orders [208]. Thus, this study considered the impact due to operation as adopted by authors of reference [208]. The authors define *GWI* as the summation of input power $P_{j,t}$ of every fossil-fuel unit j in every time step $t \in T$ multiplied by specific operational emission factor $SEF_{j,t}$ and the period Δt_t of time the step represented as:

$$GWI_g = \sum_{t \in T} \left[\Delta t_t \sum_j SEF_{j,t} * P_{j,t} \right] \tag{5.29}$$

where:

$$SEF_{j,t} = \frac{emission\ due\ to\ electrical\ energ\ genarated}{electrical\ energ\ genarated} \tag{5.30}$$

In order to estimate carbon emission cost, the formulated model given by references [17] and [209] was adopted as:

$$CE\ \left(\frac{\$}{m^3}\right) = Energy\ supply\ \left(\frac{kwh}{m^3}\right) * Emission\ factor\ \left(\frac{kgCO_{2-e}}{kwh}\right) *$$

$$Carbon\ tax\ \left(\frac{\$}{kgCO_{2-e}}\right) \tag{5.31}$$

The grid-specific emission factor and carbon tax depend on the country of location of the plant. This study adopted the calculated emission factor for South Africa by reference [210]. The value of the emission factor is 1.069 $kgCO_2$/kwh. The new South African carbon tax rate ranges from R6-R48 ($0.40-$3.17) [211]. The lowest value of $0.40 is considered in this study.

5.2.8 Optimization Problem Formulation

In this study, the ACS matrix is used for the economic evaluation of the RO desalination system powered by a grid and RES to determine the cost of freshwater and the LCOE. The *ACS* involves the *CRF* and the total system cost, which includes *TICC* and TMC of all the components that make

up the system [168];[206]; [207]. Also included in the ACS is DR cost (ΔLC) and total carbon emission cost (EC).

$$TICC = IC_{PV} + IC_{WT} + IC_{RO} + IC_{ED} + IC_{CRY} + ICW_{TK} \quad (5.32)$$

$$TMC = AMC_{PV} + AMC_{WT} + AMC_{RO} + AMC_{ED} + AMC_{CRY} \quad (5.33)$$

$$ACS = TICC * CRF + TMC + AC_{MR} * CRF + AC_{CH} + CGP + \Delta LC + EC \quad (5.34)$$

where:

$$CRF = \frac{i(1+i)^n}{(1+i)^n - 1} \qquad n = 1 \dots 19 \quad (5.35)$$

n is the number of years in the lifetime of the system of which the interest rate *i* is considered.

$$COP = {}^{ACS}/_{\sum TQW(t) + Saltp} \quad (5.36)$$

$$LCOE = \frac{ACS + P_{WD}(t) + P_B(t)}{\sum P_{PV}(t) + W_p(t) + GP_i(t)} \quad (5.37)$$

$$\forall t = 1,2,3 \dots 8760$$

The optimization problem is formulated as a multi-objective linear programming problem as expressed in (5.38), with the objective of minimizing the ACS and carbon emission while maximizing the quantity of freshwater production subject to constraints expressed by (5.39) - (5.44). The weighting factors (W_1, W_2, W_3 and W_4) were allocated based on the preference of significant concern, with the GWI of emission ranked highest. The ACS and quantity of water produced rank lowest, since meeting water demand is more excess water production. This multi-optimization problem is solved using the CPLEX solver of the AIMMS.

Objective Function

$$Min\left[w_1 * ACS + w_2 * \sum GWI + w_3 * \sum QB(t) - w_4 * \sum TQW(t)\right] \quad (5.38)$$

S.t.

$$P_{PV}(t) + W_p(t) + GP_i(t) = P_{WD}(t) + P_B(t) + \Delta L(t) + GP_e(t) \quad (5.39)$$

$$TQW(t) \geq WD(t) \quad (5.40)$$

$$QW^{min} \leq QW_{RO}(t) \leq QW^{max} \quad (5.41)$$

$$P_{WD}{}^{min} \leq P_{WD}(t) \leq P_{WD}{}^{max} \quad (5.42)$$

$$\forall t = 1,2,3 \ldots 8760$$

$$APV \geq 0 \quad (5.43)$$

$$AWT \geq 0 \quad (5.44)$$

Constraint (5.39) expresses the power balance that ensures that power supply from PV, a wind generator and the grid at any time t equals the total demand by the RO desalination and brine treatment unit and the power exported to the grid at the same time t. Constraint (5.40) is a water balance that ensures that the total amount of water produced at any hour t is equal to or in excess of the water demand at that hour t, while constraint (5.41) ensures that the water produced per hour remains within the required limits. Constraint (5.42) is the limit of power required by RO to produce water at any time t, and constraint (5.43) expresses the limit of the area of PV while constraint (5.44) limits the area of the wind turbine. Other constraints include (5.1), (5.2), (5.3) and (5.25), which express the limit of grid imported power, limit of grid exported power, maximum allowable transfer power and limit of the DR load respectively. Constraint (5.27) also ensures even distribution of load shift. Model's flowchart is similar to that of Figure 3.1.

5.3 Case Study

In this chapter, as in previous chapters, the metrological data from Stellenbosch University, Western Cape province of South Africa, is used, including the hourly wind speed, as represented in Figure 5.2.

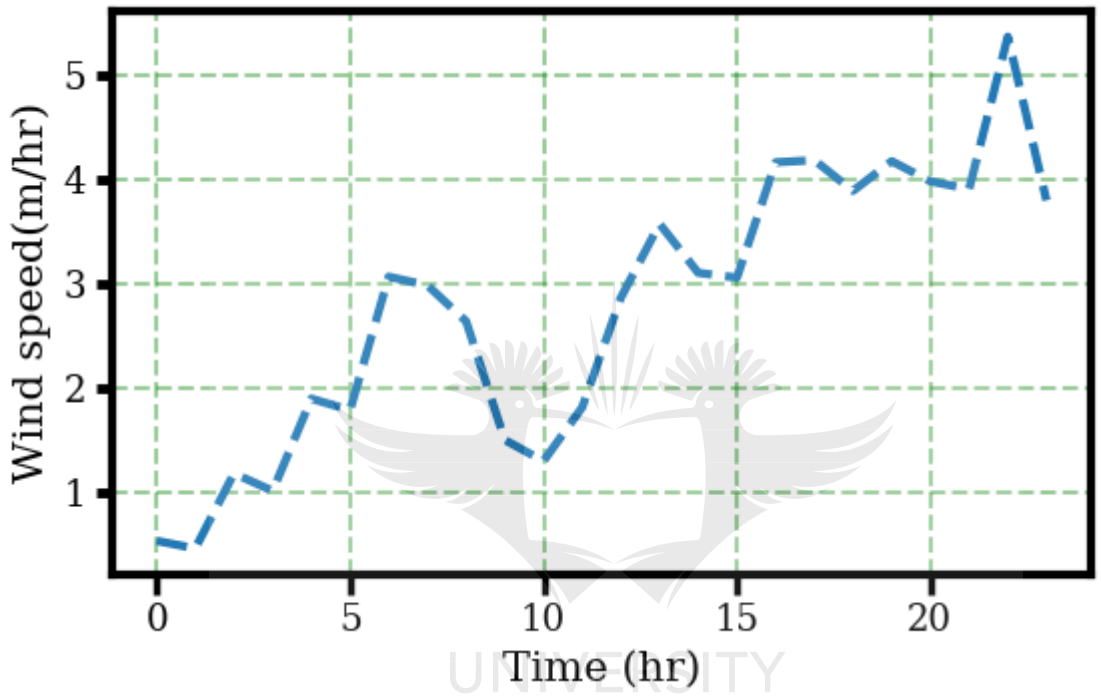

Fig. 5.2 Hourly wind speed

5.4 Results and Discussion

5.4.1 Results

Figure 5.3 shows the hourly power supply and power sold back to the grid, the power from the wind generator and the power output of the PV generator. A simulation of an average day is used for the sake of simplicity. Figure 5.4 depicts the hourly volume of freshwater produced from the three units, RO, ED and CRY. Figure 5.5 represents the hourly volume of brine, freshwater and salt produced, while Table 5.1 is the summary results of the other optimized parameters.

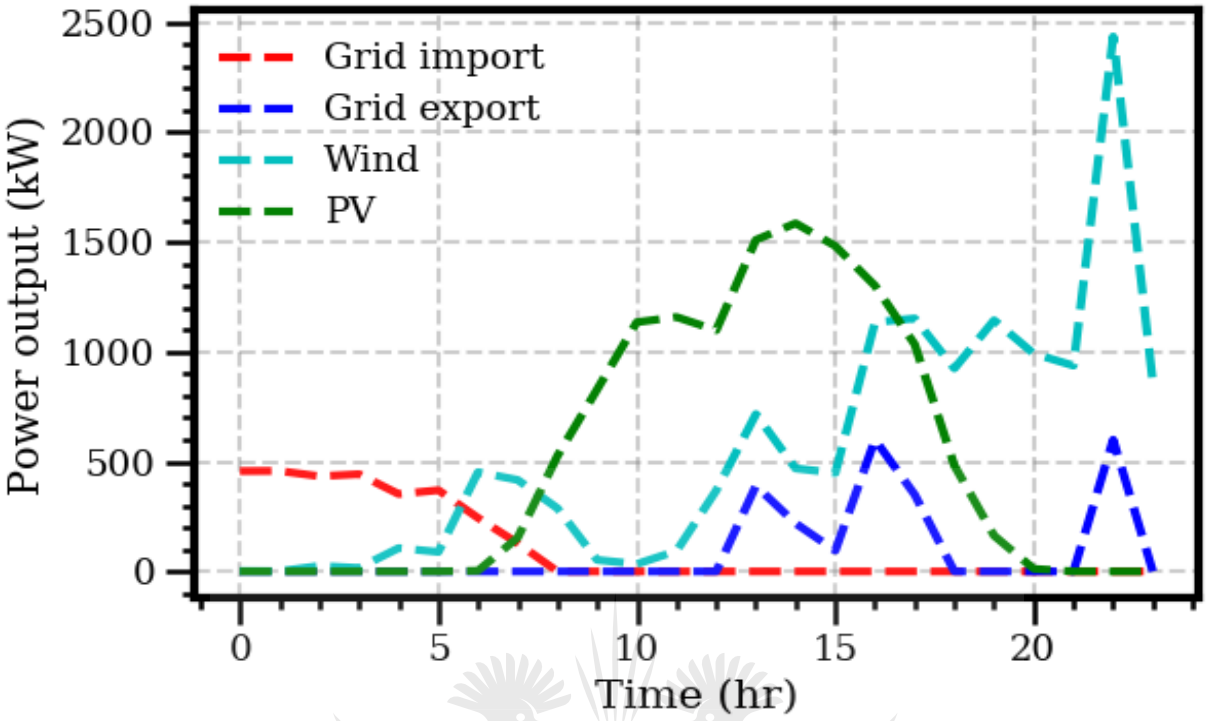

Fig. 5.3 Hourly energy dispensed

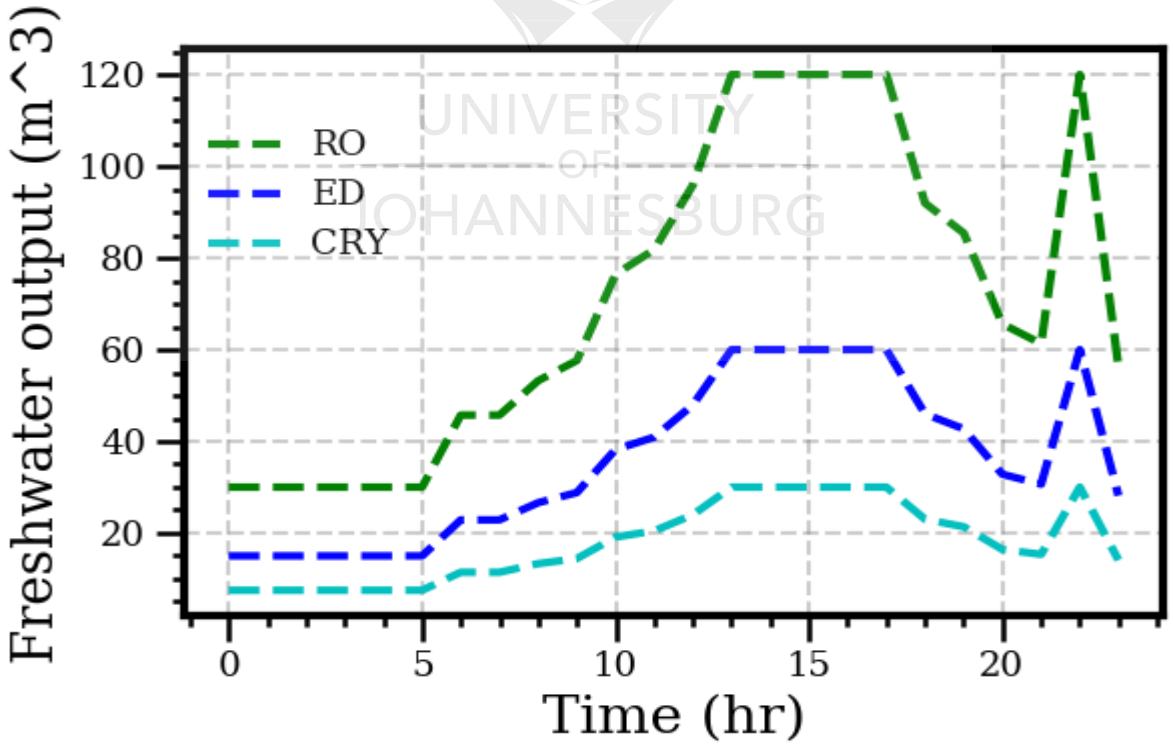

Fig. 5.4 Hourly freshwater dispensed

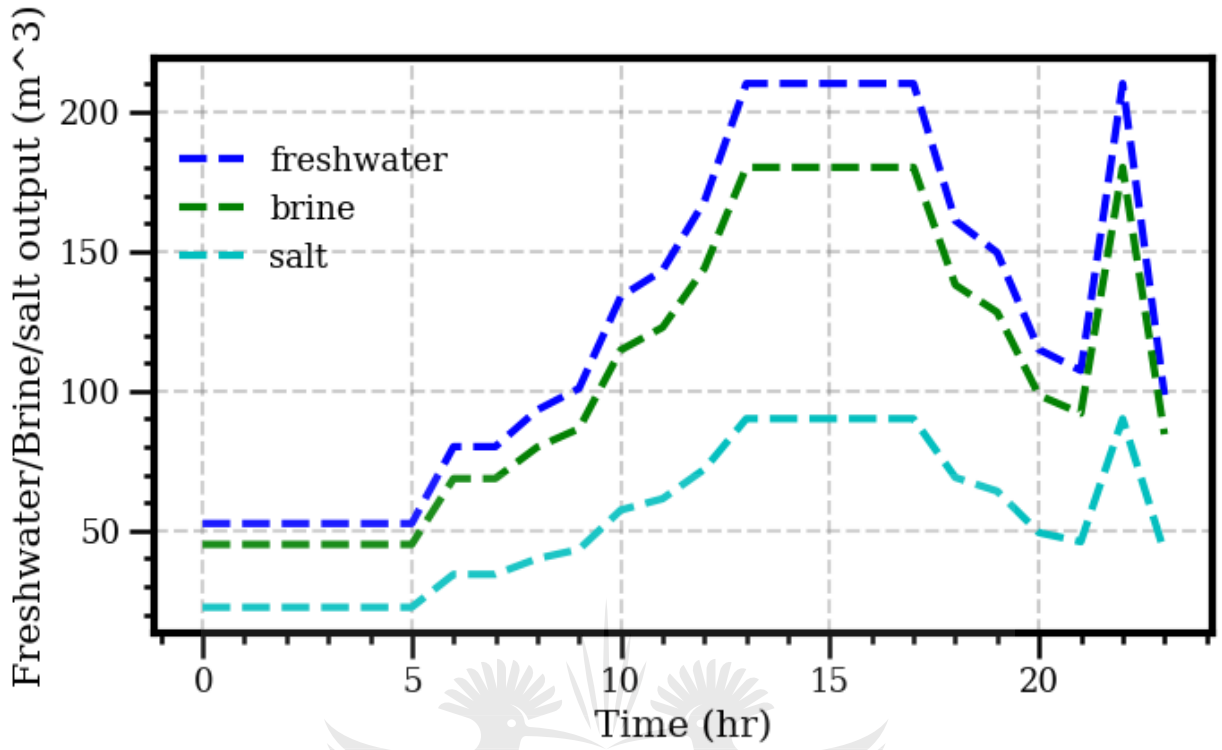

Fig. 5.5 Hourly freshwater, brine and salt produced

Table 5.1: Summary results of optimized parameters

ACS ($)	Emission ($kgCO_{2\text{-}e}$)	Emission cost ($)	Daily water produced (m^3)	Daily salt produced (m^3)	LCOE ($/kW)	Unit cost of production of freshwater and salt ($/$m^3$)	APV (m^2)	AWT (m^2)
1 401 367	637 708	261 460	3 005	1 288	0.89	1.056	9 431	50 891

5.4.2 Discussion

The result represented in Figure 5.3 shows the impact of TOU DR in shifting load from peak hours to off-peak and standard hours for cost-effective energy management. The selection of the energy sources and the subsequent power output depends on the cost and the carbon emission of the energy source, hence the resulting low power output from the grid, which depends mainly on fossil fuel generators. The carbon emitted from the grid generator comes at a cost (261 460 $/year), therefore increasing the cost of grid power supply. This gives the advantage to the RES (wind and PV generators), hence the high power output from the two sources.

The hourly volume of freshwater produced by the three units (RO, ED and CRY), as depicted in Figure 5.4, shows that the RO unit, which is the main desalination unit, produces the highest quantity of freshwater, followed by the ED unit. The crystallization unit produces only a small volume of freshwater, since the larger volume of brine passed into it has a high concentration of salt. The crystallization process is, therefore, the main brine treatment unit producing soluble salts and a small volume of freshwater, leaving zero brine discharge.

The total potable water produced from RO-ED-CRY at every hour of the day alongside the hourly brine production from the RO unit, as well as the salt produced from the brine, is shown in Figure 5.5. This result indicates that a large volume of the feed water is converted into freshwater while the remainder is crystallized into salts. Furthermore, the volume of freshwater produced (3 005 m^3/day) from this combined model of desalination and brine treatment, as shown in Table 5.1, is higher than the volume produced by a standalone RO unit previously presented by reference [217], with similar input parameters, which is also the expected desalination capacity to meet the baseline daily water demand (1 250 m^3/day). Moreover, this study presents the unit cost of

freshwater and salt as a single unit cost of production, since it is difficult to separate the cost of production of freshwater and salt because the system is designed as a single unit with the same component costs, energy sources and their costs. The unit cost of production of freshwater and salt ($0.89) is within the range of cost of water for standalone desalination units presented in literature, which is from $0.5-2.39 [19]; [20]; [217]. Furthermore, most standalone RO desalination systems do not account for carbon emission cost and brine treatment; therefore, they use less energy and treatment chemicals and require less frequent membrane replacement than a combined model that produces freshwater and treats brine with zero discharge. Hence, the unit cost of production of this combined model is relatively low, considering the economic and environmental factors. On the other hand, the LCOE of this model (1.06 $/kWh) is within the average value of those of standalone RO desalination systems that usually range between 0.5-1.2 $/kWh, suggesting similar cost of energy for a standalone desalination unit and a combined desalination-brine treatment unit. This is because the component cost of similar energy sources used for a standalone unit is the same for a combined unit and depends mainly on the size of the system and the volume of production.

5.5 SUMMARY

This chapter presents efficient energy and brine management in the production of freshwater using the integration of RO, ED and crystallization methods. The objective of this study is to minimize LCOE and brine production while maximizing freshwater and salt production at a minimal cost. The proposed design is such that the feed water (saline water) is passed through the RO unit for desalination; the brine produced from the RO unit is further desalinated by the ED method, leaving a very high concentrate to be crystallized into soluble salts, thus achieving zero brine production. Furthermore, for energy-efficient management, optimal sizing of energy sources, which include grid power, wind power and solar power, was carried out considering mitigation of carbon

emission and its cost and the intermittent limitation of the RES. This integrated design ensured that the internal and external costs of desalination were evaluated and minimized. The results show the impact of emission and its cost on the energy cost, increasing the cost of grid energy supply and making RES more cost-effective as well as environmentally friendly. The LCOE is within the average value of those of standalone desalination units, suggesting similar cost of energy for a standalone desalination unit and a combined desalination-brine treatment unit. This is because the component costs of similar energy sources used for a standalone unit are the same for a combined unit and depend mainly on the size of the system and the volume of production. Further study can investigate the cost of salt based on location, as it is expected that the salt produced, if further treated, can be an added advantage of the combined model of desalination and brine treatment, as it can be of use. Furthermore, the annual carbon emission (637 708 $kgCO_{2\text{-}e}$) is still very high, and a further reduction can be achieved with the integration of a storage system to supplement the inconsistency of the RES. This will reduce dependence on grid power but might increase the cost of production.

CHAPTER 6
COMPARISON OF RESULTS AND SENSITIVITY ANALYSIS

6.1 Introduction

This chapter presents a comparison of results from the three models in the previous chapters and sensitivity analyses are also performed using some key parameters to determine the behavior of the models in different circumstances.

In Chapter 3, a comparison was made of three cases of Model 1, consisting of an energy mix that includes (i) Conventional grid power and a DG, (ii) Conventional grid power, DG and PV, and (iii) Grid power, DG and PV with a TOU DR program. The comparative result of the three cases of Model 1 shows that Case 3 (the system with DG, PV and grid-connected with a TOU DR program) is more promising. Hence the result of Case 3 of Model 1 is compared with the results from other subsequent models.

Chapter 4, similar to Chapter 3, compares three cases of Model 2 with an energy mix that includes (i) Grid only, (ii) DG and grid, and (iii) DG, PV and grid. Model 2 also considered carbon emission and its cost in all the cases of the model formation. The comparison of the cases of Model 2 extends to cases with the same energy mix, with or without the TOU DR program. The result of the comparison of the different cases of Model 2 shows that Case 3 (the system with DG, PV and grid-connected energy sources with TOU DR) is more promising. Therefore, the result of Case 3 with DR taken from Model 2 is compared with the result from Models 1 and 3.

Chapter 5 presents Model 3, which is formulated to consist of an energy mix that includes PV, wind and the grid to power a combined desalination and brine treatment unit. This model also considered carbon emission and its cost, as well as the implementation of a DR program.

6.2 Comparative Analysis

Table 6.1 shows the summary results of key optimized parameters from the three models for a simple comparison. The three models incorporate the TOU DR program and integrate an energy mix of grid and PV; Model 3 includes wind energy in its energy mix. Models 2 and 3 consider carbon emission and its cost, but Model 1 does not. Other parameters, such as daily water demand, system components cost (for energy sources and desalination units) and metrological data used in the three models are the same.

Table 6.1: Comparison of Model Results

Optimized parameters	Model 1	Model 2	Model 3
Daily freshwater produced (m^3/day)	1521	1790	3005
Unit cost of water ($/$m^3$)	1.36	1.77	1.056
LCOE ($/kW/h)	0.86	1.20	0.89

The comparative result shows that the three models have a relatively low cost of water and LEOC, with Model 3 producing more water than both Model 1 and Model 2. This implies that a combined system of desalination and a brine treatment unit has the capacity to produce more freshwater at a reduced cost, considering carbon emission and zero brine discharge. This characteristic makes Model 3 a more promising approach to solving the freshwater scarcity problem at a low cost and in an environmentally friendly way.

6.3 Sensitivity Analysis from Model 2

Sensitivity analyses are performed on the three cases of Model 2 with and without DR. The results, shown in Figure 6.1 and Figure 6.2, reflect the effect of an increased carbon tax rate on LCOE and the cost of water produced. The relationship between the carbon tax rate and LCOE is directly proportional. The cost of water produced also tends to increase with an increase in carbon tax. Case 3 proves to be less affected, as its proportional cost variation is significantly less than that of Case 1 and Case 2.

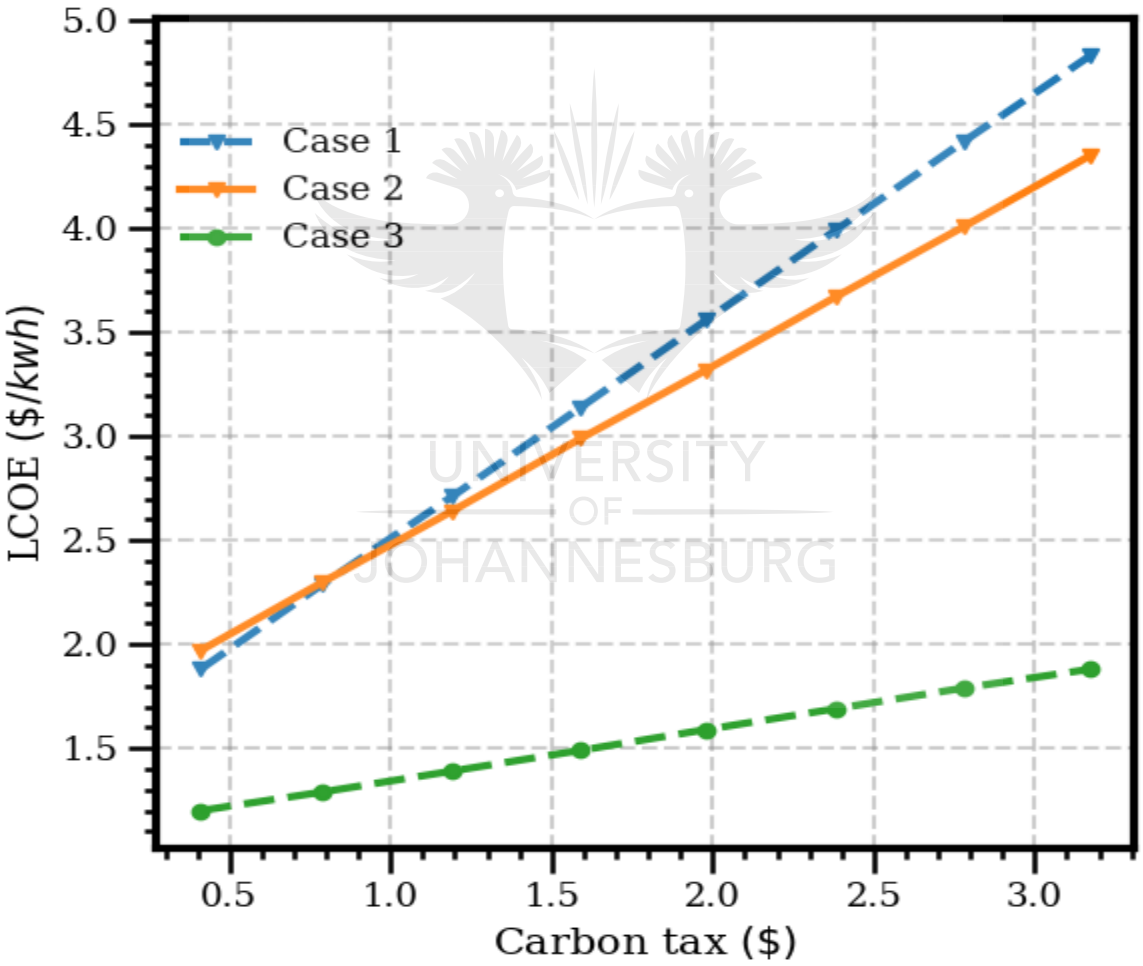

Fig. 6.1 Effect of increase in carbon tax on levelized cost of energy for the three cases with demand response

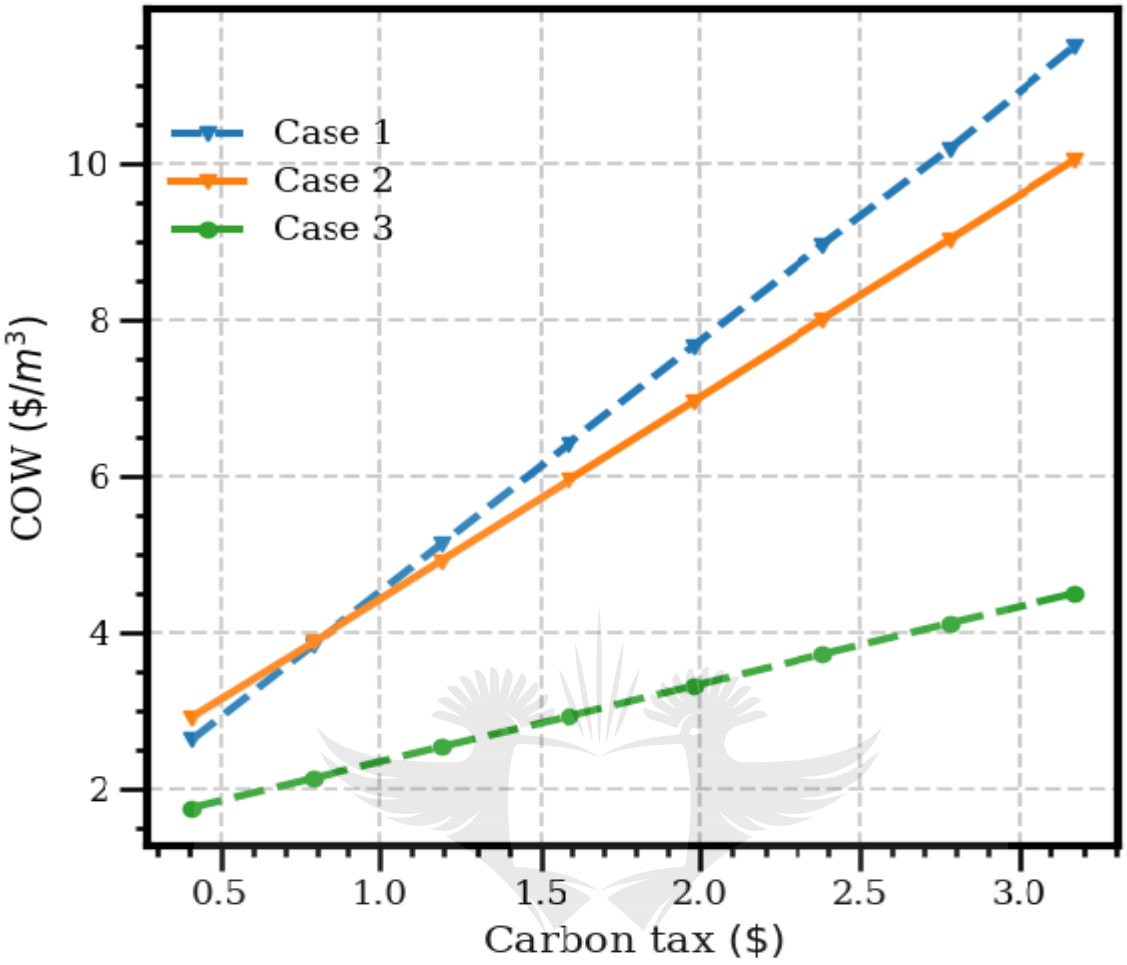

Fig. 6.2 Effect of increase in carbon tax on cost of water for the three cases with demand response

Again, the impact of DR in the model is highlighted in Table 4, which shows that the increase in both LCOW and COW as a result of an increase in the carbon tax is significantly higher in the cases without DR compared to the ones with DR.

Table 6.2: Summary results of cost parameters

Carbon tax ($)	Case 1				Case 2				Case 3			
	Without DR		With DR		Without DR		With DR		Without DR		With DR	
	LCOE	COW	LCOE	COW	LCOE	COW	LCOE	COW	LCOE	COW	LCOE	COW
0.4	1.88	2.64	1.88	2.64	1.98	2.93	1.97	2.93	1.29	1.92	1.20	1.77
0.79	2.29	3.86	2.29	3.86	2.32	3.96	2.30	3.89	1.40	2.36	1.29	2.15
1.19	2.71	5.14	2.71	5.14	2.68	5.04	2.64	4.93	1.52	2.82	1.39	2.55
1.59	3.14	6.43	3.14	6.43	3.04	6.12	2.99	5.96	1.65	3.28	1.49	2.94
1.98	3.56	7.68	3.56	7.68	3.39	7.18	3.32	6.97	1.76	3.73	1.59	3.33
2.38	3.99	8.96	3.99	8.96	3.75	8.26	3.67	8.01	1.88	4.19	1.69	3.73
2.78	4.42	10.2	4.42	10.2	4.11	9.34	4.01	9.04	2.00	4.65	1.79	4.13
3.17	4.83	11.5	4.83	11.5	4.47	10.4	4.35	10.05	2.12	5.10	1.88	4.51

6.4 Sensitivity Analysis from Model 3

Sensitivity analysis was also performed to evaluate the impact of the percentage increase of water demand on three cost matrices (ACS, LCOE and cost of products, COP) in Model 3, as depicted in Figures 6.3, 6.4 and 6.5, respectively.

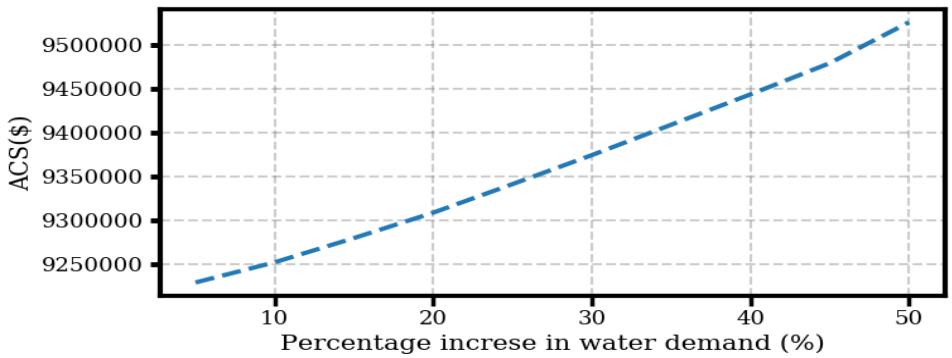

Fig. 6.3 Impact of percentage increase on the annual cost of the system

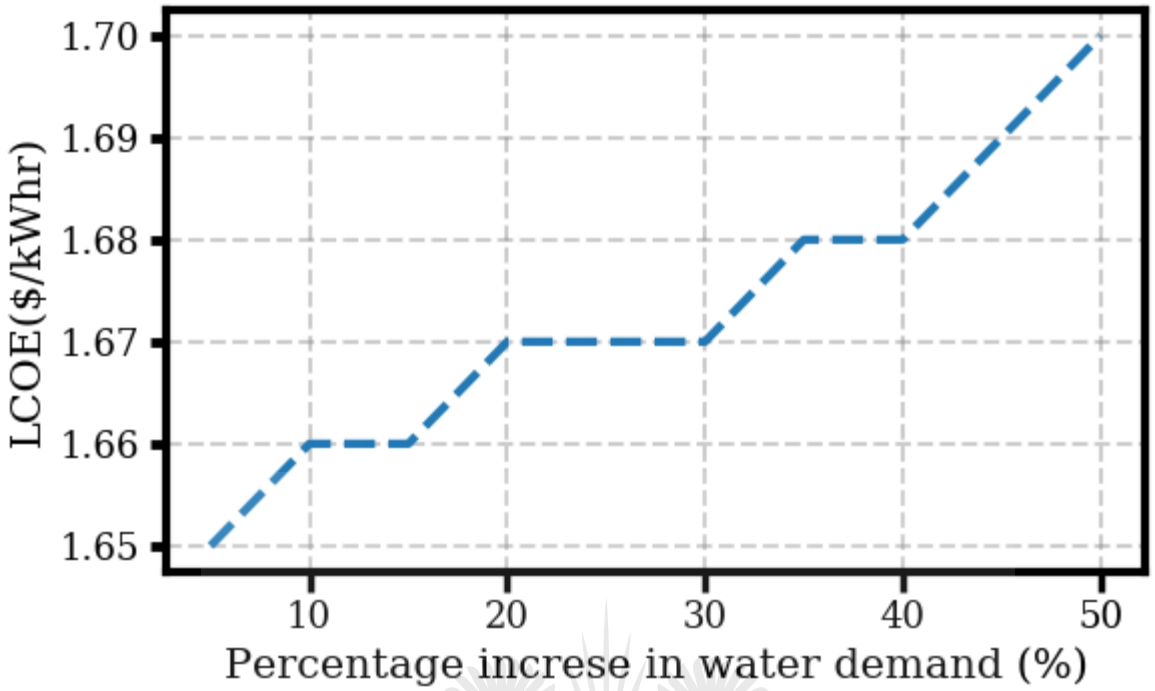

Fig. 6.4 Impacts of percentage increased on levelized cost of energy

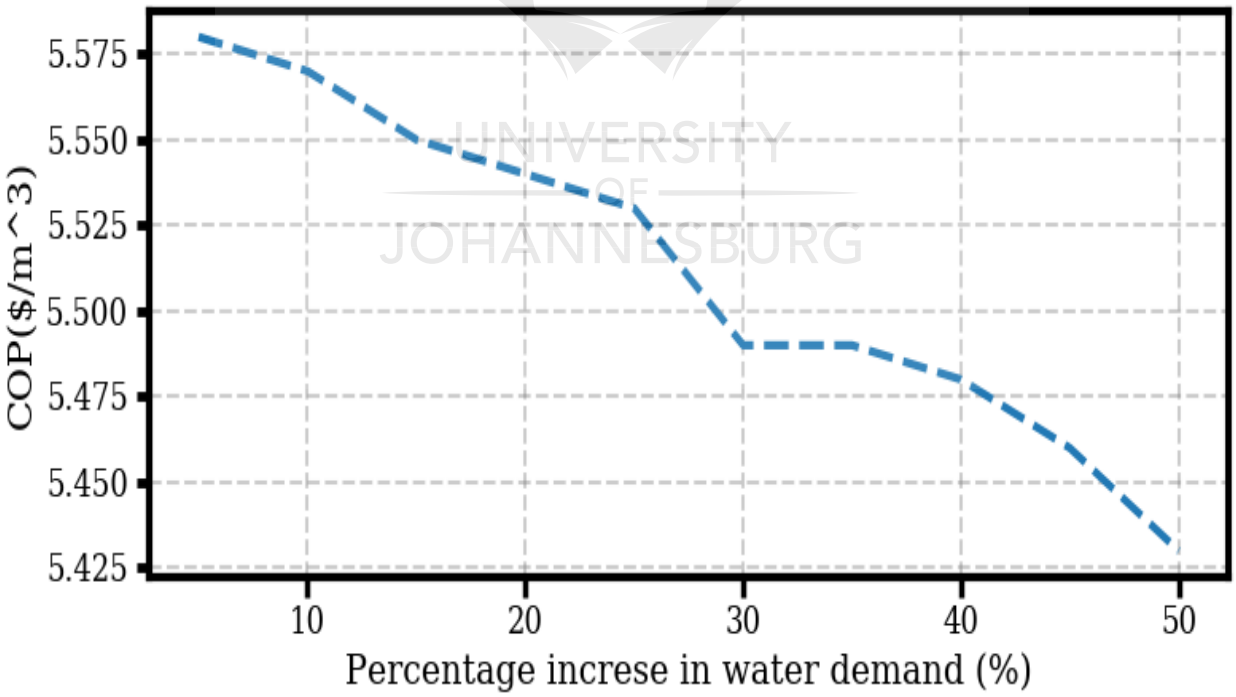

Fig. 6.5 Impacts of percentage increase in cost of water and salt

The results of the sensitivity analysis show a proportional increase in ACS, a moderate increase in LCOE and a decrease in the COP against the percentage increase in water demand. This implies that the increase in water demand results in a rise in ACS and LCOE, but the unit cost of production of water and salt is reduced, with more freshwater production to meet the increased water demand.

6.5 SUMMARY

This chapter presents a comparison of results from the three models in the previous chapters and sensitivity analyses are also performed using some key parameters to determine the behavior of the models in different circumstances. The comparative result shows that the three models have a relatively low cost of water and LCOE, with Model 3 producing more water than both Model 1 and Model 2. This implies that a combined system of desalination and a brine treatment unit has the capacity to produce more freshwater at a reduced cost, considering carbon emission and zero brine discharge. This characteristic makes Model 3 a more promising approach to solving the freshwater scarcity problem at a low cost and in an environmentally friendly way. Sensitivity analysis shows that when carbon emission and its cost are considered, the increase in carbon tax rate is proportional to LCOE and the cost of water produced. Furthermore, the sensitivity analysis from Model 3 shows that the percentage increase in freshwater and salt production is inversely proportional to the unit cost of production. This implies that it is cheaper to produce a larger quantity in the long term than producing at a small capacity.

CHAPTER 7
CONCLUSION

7.1 Conclusion

This thesis has extensively researched the integration of RES into power desalination systems. Two common forms of RES (PV and wind energy) were considered alongside grid energy to power the RO desalination system, with the implementation of TOU DR to obtain an optimal energy-efficient schedule. Furthermore, the integration of RO, ED and crystallization methods of desalination was explored to maximize freshwater production and minimize brine production. Techno-economic analyses of the integrated modelled systems were presented; the results were compared and sensitivity analysis was performed. The results showed that, for optimal performance considering economic cost and environmental impact, the RO desalination system is better integrated with other methods of desalination and powered with an energy mix of both grid energy and RES. The application of the TOU DR program also improved productivity at a reduced cost.

7.2 Contributions to Knowledge

The following are the contributions of this thesis to the body of knowledge:

I. This thesis has extensively researched the integration of RES to power a desalination system and has presented the merits of different segments of this integration, such as the impact of TOU DR, the impact of carbon emission cost and the impact of RES. The study also presents different optimization approaches for techno-economic analyses.

II. A mathematical model of an optimal energy mix that includes a DR program for an efficient energy schedule to power an RO desalination unit at minimal LCOE was developed.

III. A mathematical optimization model that enhances effective techno-economic analysis of a RES-powered RO desalination system considering carbon emission and its cost while maximizing freshwater production was developed.

IV. A techno-economic optimization model of a combined desalination and brine treatment unit for freshwater production and brine management was developed.

7.3 Future Work

The following areas can still be explored in future research:

I. Thermo-economic analysis of RES-RO desalination has become a central research focus, but the optimization of the thermodynamic parameters such as exergy destruction and specific energy consumption has not been extensively explored. It is therefore recommended that in the future, more work can be done by applying optimization techniques to the thermodynamic analysis of RES-RO desalination systems.

II. For more extensive optimization and analysis of RES-RO systems, a combined optimization approach should be considered, taking into account the sizing, operation and thermodynamic effect of the system.

III. Furthermore, in response to the trend in the application of different metaheuristic optimization techniques, attention has shifted away from mathematical techniques. However, for accurate results, mathematical techniques are still very promising, especially in view of the availability of different computer software solvers. More metaheuristic optimization techniques can still be explored; thus far, only very few have been used in this area.

IV. Moreover, optimization objectives in this area have concentrated more strongly on economic performance indicators. In the future, more extensive work should incorporate both an economic and a reliability index in the formation of objective functions. In general, there is still much work

to be done in this area of optimization of RES-RO systems, especially the exploration of RES such as geothermal and ocean energy, including salinity gradient energy.

REFERENCES

[1] M. A. Abdelkareem, M. El Haj Assad, E. T. Sayed, and B. Soudan, "Recent progress in the use of renewable energy sources to power water desalination plants," *Desalination*, vol. 435, no. November 2017, pp. 97–113, 2018, doi: 10.1016/j.desal.2017.11.018.

[2] Z. Jian-yun, S. Man-ting, H. Rui-min, S. Shahid, X. Xing-hui, and W. Xiao-jun, "Catastrophe theory to assess water security and adaptation strategy in the context of environmental change," *Mitig. Adapt. Strateg. Glob. Chang.*, vol. 19, no. 4, pp. 463–477, 2012, doi: 10.1007/s11027-012-9443-x.

[3] UNESCO, *Water for a sustainable world (2015 report) UNESCO*. 2015.

[4] M. Prisciandaro, M. Capocelli, V. Piemonte, and D. Barba, "Process analysis applied to water reuse for a 'closed water cycle' approach," *Chem. Eng. J.*, vol. 304, pp. 602–608, 2016, doi: 10.1016/j.cej.2016.06.134.

[5] J. R. Ziolkowska and R. Reyes, "Impact of socio-economic growth on desalination in the US," *J. Environ. Manage.*, vol. 167, pp. 15–22, 2016, doi: 10.1016/j.jenvman.2015.11.013.

[6] A. Maleki, M. G. Khajeh, and M. A. Rosen, "Weather forecasting for optimization of a hybrid solar-wind–powered reverse osmosis water desalination system using a novel optimizer approach," *Energy*, vol. 114, pp. 1120–1134, 2016, doi: 10.1016/j.energy.2016.06.134.

[7] A. Maleki, F. Pourfayaz, and M. H. Ahmadi, "Design of a cost-effective wind/photovoltaic/hydrogen energy system for supplying a desalination unit by a heuristic approach," *Sol. Energy*, vol. 139, pp. 666–675, 2016, doi: 10.1016/j.solener.2016.09.028.

[8] A. Maleki, "Design and optimization of autonomous solar-wind-reverse osmosis desalination systems coupling battery and hydrogen energy storage by an improved bee algorithm," *Desalination*, vol. 435, no. August 2017, pp. 221–234, 2018, doi:

10.1016/j.desal.2017.05.034.

[9] L. Marletta, G. Evola, M. De Simone, R. Bruno, G. Oliveti, and N. Arcuri, “Solar Energy,” pp. 159–214, 2014, doi: 10.1007/978-3-319-03074-6_4.

[10] S. L. Gbadamosi, N. I. Nwulu, and Y. Sun, “Harmonic and power loss minimization in power systems incorporating renewable energy sources and locational marginal pricing,” *J. Renew. Sustain. Energy*, vol. 10, no. 5, 2018, doi: 10.1063/1.5041923.

[11] S. L. Gbadamosi, N. I. Nwulu, and Y. Sun, “Multi-objective optimisation for composite generation and transmission expansion planning considering offshore wind power and feed-in tariffs,” *IET Renew. Power Gener.*, vol. 12, no. 14, pp. 1687–1697, 2018, doi: 10.1049/iet-rpg.2018.5531.

[12] C. Laspidou *et al.*, “Energy modelling and the Nexus concept,” *Energy Strateg. Rev.*, vol. 19, pp. 1–6, 2017, doi: 10.1016/j.esr.2017.10.005.

[13] N. I. Nwulu and M. Fahrioglu, “A neural network model for optimal demand management contract design,” *2011 10th Int. Conf. Environ. Electr. Eng. EEEIC.EU 2011 - Conf. Proc.*, pp. 1–4, 2011, doi: 10.1109/EEEIC.2011.5874776.

[14] W. N. Lubega and A. M. Farid, “A Reference System Architecture for the Energy-Water Nexus,” *IEEE Syst. J.*, vol. 10, no. 1, pp. 106–116, 2016, doi: 10.1109/JSYST.2014.2302031.

[15] A. Giwa, V. Dufour, F. Al Marzooqi, M. Al Kaabi, and S. W. Hasan, “Brine management methods : Recent innovations and current status,” *Desalination*, vol. 407, pp. 1–23, 2017, doi: 10.1016/j.desal.2016.12.008.

[16] E. Jones, M. Qadir, M. T. H. van Vliet, V. Smakhtin, and S. mu Kang, “The state of desalination and brine production: A global outlook,” *Sci. Total Environ.*, vol. 657, pp.

1343–1356, 2019, doi: 10.1016/j.scitotenv.2018.12.076.

[17] M. Molinos-Senante and D. González, "Evaluation of the economics of desalination by integrating greenhouse gas emission costs: An empirical application for Chile," *Renew. Energy*, vol. 133, pp. 1327–1337, 2018, doi: 10.1016/j.renene.2018.09.019.

[18] Eskom, "Schedule of standard prices for Eskom tariffs 1 April 2019 to 31 March 2020 for non-local authority supplies and 1 July 2019 to 30 June 2020 for local authority supplies," vol. 0207, no. MARCH, pp. 1–48, 2019.

[19] A. M. Abdelshafy, H. Hassan, and J. Jurasz, "Optimal design of a grid-connected desalination plant powered by renewable energy resources using a hybrid PSO–GWO approach," *Energy Convers. Manag.*, vol. 173, no. August, pp. 331–347, 2018, doi: 10.1016/j.enconman.2018.07.083.

[20] B. Wu, A. Maleki, F. Pourfayaz, and M. A. Rosen, "Optimal design of stand-alone reverse osmosis desalination driven by a photovoltaic and diesel generator hybrid system," *Sol. Energy*, vol. 163, no. February, pp. 91–103, 2018, doi: 10.1016/j.solener.2018.01.016.

[21] C. Yildirim and I. Solmuş, "A parametric study on a humidification-dehumidification (HDH) desalination unit powered by solar air and water heaters," *Energy Convers. Manag.*, vol. 86, no. 0, pp. 568–575, 2014, doi: 10.1016/j.enconman.2014.06.016.

[22] H. Ettouney, "Design and analysis of humidification dehumidification desalination process," *Desalination*, vol. 183, no. 1–3, pp. 341–352, 2005, doi: 10.1016/j.desal.2005.03.039.

[23] M. Capocelli, M. Balsamo, A. Lancia, and D. Barba, "Process analysis of a novel humidification-dehumidification-adsorption (HDHA) desalination method," *Desalination*, vol. 429, no. September 2017, pp. 155–166, 2018, doi: 10.1016/j.desal.2017.12.020.

[24] G. P. Narayan, E. K. Summers, J. H. Lienhard, M. H. Sharqawy, M. A. Antar, and S. M. Zubair, "The potential of solar-driven humidification–dehumidification desalination for small-scale decentralized water production," *Renew. Sustain. Energy Rev.*, vol. 14, no. 4, pp. 1187–1201, 2009, doi: 10.1016/j.rser.2009.11.014.

[25] R. Segurado, M. Costa, N. Duić, and M. G. Carvalho, "Integrated analysis of energy and water supply in islands. Case study of S. Vicente, Cape Verde," *Energy*, vol. 92, no. Part 3, pp. 639–648, 2014, doi: 10.1016/j.energy.2015.02.013.

[26] H. Müller-Holst, M. Engelhardt, and W. Schölkopf, "Small-scale thermal seawater desalination simulation and optimization of system design," *Desalination*, vol. 122, no. 2–3, pp. 255–262, 1999, doi: 10.1016/S0011-9164(99)00046-6.

[27] H. Müller-Holst, "Solar thermal desalination using the multiple effect humidification (meh)-method hendrik müller-holst *," *Springer*, no. Solar Desalination for the 21st Century, pp. 215–225, 2007.

[28] D. Lawal, M. Antar, A. Khalifa, S. Zubair, and F. Al-Sulaiman, "Humidification-dehumidification desalination system operated by a heat pump," *Energy Convers. Manag.*, vol. 161, no. September 2017, pp. 128–140, 2018, doi: 10.1016/j.enconman.2018.01.067.

[29] C. S. Bandi, R. Uppaluri, and A. Kumar, "Global optimization of MSF seawater desalination processes," *Desalination*, vol. 394, pp. 30–43, 2016, doi: 10.1016/j.desal.2016.04.012.

[30] I. Darawsheh, M. D. Islam, and F. Banat, "Experimental characterization of a solar powered MSF desalination process performance," *Therm. Sci. Eng. Prog.*, vol. 10, no. March 2018, pp. 154–162, 2019, doi: 10.1016/j.tsep.2019.01.018.

[31] E. A. M. Hawaidi and I. M. Mujtaba, "Simulation and optimization of MSF desalination

process for fixed freshwater demand: Impact of brine heater fouling," *Chem. Eng. J.*, vol. 165, no. 2, pp. 545–553, 2010, doi: 10.1016/j.cej.2010.09.071.

[32] H. El-Dessouky, I. Alatiqi, and H. Ettouney, "Process synthesis: the multi-stage flash desalination system," *Desalination*, vol. 115, no. 2, pp. 155–179, 1998, doi: 10.1016/S0011-9164(98)00035-6.

[33] M. S. Tanvir and I. M. Mujtaba, "Optimisation of design and operation of MSF desalination process using MINLP technique in gPROMS," *Desalination*, vol. 222, no. 1–3, pp. 419–430, 2008, doi: 10.1016/j.desal.2007.02.068.

[34] M. Abduljawad and U. Ezzeghni, "Optimization of Tajoura MSF desalination plant," *Desalination*, vol. 254, no. 1–3, pp. 23–28, 2010, doi: 10.1016/j.desal.2009.12.019.

[35] M. G. Marcovecchio, S. F. Mussati, P. A. Aguirre, and N. J. Scenna, "Optimization of hybrid desalination processes including multi stage flash and reverse osmosis systems," *Desalination*, vol. 182, no. 1–3, pp. 111–122, 2005, doi: 10.1016/j.desal.2005.03.011.

[36] M. A. Deyab, "Enhancement of corrosion resistance in MSF desalination plants during acid cleaning operation by cationic surfactant," *Desalination*, vol. 456, no. January, pp. 32–37, 2019, doi: 10.1016/j.desal.2019.01.018.

[37] M. Mannan, M. Alhaj, A. N. Mabrouk, and S. G. Al-Ghamdi, "Examining the life-cycle environmental impacts of desalination: A case study in the State of Qatar," *Desalination*, vol. 452, no. November 2018, pp. 238–246, 2019, doi: 10.1016/j.desal.2018.11.017.

[38] A. Al-Karaghouli and L. L. Kazmerski, "Energy consumption and water production cost of conventional and renewable-energy-powered desalination processes," *Renew. Sustain. Energy Rev.*, vol. 24, pp. 343–356, 2013, doi: 10.1016/j.rser.2012.12.064.

[39] J. Shen, G. Feng, Z. Xing, and X. Wang, "Theoretical study of two-stage water vapor

compression systems," *Appl. Therm. Eng.*, vol. 147, no. November 2018, pp. 972–982, 2019, doi: 10.1016/j.applthermaleng.2018.11.012.

[40] R. Saidur, E. T. Elcevvadi, S. Mekhilef, A. Safari, and H. A. Mohammed, "An overview of different distillation methods for small scale applications," *Renew. Sustain. Energy Rev.*, vol. 15, no. 9, pp. 4756–4764, 2011, doi: 10.1016/j.rser.2011.07.077.

[41] Z. Xing, K. Zhang, X. Wang, Z. He, and J. Shen, "Development of a water-injected twin-screw compressor for mechanical vapor compression desalination systems," *Appl. Therm. Eng.*, vol. 95, pp. 125–135, 2015, doi: 10.1016/j.applthermaleng.2015.11.057.

[42] C. Wang, J. Shen, X. Wang, Z. Xing, and Y. Tian, "Modeling and performance study of a water-injected twin-screw water vapor compressor," *Int. J. Refrig.*, vol. 83, pp. 75–87, 2017, doi: 10.1016/j.ijrefrig.2017.04.008.

[43] J. Veza, "Mechanical vapour compression desalination plants - A case study," *Desalination*, vol. 101, no. 1, pp. 1–10, 1995, doi: 10.1016/0011-9164(95)00002-J.

[44] G. Kronenberg and F. Lokiec, "Low-temperature distillation processes in single-and dual-purpose plants," *Desalination*, vol. 136, no. 1–3, pp. 189–197, 2001, doi: 10.1016/S0011-9164(01)00181-3.

[45] J. Yang, C. Zhang, Z. Zhang, L. Yang, and W. Lin, "Study on mechanical vapor recompression system with wet compression single screw compressor," *Appl. Therm. Eng.*, vol. 103, pp. 205–211, 2016, doi: 10.1016/j.applthermaleng.2016.04.053.

[46] R. Bahar, M. N. A. Hawlader, and L. S. Woei, "Performance evaluation of a mechanical vapor compression desalination system," *Desalination*, vol. 166, no. 1–3, pp. 123–127, 2004, doi: 10.1016/j.desal.2004.06.066.

[47] Q. Chen, M. K. Ja, Y. Li, and K. J. Chua, "Energy, exergy and economic analysis of a hybrid

spray-assisted low-temperature desalination/thermal vapor compression system," *Energy*, vol. 166, pp. 871–885, 2019, doi: 10.1016/j.energy.2018.10.154.

[48] Z. Cao, J. Deng, F. Ye, and C. A. Garris, "Analysis of a hybrid Thermal Vapor Compression and Reverse Osmosis desalination system at variable design conditions," *Desalination*, vol. 438, no. March, pp. 54–62, 2018, doi: 10.1016/j.desal.2018.03.019.

[49] C. zhuo Jin, Q. li Chou, D. sheng Jiao, and P. cheng Shu, "Vapour Compression Flash seawater desalination system and its exergy analysis," *Desalination*, vol. 353, pp. 75–83, 2014, doi: 10.1016/j.desal.2014.09.001.

[50] M. A. Jamil and S. M. Zubair, "On thermoeconomic analysis of a single-effect mechanical vapor compression desalination system," *Desalination*, vol. 420, no. July, pp. 292–307, 2017, doi: 10.1016/j.desal.2017.07.024.

[51] M. A. Jamil and S. M. Zubair, "Design and analysis of a forward feed multi-effect mechanical vapor compression desalination system: An exergo-economic approach," *Energy*, vol. 140, pp. 1107–1120, 2017, doi: 10.1016/j.energy.2017.08.053.

[52] W. F. He, C. Ji, D. Han, Y. K. Wu, L. Huang, and X. K. Zhang, "Performance analysis of the mechanical vapor compression desalination system driven by an organic Rankine cycle," *Energy*, vol. 141, pp. 1177–1186, 2017, doi: 10.1016/j.energy.2017.10.014.

[53] D. Han, W. F. He, C. Yue, and W. H. Pu, "Study on desalination of zero-emission system based on mechanical vapor compression," *Appl. Energy*, vol. 185, pp. 1490–1496, 2017, doi: 10.1016/j.apenergy.2015.12.061.

[54] M. C. Garg, *Renewable Energy-Powered Membrane Technology: Cost Analysis and Energy Consumption*. Elsevier Inc., 2018.

[55] M. L. Elsayed, O. Mesalhy, R. H. Mohammed, and L. C. Chow, "Transient performance of

MED processes with different feed configurations," *Desalination*, vol. 438, no. March, pp. 37–53, 2018, doi: 10.1016/j.desal.2018.03.016.

[56] A. Al-Karaghouli, D. Renne, and L. L. Kazmerski, "Technical and economic assessment of photovoltaic-driven desalination systems," *Renew. Energy*, vol. 35, no. 2, pp. 323–328, 2010, doi: 10.1016/j.renene.2009.05.018.

[57] H. J. Lee, F. Sarfert, H. Strathmann, and S. H. Moon, "Designing of an electrodialysis desalination plant," *Desalination*, vol. 142, no. 3, pp. 267–286, 2002, doi: 10.1016/S0011-9164(02)00208-4.

[58] N. Ishimaru, "Solar photovoltaic desalination of brackish water in remote areas by electrodialysis," *Desalination*, vol. 98, no. 1–3, pp. 485–493, 1994, doi: 10.1016/0011-9164(94)00175-8.

[59] A. Campione, L. Gurreri, M. Ciofalo, G. Micale, A. Tamburini, and A. Cipollina, "Electrodialysis for water desalination: A critical assessment of recent developments on process fundamentals, models and applications," *Desalination*, vol. 434, no. February, pp. 121–160, 2018, doi: 10.1016/j.desal.2017.12.044.

[60] A. Daniilidis, D. A. Vermaas, R. Herber, and K. Nijmeijer, "Experimentally obtainable energy from mixing river water, seawater or brines with reverse electrodialysis," *Renew. Energy*, vol. 64, pp. 123–131, 2014, doi: 10.1016/j.renene.2013.11.001.

[61] M. L. La Cerva *et al.*, "Coupling CFD with a one-dimensional model to predict the performance of reverse electrodialysis stacks," *J. Memb. Sci.*, vol. 541, no. July, pp. 595–610, 2017, doi: 10.1016/j.memsci.2017.07.030.

[62] M. Tedesco, A. Cipollina, A. Tamburini, and G. Micale, "Towards 1 kW power production in a reverse electrodialysis pilot plant with saline waters and concentrated brines," *J. Memb.*

Sci., vol. 522, pp. 226–236, 2017, doi: 10.1016/j.memsci.2016.09.015.

[63] N. Kress, "Desalination Technologies," *Mar. Impacts Seawater Desalin.*, no. 4, pp. 11–34, 2019, doi: 10.1016/b978-0-12-811953-2.00002-5.

[64] S. Ahualli, G. R. Iglesias, and Á. V. Delgado, "Principles and Theoretical Models of CDI: Experimental Approaches," *Interface Sci. Technol.*, vol. 24, pp. 169–192, 2018, doi: 10.1016/B978-0-12-811370-7.00008-5.

[65] K. Tang *et al.*, "Seawater desalination by over-potential membrane capacitive deionization: Opportunities and hurdles," *Chem. Eng. J.*, vol. 357, no. September 2018, pp. 103–111, 2019, doi: 10.1016/j.cej.2018.09.121.

[66] M. W. Saleem and W. S. Kim, "Parameter-based performance evaluation and optimization of a capacitive deionization desalination process," *Desalination*, vol. 437, no. March, pp. 133–143, 2018, doi: 10.1016/j.desal.2018.02.023.

[67] J. B. Lee, K. K. Park, H. M. Eum, and C. W. Lee, "Desalination of a thermal power plant wastewater by membrane capacitive deionization," *Desalination*, vol. 196, no. 1–3, pp. 125–134, 2006, doi: 10.1016/j.desal.2006.01.011.

[68] Z. Wang, H. Gong, Y. Zhang, P. Liang, and K. Wang, "Nitrogen recovery from low-strength wastewater by combined membrane capacitive deionization (MCDI) and ion exchange (IE) process," *Chem. Eng. J.*, vol. 316, pp. 1–6, 2017, doi: 10.1016/j.cej.2017.01.082.

[69] Y. A. Chen, C. S. Fan, and C. H. Hou, "Optimizing the energetic performance of capacitive deionization devices with unipolar and bipolar connections under constant current charging," *J. Taiwan Inst. Chem. Eng.*, vol. 93, pp. 201–210, 2018, doi: 10.1016/j.jtice.2018.06.039.

[70] X. Liu *et al.*, "Bipolarly stacked electrolyser for energy and space efficient fabrication of

supercapacitor electrodes," *J. Power Sources*, vol. 307, pp. 208–213, 2016, doi: 10.1016/j.jpowsour.2016.01.006.

[71] C. Zhang, D. He, J. Ma, W. Tang, and T. D. Waite, "Faradaic reactions in capacitive deionization (CDI) - problems and possibilities: A review," *Water Res.*, vol. 128, pp. 314–330, 2018, doi: 10.1016/j.watres.2017.10.024.

[72] S. Sen Gupta, M. R. Islam, and T. Pradeep, *Capacitive Deionization (CDI): An Alternative Cost-Efficient Desalination Technique*, no. CDI. Elsevier Inc., 2019.

[73] J. Kang, T. Kim, H. Shin, J. Lee, J. I. Ha, and J. Yoon, "Direct energy recovery system for membrane capacitive deionization," *Desalination*, vol. 398, pp. 144–150, 2016, doi: 10.1016/j.desal.2016.07.025.

[74] R. Zhao, S. Porada, P. M. Biesheuvel, and A. Van der Wal, "Energy consumption in membrane capacitive deionization for different water recoveries and flow rates, and comparison with reverse osmosis," *Desalination*, vol. 330, pp. 35–41, 2013, doi: 10.1016/j.desal.2013.08.017.

[75] V. Soni, J. Abildskov, G. Jonsson, and R. Gani, "A general model for membrane-based separation processes," *Comput. Chem. Eng.*, vol. 33, no. 3, pp. 644–659, 2009, doi: 10.1016/j.compchemeng.2008.08.004.

[76] D. González, J. Amigo, and F. Suárez, "Membrane distillation: Perspectives for sustainable and improved desalination," *Renew. Sustain. Energy Rev.*, vol. 80, no. April 2016, pp. 238–259, 2017, doi: 10.1016/j.rser.2017.05.078.

[77] S. Al-Obaidani, E. Curcio, F. Macedonio, G. Di Profio, H. Al-Hinai, and E. Drioli, "Potential of membrane distillation in seawater desalination: Thermal efficiency, sensitivity study and cost estimation," *J. Memb. Sci.*, vol. 323, no. 1, pp. 85–98, 2008, doi:

10.1016/j.memsci.2008.06.006.

[78] D. Winter, J. Koschikowski, and M. Wieghaus, "Desalination using membrane distillation: Experimental studies on full scale spiral wound modules," *J. Memb. Sci.*, vol. 375, no. 1–2, pp. 104–112, 2011, doi: 10.1016/j.memsci.2011.03.030.

[79] B. B. Ashoor, S. Mansour, A. Giwa, V. Dufour, and S. W. Hasan, "Principles and applications of direct contact membrane distillation (DCMD): A comprehensive review," *Desalination*, vol. 398, pp. 222–246, 2016, doi: 10.1016/j.desal.2016.07.043.

[80] P. S. Goh, T. Matsuura, A. F. Ismail, and N. Hilal, "Recent trends in membranes and membrane processes for desalination," *Desalination*, vol. 391, pp. 43–60, 2016, doi: 10.1016/j.desal.2015.12.016.

[81] C. Fritzmann, J. Lowenberg, T. Wintgens, and T. Melin, "State o the art of reverse osmosis desalination," *Desalination*, vol. 216, no. 1–3, pp. 1–76, 2007, doi: 10.1016/j.desal.2006.12.009.

[82] S. Abdallah, M. Abu-Hilal, and M. S. Mohsen, "Performance of a photovoltaic powered reverse osmosis system under local climatic conditions," *Desalination*, vol. 183, no. 1–3, pp. 95–104, 2005, doi: 10.1016/j.desal.2005.03.030.

[83] S. Lin and M. Elimelech, "Kinetics and energetics trade-off in reverse osmosis desalination with different configurations," *Desalination*, vol. 401, pp. 42–52, 2017, doi: 10.1016/j.desal.2016.09.008.

[84] J. Jaafar *et al.*, "Forward Osmosis for Desalination Application," *Membr. Sep. Princ. Appl.*, pp. 315–337, 2018, doi: 10.1016/b978-0-12-812815-2.00010-7.

[85] G. P. Syed Ibrahim, A. M. Isloor, and E. Yuliwati, *Current Trends and Future Developments on (Bio-) Membranes*. Elsevier Inc., 2019.

[86] B. Peñate and L. García-Rodríguez, "Current trends and future prospects in the design of seawater reverse osmosis desalination technology," *Desalination*, vol. 284, pp. 1–8, 2012, doi: 10.1016/j.desal.2011.09.010.

[87] Y. J. Choi, J. S. Choi, H. J. Oh, S. Lee, D. R. Yang, and J. H. Kim, "Toward a combined system of forward osmosis and reverse osmosis for seawater desalination," *Desalination*, vol. 247, no. 1–3, pp. 239–246, 2009, doi: 10.1016/j.desal.2008.12.028.

[88] N. Akther, A. Sodiq, A. Giwa, S. Daer, H. A. Arafat, and S. W. Hasan, "Recent advancements in forward osmosis desalination: A review," *Chem. Eng. J.*, vol. 281, pp. 502–522, 2015, doi: 10.1016/j.cej.2015.05.080.

[89] M. A. Abdel-Fatah, "Nanofiltration systems and applications in wastewater treatment: Review article," *Ain Shams Eng. J.*, vol. 9, no. 4, pp. 3077–3092, 2018, doi: 10.1016/j.asej.2018.08.001.

[90] A. Matin, F. Rahman, H. Z. Shafi, and S. M. Zubair, "Scaling of reverse osmosis membranes used in water desalination: Phenomena, impact, and control; future directions," *Desalination*, vol. 455, no. September 2018, pp. 135–157, 2019, doi: 10.1016/j.desal.2018.12.009.

[91] Y. H. Teow and A. W. Mohammad, "New generation nanomaterials for water desalination: A review," *Desalination*, vol. 451, no. May 2017, pp. 2–17, 2019, doi: 10.1016/j.desal.2017.11.041.

[92] B. Kalista, H. Shin, J. Cho, and A. Jang, "Current development and future prospect review of freeze desalination," *Desalination*, vol. 447, no. September, pp. 167–181, 2018, doi: 10.1016/j.desal.2018.09.009.

[93] W. Cao, C. Beggs, and I. M. Mujtaba, "Theoretical approach of freeze seawater desalination

on flake ice maker utilizing LNG cold energy," *Desalination*, vol. 355, pp. 22–32, 2014, doi: 10.1016/j.desal.2014.09.034.

[94] F. E. Ahmed, R. Hashaikeh, and N. Hilal, "Solar powered desalination – Technology, energy and future outlook," *Desalination*, vol. 453, no. November 2018, pp. 54–76, 2019, doi: 10.1016/j.desal.2018.12.002.

[95] T. Mezher, H. Fath, Z. Abbas, and A. Khaled, "Techno-economic assessment and environmental impacts of desalination technologies," *Desalination*, vol. 266, no. 1–3, pp. 263–273, 2011, doi: 10.1016/j.desal.2010.08.035.

[96] M. W. Shahzad, M. Burhan, L. Ang, and K. C. Ng, "Energy-water-environment nexus underpinning future desalination sustainability," *Desalination*, vol. 413, pp. 52–64, 2017, doi: 10.1016/j.desal.2017.03.009.

[97] B. Mayor, "Growth patterns in mature desalination technologies and analogies with the energy field," *Desalination*, vol. 457, no. January, pp. 75–84, 2019, doi: 10.1016/j.desal.2019.01.029.

[98] S. Lin and M. Elimelech, "Kinetics and energetics trade-off in reverse osmosis desalination with different configurations," *Desalination*, vol. 401, pp. 42–52, 2017, doi: 10.1016/j.desal.2016.09.008.

[99] M. A. Jamil, S. M. Elmutasim, and S. M. Zubair, "Exergo-economic analysis of a hybrid humidification dehumidification reverse osmosis (HDH-RO) system operating under different retrofits," *Energy Convers. Manag.*, vol. 158, no. September 2017, pp. 286–297, 2018, doi: 10.1016/j.enconman.2017.11.025.

[100] G. P. Narayan, R. K. McGovern, S. M. Zubair, and J. H. Lienhard, "High-temperature-steam-driven, varied-pressure, humidification-dehumidification system coupled with

reverse osmosis for energy-efficient seawater desalination," *Energy*, vol. 37, no. 1, pp. 482–493, 2012, doi: 10.1016/j.energy.2011.11.007.

[101] A. Eslamimanesh and M. S. Hatamipour, "Economical study of a small-scale direct contact humidification-dehumidification desalination plant," *Desalination*, vol. 250, no. 1, pp. 203–207, 2010, doi: 10.1016/j.desal.2008.11.015.

[102] A. Almulla, A. Hamad, and M. Gadalla, "Integrating hybrid systems with existing thermal desalination plants," *Desalination*, vol. 174, no. 2, pp. 171–192, 2005, doi: 10.1016/j.desal.2004.08.041.

[103] C. S. Bandi, R. Uppaluri, and A. Kumar, "Global optimality of hybrid MSF-RO seawater desalination processes," *Desalination*, vol. 400, pp. 47–59, 2016, doi: 10.1016/j.desal.2016.09.021.

[104] B. Heidary, T. T. Hashjin, B. Ghobadian, and R. Roshandel, "Optimal integration of small scale hybrid solar wind RO-MSF desalination system," *Renew. Energy Focus*, vol. 27, no. December, pp. 120–134, 2018, doi: 10.1016/j.ref.2018.05.003.

[105] G. Filippini, M. A. Al-Obaidi, F. Manenti, and I. M. Mujtaba, "Performance analysis of hybrid system of multi effect distillation and reverse osmosis for seawater desalination via modelling and simulation," *Desalination*, vol. 448, no. September, pp. 21–35, 2018, doi: 10.1016/j.desal.2018.09.010.

[106] M. H. Khoshgoftar Manesh, H. Ghalami, M. Amidpour, and M. H. Hamedi, "Optimal coupling of site utility steam network with MED-RO desalination through total site analysis and exergoeconomic optimization," *Desalination*, vol. 316, pp. 42–52, 2013, doi: 10.1016/j.desal.2013.01.022.

[107] S. Lee, J. Choi, Y. G. Park, H. Shon, C. H. Ahn, and S. H. Kim, "Hybrid desalination

processes for beneficial use of reverse osmosis brine: Current status and future prospects," *Desalination*, vol. 454, no. September 2017, pp. 104–111, 2019, doi: 10.1016/j.desal.2018.02.002.

[108] K. G. Nayar, J. Fernandes, R. K. McGovern, B. S. Al-Anzi, and J. H. Lienhard, "Cost and energy needs of RO-ED-crystallizer systems for zero brine discharge seawater desalination," *Desalination*, vol. 457, no. January, pp. 115–132, 2019, doi: 10.1016/j.desal.2019.01.015.

[109] G. P. Thiel, A. Kumar, A. Gómez-González, and J. H. Lienhard, "Utilization of Desalination Brine for Sodium Hydroxide Production: Technologies, Engineering Principles, Recovery Limits, and Future Directions," *ACS Sustain. Chem. Eng.*, vol. 5, no. 12, pp. 11147–11162, 2017, doi: 10.1021/acssuschemeng.7b02276.

[110] M. B. Minhas, Y. A. C. Jande, and W. S. Kim, "Combined reverse osmosis and constant-current operated capacitive deionization system for seawater desalination," *Desalination*, vol. 344, pp. 299–305, 2014, doi: 10.1016/j.desal.2014.03.043.

[111] Y. Choi *et al.*, "Experimental comparison of submerged membrane distillation configurations for concentrated brine treatment," *Desalination*, vol. 420, no. June, pp. 54–62, 2017, doi: 10.1016/j.desal.2017.06.024.

[112] Z. Yan *et al.*, "Reverse osmosis brine treatment using direct contact membrane distillation: Effects of feed temperature and velocity," *Desalination*, vol. 423, no. September, pp. 149–156, 2017, doi: 10.1016/j.desal.2017.09.010.

[113] J. A. Sanmartino, M. Khayet, M. C. García-Payo, H. El-Bakouri, and A. Riaza, "Treatment of reverse osmosis brine by direct contact membrane distillation: Chemical pretreatment approach," *Desalination*, vol. 420, no. July, pp. 79–90, 2017, doi:

10.1016/j.desal.2017.06.030.

[114] J. Ge, Y. Peng, Z. Li, P. Chen, and S. Wang, “Membrane fouling and wetting in a DCMD process for RO brine concentration,” *Desalination*, vol. 344, pp. 97–107, 2014, doi: 10.1016/j.desal.2014.03.017.

[115] D. Zhou, L. Zhu, Y. Fu, M. Zhu, and L. Xue, “Development of lower cost seawater desalination processes using nanofiltration technologies - A review,” *Desalination*, vol. 376, no. 1219, pp. 109–116, 2015, doi: 10.1016/j.desal.2015.08.020.

[116] D. G. Randall and J. Nathoo, “A succinct review of the treatment of Reverse Osmosis brines using Freeze Crystallization,” *J. Water Process Eng.*, vol. 8, pp. 186–194, 2015, doi: 10.1016/j.jwpe.2015.10.005.

[117] K. Bourouni, J. C. Deronzier, and L. Tadrist, “Experimentation and modelling of an innovative geothermal desalination unit,” *Desalination*, vol. 125, no. 1–3, pp. 147–153, 1999, doi: 10.1016/S0011-9164(99)00133-2.

[118] S. Bouguecha and M. Dhahbi, “Fluidised bed crystalliser and air gap membrane distillation as a solution to geothermal water desalination,” *Desalination*, vol. 152, no. 1–3, pp. 237–244, 2003, doi: 10.1016/S0011-9164(02)01069-X.

[119] V. G. Gude, “Geothermal source potential for water desalination - Current status and future perspective,” *Renew. Sustain. Energy Rev.*, vol. 57, pp. 1038–1065, 2016, doi: 10.1016/j.rser.2015.12.186.

[120] S. Loutatidou and H. A. Arafat, “Techno-economic analysis of MED and RO desalination powered by low-enthalpy geothermal energy,” *Desalination*, vol. 365, pp. 277–292, 2015, doi: 10.1016/j.desal.2015.03.010.

[121] M. Lehmann, F. Karimpour, C. A. Goudey, P. T. Jacobson, and M. R. Alam, “Ocean wave

energy in the United States: Current status and future perspectives," *Renew. Sustain. Energy Rev.*, vol. 74, no. November 2016, pp. 1300–1313, 2017, doi: 10.1016/j.rser.2016.11.101.

[122] M. Bilgili, A. Ozbek, B. Sahin, and A. Kahraman, "An overview of renewable electric power capacity and progress in new technologies in the world," *Renew. Sustain. Energy Rev.*, vol. 49, pp. 323–334, 2015, doi: 10.1016/j.rser.2015.04.148.

[123] Z. Li, A. Siddiqi, L. D. Anadon, and V. Narayanamurti, "Towards sustainability in water-energy nexus: Ocean energy for seawater desalination," *Renew. Sustain. Energy Rev.*, vol. 82, no. August 2016, pp. 3833–3847, 2018, doi: 10.1016/j.rser.2017.10.087.

[124] R. A. Sawyer and D. F. Maratos, "An investigation into the economic feasibility of unsteady incompressible duct flow (waterhammer) to create hydrostatic pressure for seawater desalination using reverse osmosis," *Desalination*, vol. 138, no. 1–3, pp. 307–317, 2001, doi: 10.1016/S0011-9164(01)00279-X.

[125] R. Senthil Kumar, A. Mani, and S. Kumaraswamy, "Experimental studies on desalination system for ocean thermal energy utilisation," *Desalination*, vol. 207, no. 1–3, pp. 1–8, 2007, doi: 10.1016/j.desal.2006.08.001.

[126] A. S. Kim, H. J. Kim, H. S. Lee, and S. Cha, "Dual-use open cycle ocean thermal energy conversion (OC-OTEC) using multiple condensers for adjustable power generation and seawater desalination," *Renew. Energy*, vol. 85, pp. 344–358, 2016, doi: 10.1016/j.renene.2015.06.014.

[127] Z. jiang Jin, H. Ye, H. Wang, H. Li, and J. yuan Qian, "Thermodynamic analysis of siphon flash evaporation desalination system using ocean thermal energy," *Energy Convers. Manag.*, vol. 136, pp. 66–77, 2017, doi: 10.1016/j.enconman.2017.01.002.

[128] R. Ferreira and S. Estefen, "Ocean Power Conversion for Electricity Generation and

Desalinated Water Production," *Proc. World Renew. Energy Congr. – Sweden, 8–13 May, 2011, Linköping, Sweden*, vol. 57, pp. 2198–2205, 2011, doi: 10.3384/ecp110572198.

[129] D. F. Maratos, "Technical feasibility of wavepower for seawater desalination using the hydro-ram (Hydram)," *Desalination*, vol. 153, no. 1–3, pp. 287–293, 2003, doi: 10.1016/S0011-9164(02)01148-7.

[130] M. Folley, B. Peñate Suarez, and T. Whittaker, "An autonomous wave-powered desalination system," *Desalination*, vol. 220, no. 1–3, pp. 412–421, 2008, doi: 10.1016/j.desal.2007.01.044.

[131] C. Ling, Y. Wang, C. Min, and Y. Zhang, "Economic evaluation of reverse osmosis desalination system coupled with tidal energy," *Front. Energy*, vol. 12, no. 2, pp. 297–304, 2018, doi: 10.1007/s11708-017-0478-2.

[132] J. Leijon, J. Forslund, K. Thomas, and C. Boström, "Marine Current Energy Converters to Power a Reverse Osmosis Desalination Plant," *Energies*, vol. 11, no. 11, p. 2880, 2018, doi: 10.3390/en11112880.

[133] O. A. Alvarez-Silva, *Implementing Salinity Gradient Energy at River Mouths*. Elsevier Inc., 2017.

[134] Z. Jia, B. Wang, S. Song, and Y. Fan, "Blue energy: Current technologies for sustainable power generation from water salinity gradient," *Renew. Sustain. Energy Rev.*, vol. 31, pp. 91–100, 2014, doi: 10.1016/j.rser.2013.11.049.

[135] B. B. Sales, M. Saakes, J. W. Post, C. J. N. Buisman, P. M. Biesheuvel, and H. V. M. Hamelers, "Direct power production from a water salinity difference in a membrane-modified supercapacitor flow cell," *Environ. Sci. Technol.*, vol. 44, no. 14, pp. 5661–5665, 2010, doi: 10.1021/es100852a.

[136] A. P. Straub, A. Deshmukh, and M. Elimelech, "Pressure-retarded osmosis for power generation from salinity gradients: Is it viable?," *Energy Environ. Sci.*, vol. 9, no. 1, pp. 31–48, 2016, doi: 10.1039/c5ee02985f.

[137] H. Gu, X. Sun, W. Li, Y. Lin, S. Ma, and H. Liu, "A review on the development of tidal current energy in China," *Renew. Sustain. Energy Rev.*, vol. 15, no. 2, pp. 1141–1146, 2010, doi: 10.1016/j.rser.2010.11.042.

[138] J. Bane *et al.*, "The economics of electricity generation from Gulf Stream currents," *Energy*, vol. 134, pp. 649–658, 2017, doi: 10.1016/j.energy.2017.06.048.

[139] W. Lai, Q. Ma, H. Lu, S. Weng, J. Fan, and H. Fang, "Effects of wind intermittence and fluctuation on reverse osmosis desalination process and solution strategies," *Desalination*, vol. 395, pp. 17–27, 2016, doi: 10.1016/j.desal.2016.05.019.

[140] M. Baldea *et al.*, "Feasibility study on wind-powered desalination," *Desalination*, vol. 203, no. 1–3, pp. 463–470, 2007, doi: 10.1016/j.desal.2006.05.009.

[141] V. Romero-Ternero, L. García-Rodríguez, and C. Gómez-Camacho, "Thermoeconomic analysis of wind powered seawater reverse osmosis desalination in the Canary Islands," *Desalination*, vol. 186, no. 1–3, pp. 291–298, 2005, doi: 10.1016/j.desal.2005.06.006.

[142] L. García-Rodríguez, V. Romero-Ternero, and C. Gómez-Camacho, "Economic analysis of wind-powered desalination," *Desalination*, vol. 137, no. 1–3, pp. 259–265, 2001, doi: 10.1016/S0011-9164(01)00235-1.

[143] E. Rosales-Asensio, D. Borge-Diez, A. Pérez-Hoyos, and A. Colmenar-Santos, "Reduction of water cost for an existing wind-energy-based desalination scheme: A preliminary configuration," *Energy*, vol. 167, pp. 548–560, 2019, doi: 10.1016/j.energy.2018.11.004.

[144] G. Melián, B. Peñate, J. A. de la Fuente, L. García-Rodríguez, and A. M. Delgado-Torres,

Water Desalination by Solar-Powered RO Systems. 2018.

[145] A. B. Pouyfaucon and L. García-Rodríguez, "Solar thermal-powered desalination: A viable solution for a potential market," *Desalination*, vol. 435, no. January, pp. 60–69, 2018, doi: 10.1016/j.desal.2017.12.025.

[146] C. Li, Y. Goswami, and E. Stefanakos, "Solar assisted sea water desalination: A review," *Renew. Sustain. Energy Rev.*, vol. 19, pp. 136–163, 2013, doi: 10.1016/j.rser.2012.04.059.

[147] A. A. El-Sebaii and E. El-Bialy, "Advanced designs of solar desalination systems: A review," *Renew. Sustain. Energy Rev.*, vol. 49, pp. 1198–1212, 2015, doi: 10.1016/j.rser.2015.04.161.

[148] J. H. Reif and W. Alhalabi, "Solar-thermal powered desalination: Its significant challenges and potential," *Renew. Sustain. Energy Rev.*, vol. 48, pp. 152–165, 2015, doi: 10.1016/j.rser.2015.03.065.

[149] P. Palenzuela, G. Zaragoza, D. C. Alarcón-Padilla, E. Guillén, M. Ibarra, and J. Blanco, "Assessment of different configurations for combined parabolic-trough (PT) solar power and desalination plants in arid regions," *Energy*, vol. 36, no. 8, pp. 4950–4958, 2011, doi: 10.1016/j.energy.2011.05.039.

[150] A. Goetzberger, C. Hebling, and H. W. Schock, "Photovoltaic materials, history, status and outlook," *Mater. Sci. Eng. R Reports*, vol. 40, no. 1, pp. 1–46, 2003, doi: 10.1016/S0927-796X(02)00092-X.

[151] M. T. Ali, H. E. S. Fath, and P. R. Armstrong, "A comprehensive techno-economical review of indirect solar desalination," *Renew. Sustain. Energy Rev.*, vol. 15, no. 8, pp. 4187–4199, 2011, doi: 10.1016/j.rser.2011.05.012.

[152] A. Kasaeian, F. Rajaee, and W. M. Yan, "Osmotic desalination by solar energy: A critical

review," *Renew. Energy*, vol. 134, pp. 1473–1490, 2019, doi: 10.1016/j.renene.2018.09.038.

[153] M. Freire-Gormaly and A. M. Bilton, "Experimental quantification of the effect of intermittent operation on membrane performance of solar powered reverse osmosis desalination systems," *Desalination*, vol. 435, no. September 2017, pp. 188–197, 2018, doi: 10.1016/j.desal.2017.09.013.

[154] S. Lee, S. Myung, J. Hong, and D. Har, "Reverse osmosis desalination process optimized for maximum permeate production with renewable energy," *Desalination*, vol. 398, pp. 133–143, 2016, doi: 10.1016/j.desal.2016.07.018.

[155] L. C. Kelley and S. Dubowsky, "Thermal control to maximize photovoltaic powered reverse osmosis desalination systems productivity," *Desalination*, vol. 314, pp. 10–19, 2013, doi: 10.1016/j.desal.2012.11.036.

[156] M. C. Garg and H. Joshi, "Optimization and economic analysis of small scale nanofiltration and reverse osmosis brackish water system powered by photovoltaics," *Desalination*, vol. 353, pp. 57–74, 2014, doi: 10.1016/j.desal.2014.09.005.

[157] W. He, Y. Wang, and M. H. Shaheed, "Stand-alone seawater RO (reverse osmosis) desalination powered by PV (photovoltaic) and PRO (pressure retarded osmosis)," *Energy*, vol. 86, pp. 423–435, 2015, doi: 10.1016/j.energy.2015.04.046.

[158] A. Lamei, P. van der Zaag, and E. von Münch, "Impact of solar energy cost on water production cost of seawater desalination plants in Egypt," *Energy Policy*, vol. 36, no. 5, pp. 1748–1756, 2008, doi: 10.1016/j.enpol.2007.12.026.

[159] A. Poullikkas, "An optimization model for the production of desalinated water using photovoltaic systems," *Desalination*, vol. 258, no. 1–3, pp. 100–105, 2010, doi:

10.1016/j.desal.2010.03.036.

[160] P. Bajpai and V. Dash, “Hybrid renewable energy systems for power generation in stand-alone applications: A review,” *Renew. Sustain. Energy Rev.*, vol. 16, no. 5, pp. 2926–2939, 2012, doi: 10.1016/j.rser.2012.02.009.

[161] T. D. Xuan, K. Alikulov, N. Nakagoshi, Z. Aminov, and O. Higashi, “Analysis of environmental effect of hybrid solar-assisted desalination cycle in Sirdarya Thermal Power Plant, Uzbekistan,” *Appl. Therm. Eng.*, vol. 111, pp. 894–902, 2016, doi: 10.1016/j.applthermaleng.2016.09.029.

[162] G. L. Park, A. I. Schäfer, and B. S. Richards, “Renewable energy-powered membrane technology: Supercapacitors for buffering resource fluctuations in a wind-powered membrane system for brackish water desalination,” *Renew. Energy*, vol. 50, pp. 126–135, 2013, doi: 10.1016/j.renene.2012.05.026.

[163] M. Korpås and C. J. Greiner, “Opportunities for hydrogen production in connection with wind power in weak grids,” *Renew. Energy*, vol. 33, no. 6, pp. 1199–1208, 2008, doi: 10.1016/j.renene.2007.06.010.

[164] T. R. Ayodele and A. S. O. Ogunjuyigbe, “Mitigation of wind power intermittency: Storage technology approach,” *Renew. Sustain. Energy Rev.*, vol. 44, pp. 447–456, 2015, doi: 10.1016/j.rser.2014.12.034.

[165] S. S. Rao, *Engineering Optimization Theory and Practice*, vol. 77, no. 10. 2006.

[166] S. Twaha and M. A. M. Ramli, “A review of optimization approaches for hybrid distributed energy generation systems: Off-grid and grid-connected systems,” *Sustain. Cities Soc.*, vol. 41, no. April, pp. 320–331, 2018, doi: 10.1016/j.scs.2018.05.027.

[167] R. Ooka and S. Ikeda, “A review on optimization techniques for active thermal energy

storage control," *Energy Build.*, vol. 106, pp. 225–233, 2015, doi: 10.1016/j.enbuild.2015.07.031.

[168] L. G. Acuña, M. Lake, R. V. Padilla, Y. Y. Lim, E. G. Ponzón, and Y. C. Soo Too, "Modelling autonomous hybrid photovoltaic-wind energy systems under a new reliability approach," *Energy Convers. Manag.*, vol. 172, no. January, pp. 357–369, 2018, doi: 10.1016/j.enconman.2018.07.025.

[169] M. A. Al-Obaidi, G. Filippini, F. Manenti, and I. M. Mujtaba, "Cost evaluation and optimisation of hybrid multi effect distillation and reverse osmosis system for seawater desalination," *Desalination*, vol. 456, no. September 2018, pp. 136–149, 2019, doi: 10.1016/j.desal.2019.01.019.

[170] M. Gökçek, "Integration of hybrid power (wind-photovoltaic-diesel-battery) and seawater reverse osmosis systems for small-scale desalination applications," *Desalination*, vol. 435, no. July 2017, pp. 210–220, 2018, doi: 10.1016/j.desal.2017.07.006.

[171] E. Koutroulis and D. Kolokotsa, "Design optimization of desalination systems power-supplied by PV and W/G energy sources," *Desalination*, vol. 258, no. 1–3, pp. 171–181, 2010, doi: 10.1016/j.desal.2010.03.018.

[172] N. Duić, M. G. Carvalho, J. F. A. Madeira, R. Segurado, and M. Costa, "Optimization of a wind powered desalination and pumped hydro storage system," *Appl. Energy*, vol. 177, pp. 487–499, 2016, doi: 10.1016/j.apenergy.2016.05.125.

[173] D. Zejli, R. Benchrifa, A. Bennouna, and K. Zazi, "Economic analysis of wind-powered desalination in the south of Morocco," *Desalination*, vol. 165, no. SUPPL., pp. 219–230, 2004, doi: 10.1016/j.desal.2004.06.025.

[174] M. Gökçek and Ö. B. Gökçek, "Technical and economic evaluation of freshwater

production from a wind-powered small-scale seawater reverse osmosis system (WP-SWRO)," *Desalination*, vol. 381, pp. 47–57, 2016, doi: 10.1016/j.desal.2015.12.004.

[175] G. Zhang, B. Wu, A. Maleki, and W. Zhang, "Simulated annealing-chaotic search algorithm based optimization of reverse osmosis hybrid desalination system driven by wind and solar energies," *Sol. Energy*, vol. 173, no. April, pp. 964–975, 2018, doi: 10.1016/j.solener.2018.07.094.

[176] A. Maleki, "Design and optimization of autonomous solar-wind-reverse osmosis desalination systems coupling battery and hydrogen energy storage by an improved bee algorithm," *Desalination*, vol. 435, no. May 2017, pp. 221–234, 2018, doi: 10.1016/j.desal.2017.05.034.

[177] A. J. Karabelas, C. P. Koutsou, M. Kostoglou, and D. C. Sioutopoulos, "Analysis of specific energy consumption in reverse osmosis desalination processes," *Desalination*, vol. 431, no. February 2017, pp. 15–21, 2018, doi: 10.1016/j.desal.2017.04.006.

[178] S. Lee, H. Y. Cho, and D. Har, "Operation optimization with jointly controlled modules powered by hybrid energy source: A case study of desalination," *Renew. Sustain. Energy Rev.*, vol. 81, no. December 2016, pp. 3070–3080, 2018, doi: 10.1016/j.rser.2017.08.076.

[179] A. M. Abdelshafy, H. Hassan, and J. Jurasz, "Optimal design of a grid-connected desalination plant powered by renewable energy resources using a hybrid PSO–GWO approach," *Energy Convers. Manag.*, vol. 173, no. May, pp. 331–347, 2018, doi: 10.1016/j.enconman.2018.07.083.

[180] M. Smaoui, A. Abdelkafi, and L. Krichen, "Optimal sizing of stand-alone photovoltaic/wind/hydrogen hybrid system supplying a desalination unit," *Sol. Energy*, vol. 120, pp. 263–276, 2015, doi: 10.1016/j.solener.2015.07.032.

[181] A. Hossam-Eldin, A. M. El-Nashar, and A. Ismaiel, "Investigation into economical desalination using optimized hybrid renewable energy system," *Int. J. Electr. Power Energy Syst.*, vol. 43, no. 1, pp. 1393–1400, 2012, doi: 10.1016/j.ijepes.2012.05.019.

[182] K. Bourouni, T. Ben M'Barek, and A. Al Taee, "Design and optimization of desalination reverse osmosis plants driven by renewable energies using genetic algorithms," *Renew. Energy*, vol. 36, no. 3, pp. 936–950, 2011, doi: 10.1016/j.renene.2010.08.039.

[183] I. Prieto-Prado, B. Del Río-Gamero, A. Gómez-Gotor, and S. O. Pérez-Báez, "Water and energy self-supply in isolated areas through renewable energies using hydrogen and water as a double storage system," *Desalination*, vol. 430, no. June 2017, pp. 1–14, 2018, doi: 10.1016/j.desal.2017.12.022.

[184] M. Astolfi, S. Mazzola, P. Silva, and E. Macchi, "A synergic integration of desalination and solar energy systems in stand-alone microgrids," *Desalination*, vol. 419, no. March, pp. 169–180, 2017, doi: 10.1016/j.desal.2017.05.025.

[185] N. Duić *et al.*, "Modeling of optimal energy flows for systems with close integration of sea water desalination and renewable energy sources: Case study for Jordan," *Energy Convers. Manag.*, vol. 110, pp. 249–259, 2015, doi: 10.1016/j.enconman.2015.12.029.

[186] F. Mohammadi, M. Sahraei-Ardakani, and Y. Al-Abdullah, "Coordinated Operation of Power Generation and Water Desalination," *IFAC-PapersOnLine*, vol. 51, no. 28, pp. 456–461, 2018, doi: 10.1016/j.ifacol.2018.11.745.

[187] D. Fooladivanda and J. A. Taylor, "Energy-optimal pump scheduling and water flow," *IEEE Trans. Control Netw. Syst.*, vol. 5, no. 3, pp. 1016–1026, 2018, doi: 10.1109/TCNS.2017.2670501.

[188] Y. Cerci, "Exergy analysis of a reverse osmosis desalination plant in California,"

Desalination, vol. 142, no. 3, pp. 257–266, 2002, doi: 10.1016/S0011-9164(02)00207-2.

[189] C. Guria, P. K. Bhattacharya, and S. K. Gupta, "Multi-objective optimization of reverse osmosis desalination units using different adaptations of the non-dominated sorting genetic algorithm (NSGA)," *Comput. Chem. Eng.*, vol. 29, no. 9, pp. 1977–1995, 2005, doi: 10.1016/j.compchemeng.2005.05.002.

[190] U. Sahoo, R. Kumar, S. K. Singh, and A. K. Tripathi, "Energy, exergy, economic analysis and optimization of polygeneration hybrid solar-biomass system," *Appl. Therm. Eng.*, vol. 145, no. August, pp. 685–692, 2018, doi: 10.1016/j.applthermaleng.2018.09.093.

[191] A. Noroozian, A. Mohammadi, M. Bidi, and M. H. Ahmadi, "Energy, exergy and economic analyses of a novel system to recover waste heat and water in steam power plants," *Energy Convers. Manag.*, vol. 144, pp. 351–360, 2017, doi: 10.1016/j.enconman.2017.04.067.

[192] B. Djebedjian, H. Gad, I. Khaled, M. A. Rayan, and S. D. Authority, "Optimization of Reverse Osmosis Desalination System," *Twelfth Int. Water Technol. Conf.*, no. m, pp. 1047–1067, 2008.

[193] A. Aghaei Chadegani *et al.*, "A comparison between two main academic literature collections: Web of science and scopus databases," *Asian Soc. Sci.*, vol. 9, no. 5, pp. 18–26, 2013, doi: 10.5539/ass.v9n5p18.

[194] E. Díez, P. Langston, G. Ovejero, and M. D. Romero, "Economic feasibility of heat pumps in distillation to reduce energy use," *Appl. Therm. Eng.*, vol. 29, no. 5–6, pp. 1216–1223, 2009, doi: 10.1016/j.applthermaleng.2008.06.013.

[195] M. A. Al-Obaidi, G. Filippini, F. Manenti, and I. M. Mujtaba, "Cost evaluation and optimisation of hybrid multi effect distillation and reverse osmosis system for seawater desalination," *Desalination*, vol. 456, no. January, pp. 136–149, 2019, doi:

10.1016/j.desal.2019.01.019.

[196] A. S. Nafey, M. A. Sharaf, and L. García-Rodríguez, "Thermo-economic analysis of a combined solar organic Rankine cycle-reverse osmosis desalination process with different energy recovery configurations," *Desalination*, vol. 261, no. 1–2, pp. 138–147, 2010, doi: 10.1016/j.desal.2010.05.017.

[197] V. Gude, "Exergy Evaluation of Desalination Processes," *ChemEngineering*, vol. 2, no. 2, p. 28, 2018, doi: 10.3390/chemengineering2020028.

[198] I. D. Spyrou and J. S. Anagnostopoulos, "Design study of a stand-alone desalination system powered by renewable energy sources and a pumped storage unit," *Desalination*, vol. 257, no. 1–3, pp. 137–149, 2010, doi: 10.1016/j.desal.2010.02.033.

[199] N. I. Nwulu and X. Xia, "Optimal dispatch for a microgrid incorporating renewables and demand response," *Renew. Energy*, vol. 101, pp. 16–28, 2017, doi: 10.1016/j.renene.2016.08.026.

[200] U. Damisa, N. I. Nwulu, and Y. Sun, "Microgrid energy and reserve management incorporating prosumer behind-the-meter resources," *IET Renew. Power Gener.*, vol. 12, no. 8, pp. 910–919, 2018, doi: 10.1049/iet-rpg.2017.0659.

[201] M. Majidi, B. Mohammadi-Ivatloo, and A. Anvari-Moghaddam, "Optimal robust operation of combined heat and power systems with demand response programs," *Appl. Therm. Eng.*, vol. 149, no. November 2018, pp. 1359–1369, 2019, doi: 10.1016/j.applthermaleng.2018.12.088.

[202] F. Jabari, H. Jabari, B. Mohammadi-ivatloo, and J. Ghafouri, "Optimal short-term coordination of water-heat-power nexus incorporating plug-in electric vehicles and real-time demand response programs," *Energy*, vol. 174, pp. 708–723, 2019, doi:

10.1016/j.energy.2019.02.132.

[203] C. Ghenai, A. Merabet, T. Salameh, and E. C. Pigem, "Grid-tied and stand-alone hybrid solar power system for desalination plant," *Desalination*, vol. 435, no. October 2017, pp. 172–180, 2018, doi: 10.1016/j.desal.2017.10.044.

[204] W. Peng, A. Maleki, M. A. Rosen, and P. Azarikhah, "Optimization of a hybrid system for solar-wind-based water desalination by reverse osmosis: Comparison of approaches," *Desalination*, vol. 442, no. November 2017, pp. 16–31, 2018, doi: 10.1016/j.desal.2018.03.021.

[205] E. Dehnavi and H. Abdi, "Optimal pricing in time of use demand response by integrating with dynamic economic dispatch problem," *Energy*, vol. 109, pp. 1086–1094, 2016, doi: 10.1016/j.energy.2016.05.024.

[206] M. A. Al-Obaidi, G. Filippini, F. Manenti, and I. M. Mujtaba, "Cost evaluation and optimisation of hybrid multi effect distillation and reverse osmosis system for seawater desalination," *Desalination*, vol. 456, no. January, pp. 136–149, 2019, doi: 10.1016/j.desal.2019.01.019.

[207] C. Koroneos, A. Dompros, and G. Roumbas, "Renewable energy driven desalination systems modelling," *J. Clean. Prod.*, vol. 15, no. 5, pp. 449–464, 2007, doi: 10.1016/j.jclepro.2005.07.017.

[208] N. Baumgärtner, R. Delorme, M. Hennen, and A. Bardow, "Design of low-carbon utility systems : Exploiting time-dependent grid emissions for climate-friendly demand-side management," *Appl. Energy*, vol. 247, no. March, pp. 755–765, 2019, doi: 10.1016/j.apenergy.2019.04.029.

[209] U. K. Kesieme, N. Milne, H. Aral, C. Yong, and M. Duke, "Economic analysis of

desalination technologies in the context of carbon pricing , and opportunities for membrane distillation," *DES*, vol. 323, pp. 66–74, 2013, doi: 10.1016/j.desal.2013.03.033.

[210] A. M. Brander *et al.*, "Technical Paper | Electricity-specific emission factors for grid electricity," no. August, pp. 1–22, 2011.

[211] National Treasury, Republic Of South Africa: Media Statement Publication Of The 2019 Carbon Tax Act, vol. 2019, no. 15. 2019, pp. 10–13.

[212] A. Subramani and J. G. Jacangelo, "Treatment technologies for reverse osmosis concentrate volume minimization : A review," *Sep. Purif. Technol.*, vol. 122, pp. 472–489, 2014, doi: 10.1016/j.seppur.2013.12.004.

[213] A. Panagopoulos, K. Haralambous, and M. Loizidou, "Desalination brine disposal methods and treatment technologies - A review," *Sci. Total Environ.*, vol. 693, p. 133545, 2019, doi: 10.1016/j.scitotenv.2019.07.351.

[214] E. J. Okampo and N. Nwulu, "Optimal design and techno-economic evaluation of renewable energy powered combined reverse osmosis desalination and brine treatment unit," *Desalin. Water Treat. www.deswater.com*, vol. 202, pp. 27–37, 2020, doi: 10.5004/dwt.2020.26145.

[215] Z. M. Salameh and B. S. Borowy, "Methodology for Optimally Sizing the Combination of a Battery Bank and PV Array in a Wind/PV Hybrid System," *IEEE Trans. Energy Convers.*, vol. 11, no. 2, pp. 367–375, 1996, doi: 10.1109/60.507648.

[216] K. G. Nayar *et al.*, "Cost and energy requirements of hybrid RO and ED brine concentration systems for salt production," *Desalination*, vol. 456, no. November 2018, pp. 97–120, 2019, doi: 10.1016/j.desal.2018.11.018.

[217] E. J. Okampo and N. I. Nwulu, "Optimal energy mix for a reverse osmosis desalination unit

considering demand response osmosis," *J. Eng. Des. Technol.*, 2020, doi: 10.1108/JEDT-01-2020-0025.

APPENDIX A: SAMPLE OF MODEL'S PROGRAM IN AIMMS

I. Home page

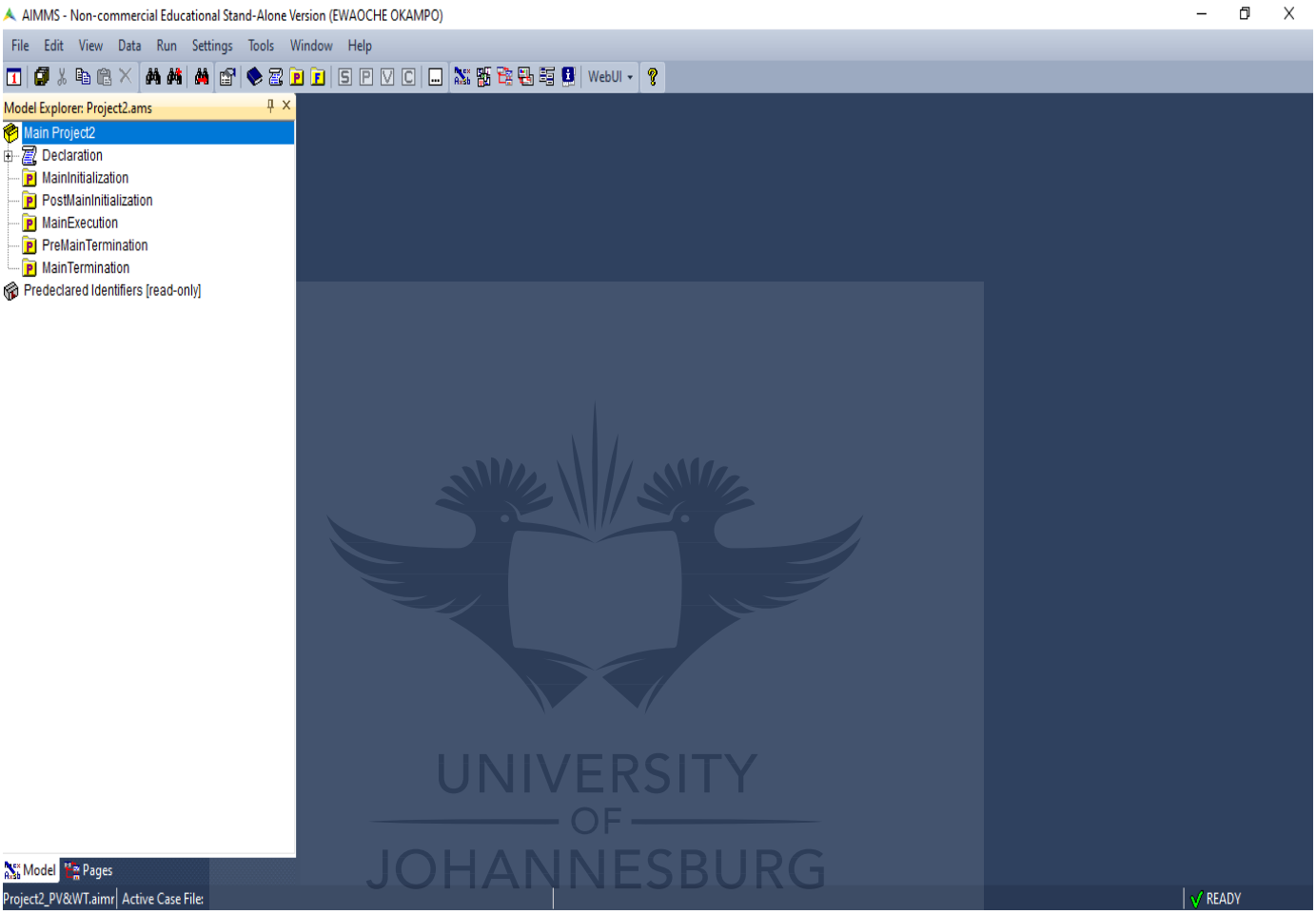

II. Decalaration Tree

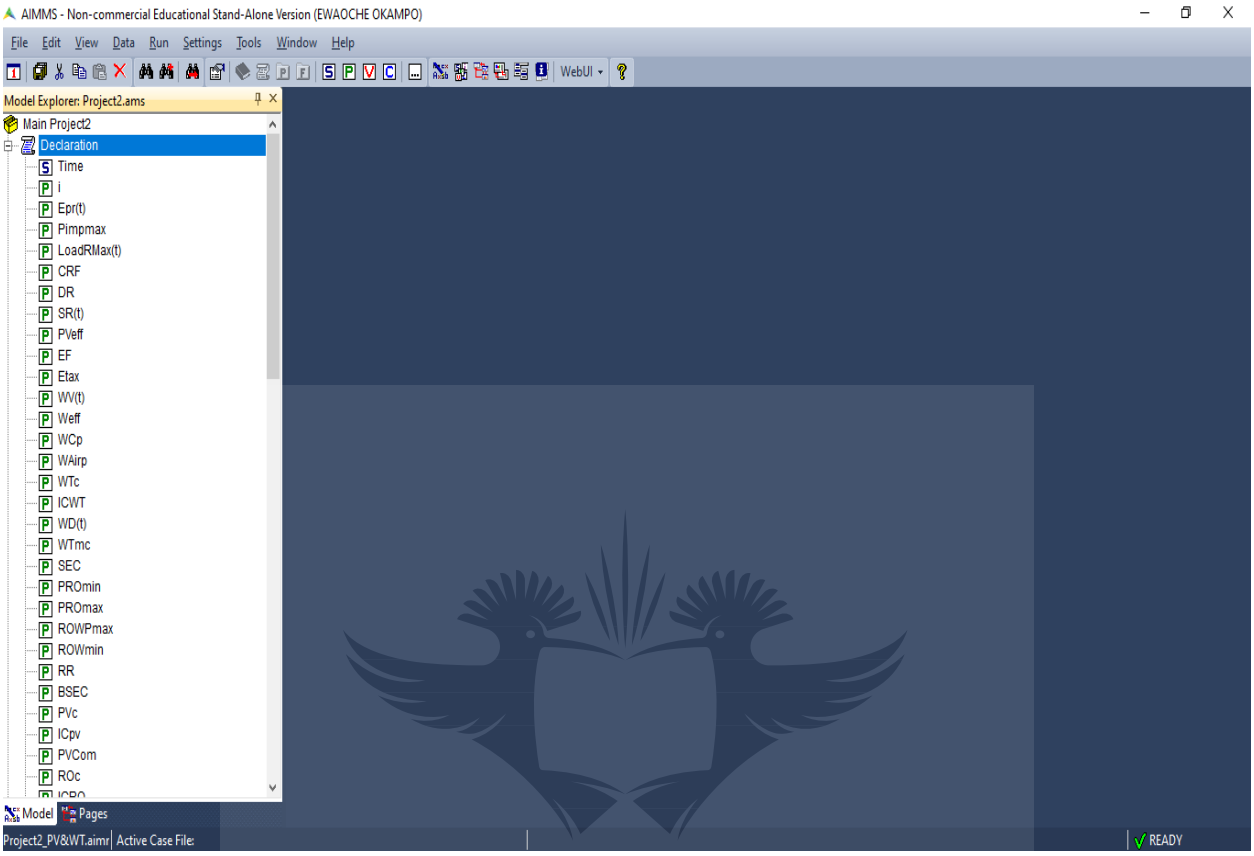

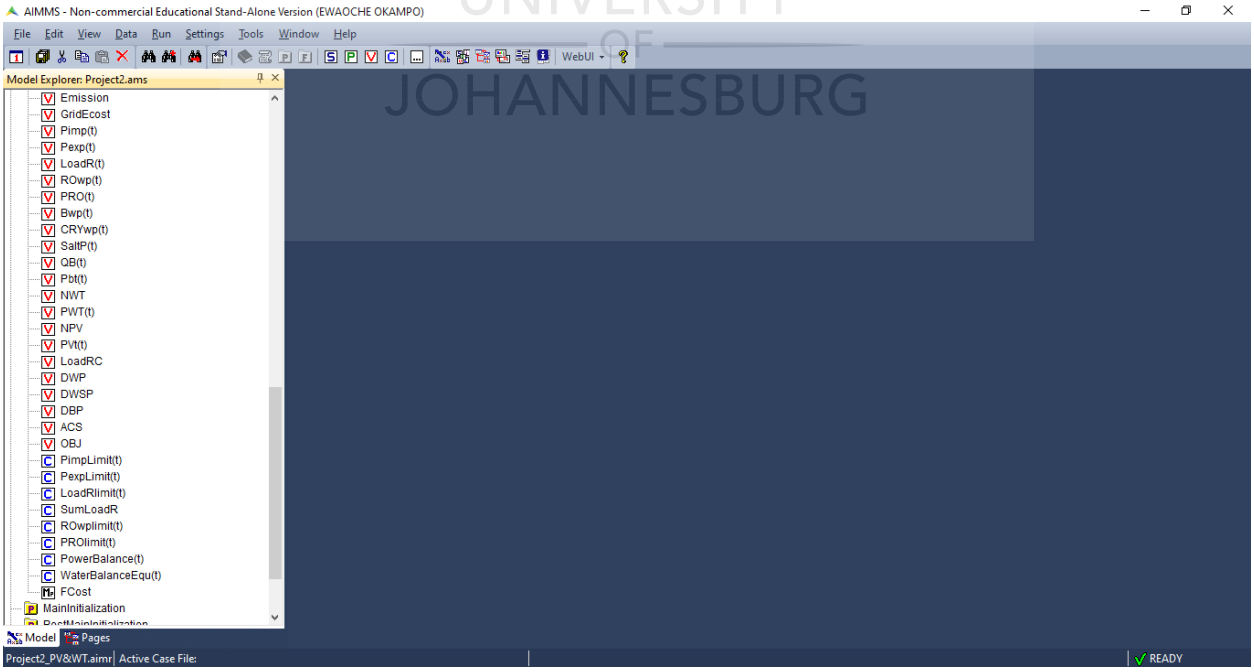

III. Data input of Set T

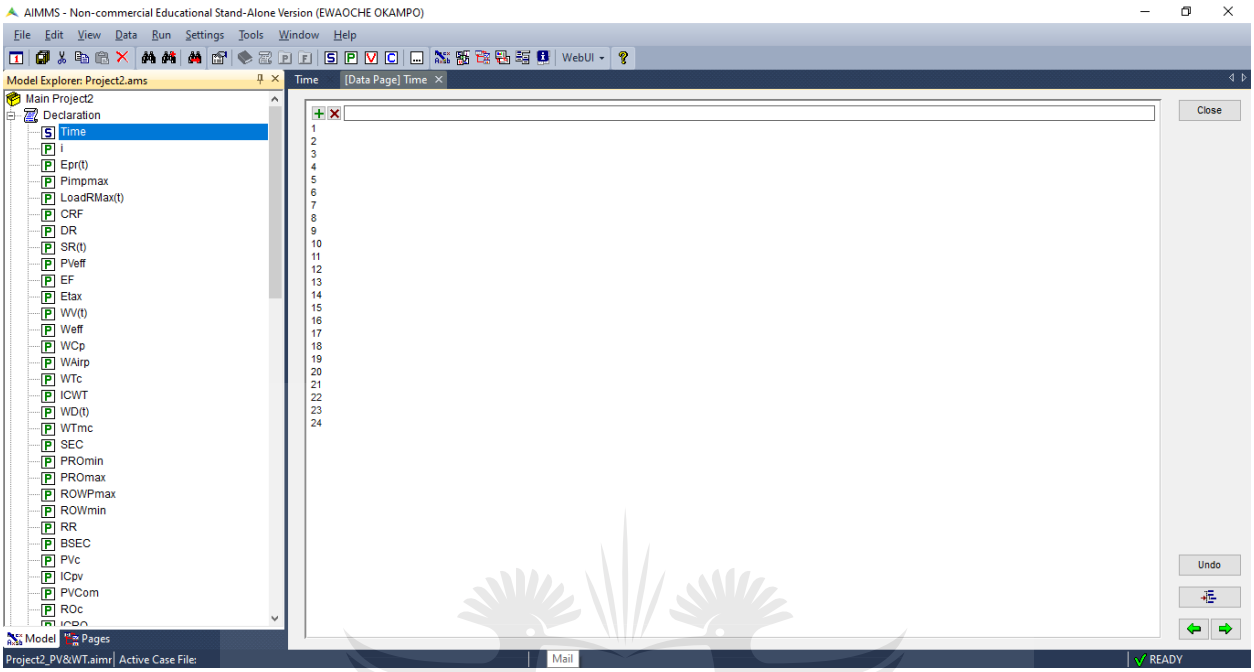

IV. Data input of parameter for water demand

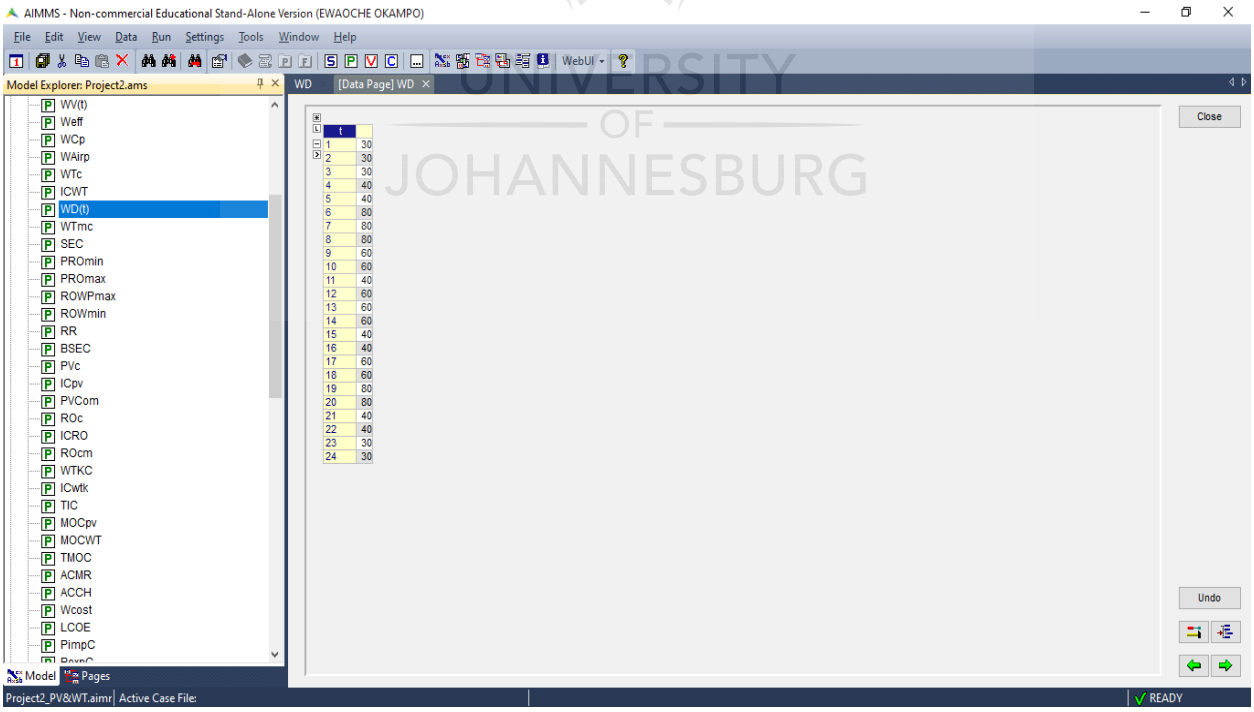

V. Variable ACS formulation

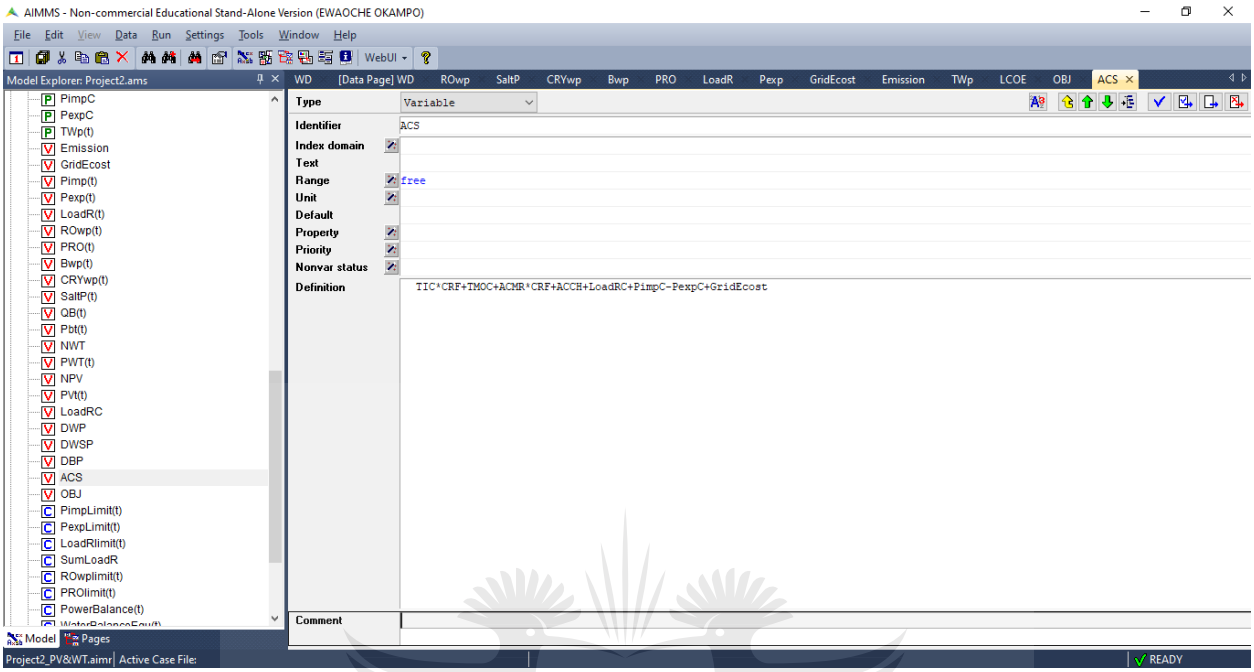

VI. Objective function formulation

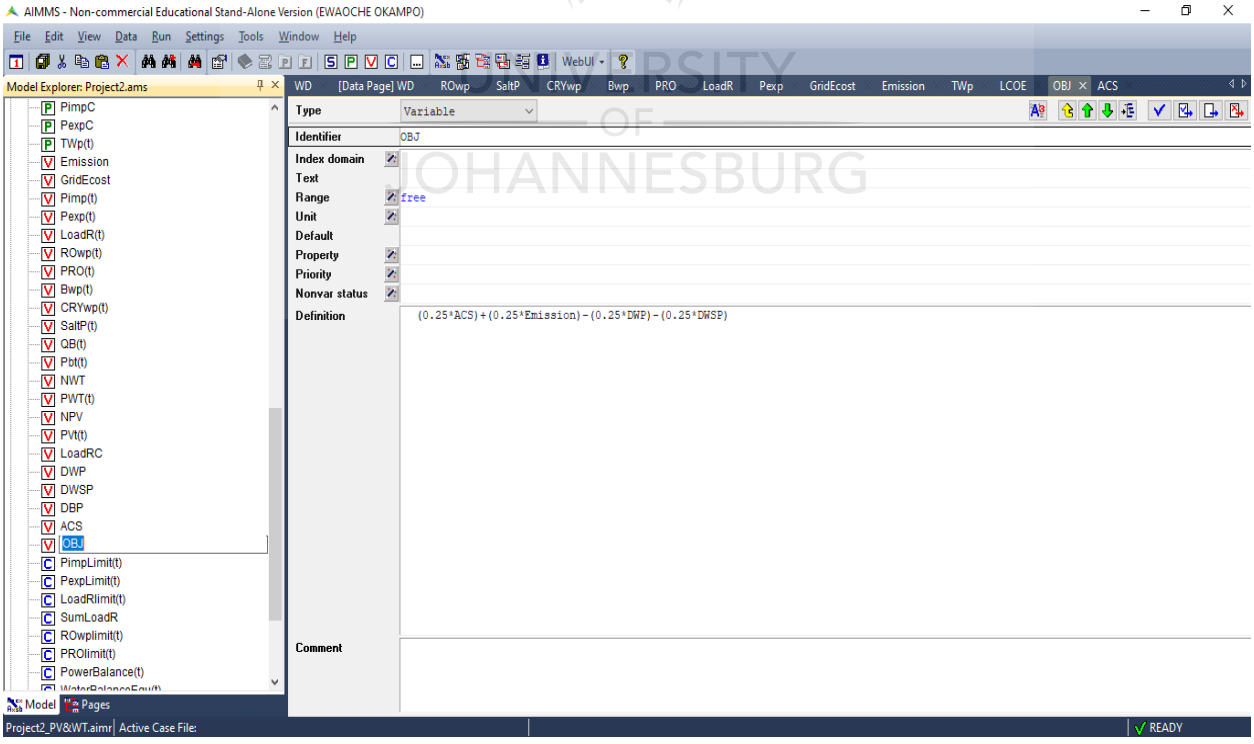

VII. Power balance constraint formation

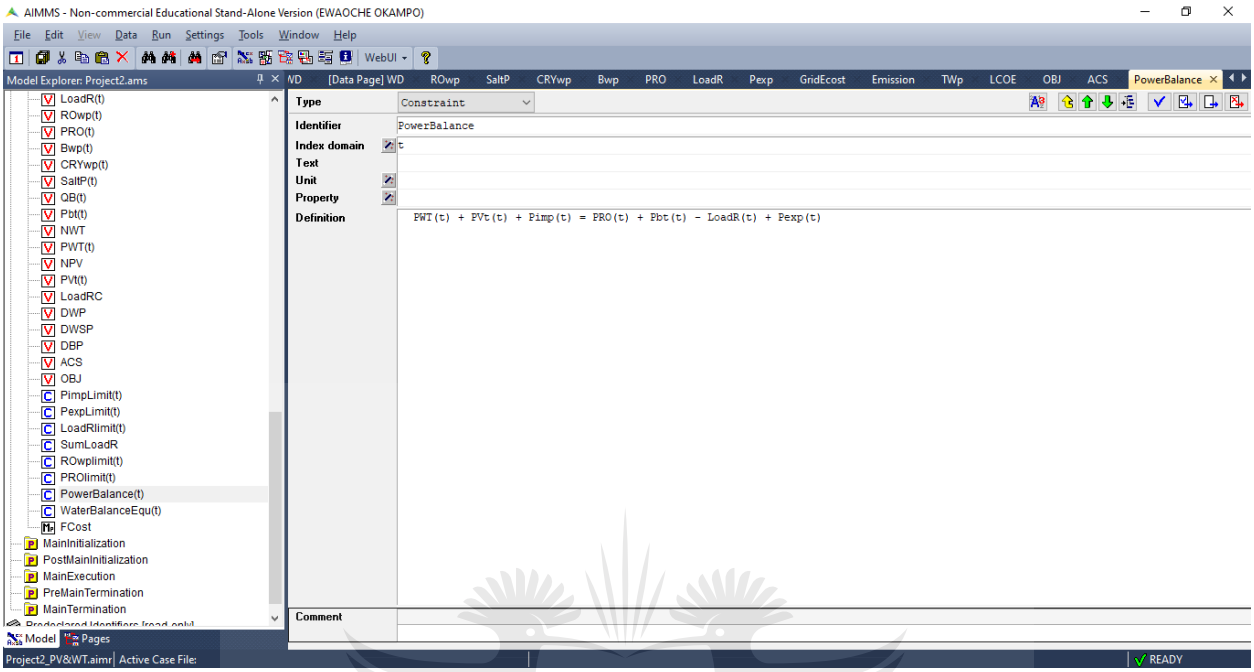

VIII. Mathematical program

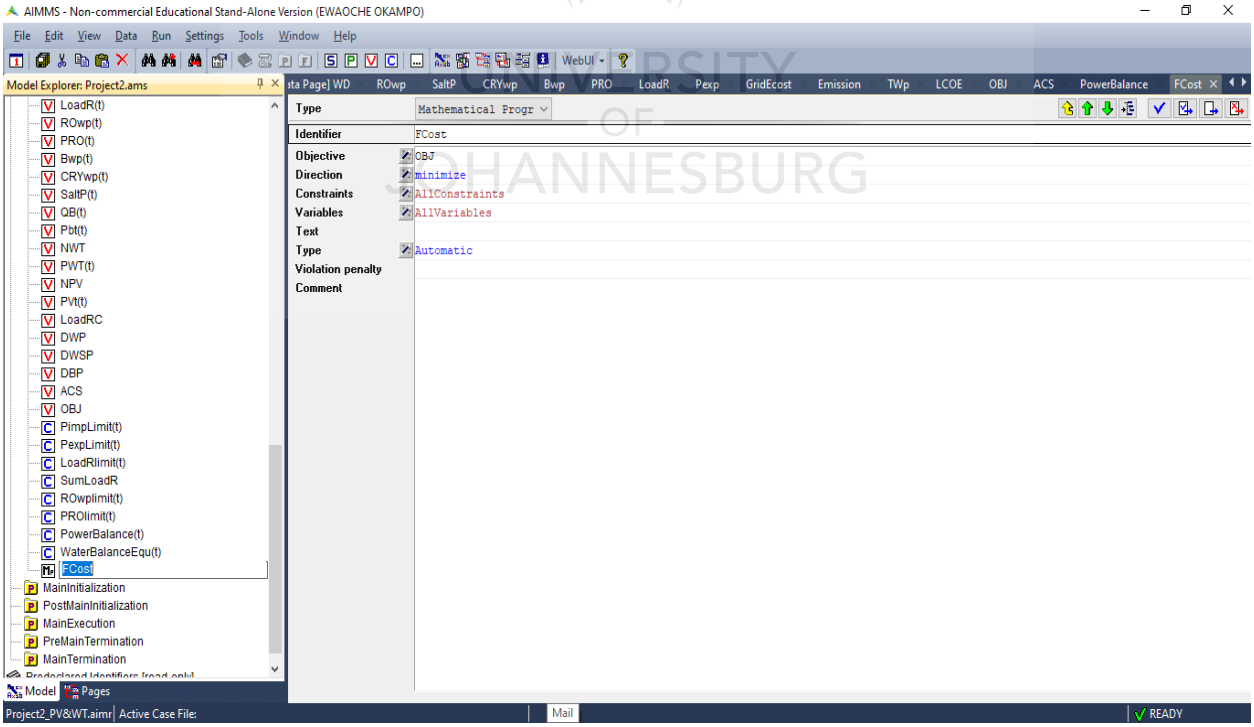

IX. Program statue box

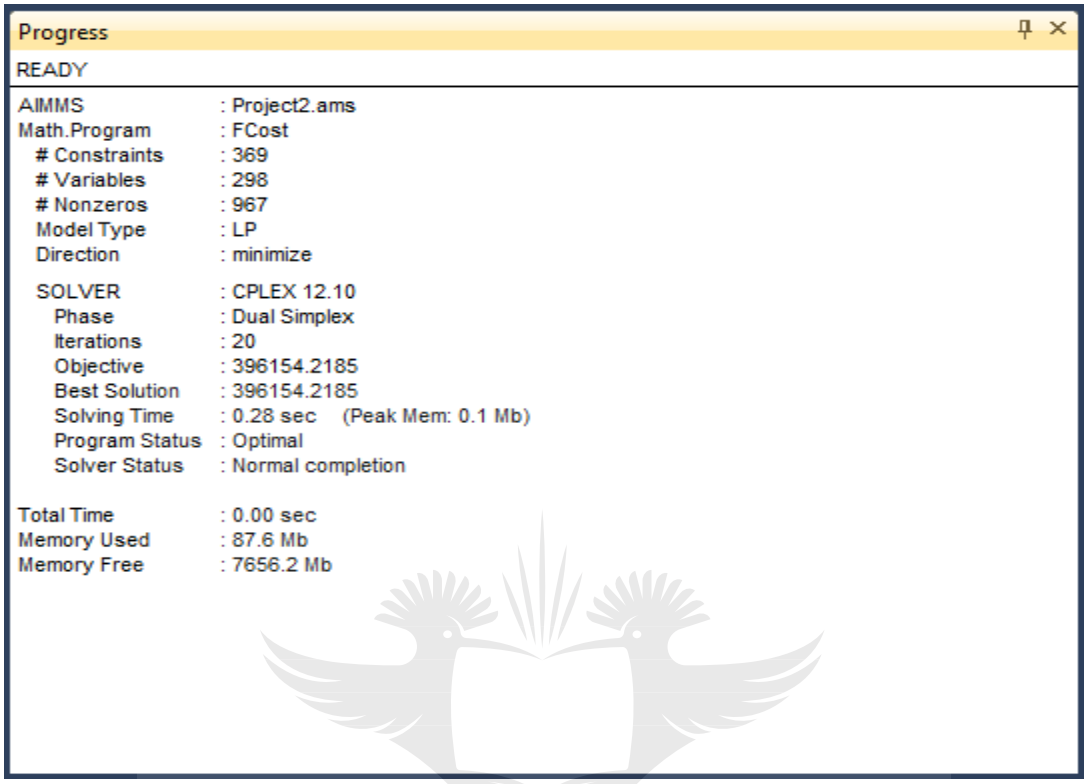

X. Math program inspector

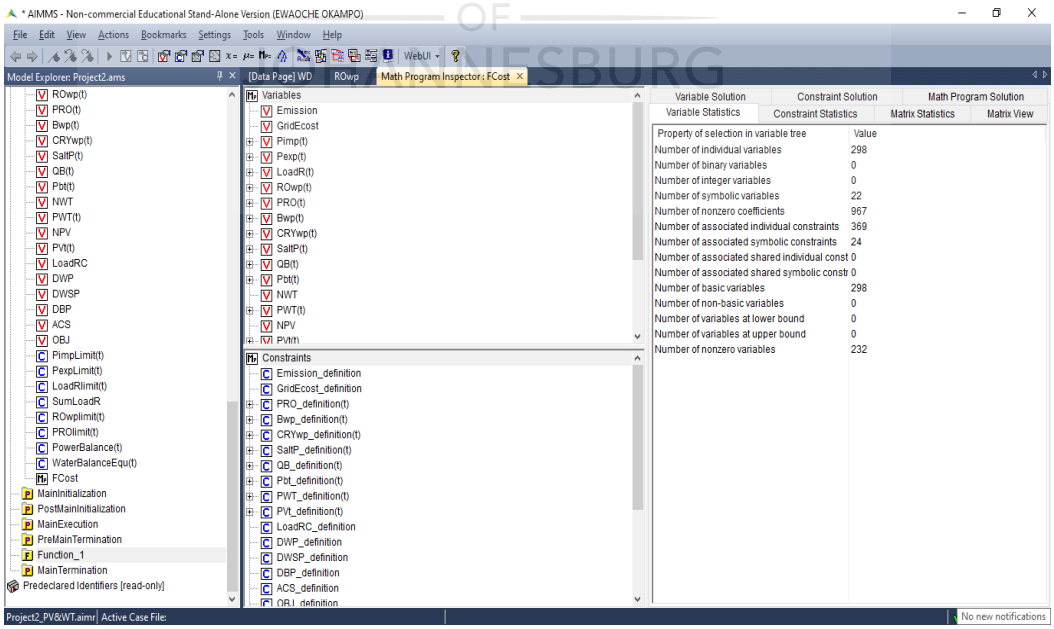

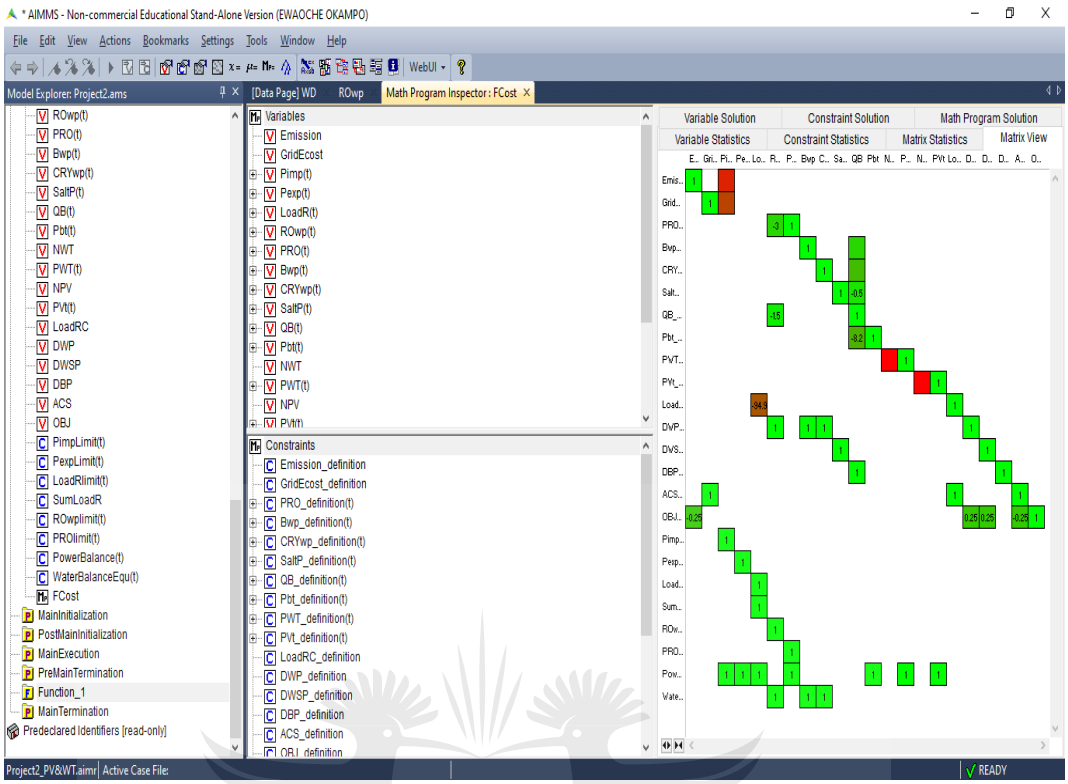

UNIVERSITY
OF
JOHANNESBURG